(12) INTERNATIONAL APPLICATION PUBLISHED UNDER THE PATENT COOPERATION TREATY (PCT)

(19) World Intellectual Property Organization
International Bureau

(43) International Publication Date
1 September 2016 (01.09.2016)

WIPO | PCT

(10) International Publication Number
WO 2016/135457 A1

(51) International Patent Classification:
A61K 48/00 (2006.01)

(21) International Application Number:
PCT/GB2016/050419

(22) International Filing Date:
19 February 2016 (19.02.2016)

(25) Filing Language: English

(26) Publication Language: English

(30) Priority Data:
1503008.3 23 February 2015 (23.02.2015) GB

(71) Applicant: **UCL BUSINESS PLC** [GB/GB]; The Network Building, 97 Tottenham Court Road, London Greater London W1T 4TP (GB).

(72) Inventors: **RIZZI, Matteo**; UCL Institute of Ophthalmology, 11-43 Bath Street, London EC1V 9EL (GB). **ALI, Robin**; UCL Institute of Ophthalmology, 11-43 Bath Street, London EC1V 9EL (GB). **SMITH, Alexander**; UCL Institute of Ophthalmology, 11-43 Bath Street, London EC1V 9EL (GB). **NISHIGUCHI, Koji**; c/o UCL Institute of Ophthalmology, 11-43 Bath Street, London EC1V 9EL (GB).

(74) Agent: **BENTHAM, Andrew**; J A Kemp, 14 South Square, Gray's Inn, London Greater London, WC1R 5JJ (GB).

(81) Designated States *(unless otherwise indicated, for every kind of national protection available)*: AE, AG, AL, AM, AO, AT, AU, AZ, BA, BB, BG, BH, BN, BR, BW, BY, BZ, CA, CH, CL, CN, CO, CR, CU, CZ, DE, DK, DM, DO, DZ, EC, EE, EG, ES, FI, GB, GD, GE, GH, GM, GT, HN, HR, HU, ID, IL, IN, IR, IS, JP, KE, KG, KN, KP, KR, KZ, LA, LC, LK, LR, LS, LU, LY, MA, MD, ME, MG, MK, MN, MW, MX, MY, MZ, NA, NG, NI, NO, NZ, OM, PA, PE, PG, PH, PL, PT, QA, RO, RS, RU, RW, SA, SC, SD, SE, SG, SK, SL, SM, ST, SV, SY, TH, TJ, TM, TN, TR, TT, TZ, UA, UG, US, UZ, VC, VN, ZA, ZM, ZW.

(84) Designated States *(unless otherwise indicated, for every kind of regional protection available)*: ARIPO (BW, GH, GM, KE, LR, LS, MW, MZ, NA, RW, SD, SL, ST, SZ, TZ, UG, ZM, ZW), Eurasian (AM, AZ, BY, KG, KZ, RU, TJ, TM), European (AL, AT, BE, BG, CH, CY, CZ, DE, DK, EE, ES, FI, FR, GB, GR, HR, HU, IE, IS, IT, LT, LU, LV, MC, MK, MT, NL, NO, PL, PT, RO, RS, SE, SI, SK, SM, TR), OAPI (BF, BJ, CF, CG, CI, CM, GA, GN, GQ, GW, KM, ML, MR, NE, SN, TD, TG).

Published:

— *with international search report (Art. 21(3))*

WO 2016/135457 A1

(54) Title: GENE THERAPY TO IMPROVE VISION

(57) Abstract: The invention relates to the use of gene therapy vectors to improve vision by introducing into healthy rod photoreceptor cells of a patient suffering from cone photoreceptor dysfunction and/or degeneration a nucleic acid encoding a gene product that is light-sensitive and/or that modulates endogenous light-sensitive signalling in a photoreceptor cell, such that the range of light intensities to which the rod photoreceptor responds is extended and/or the speed at which the rod photoreceptor responds to light is increased.

GENE THERAPY TO IMPROVE VISION

FIELD OF THE INVENTION

The present invention relates to the use of gene therapy vectors to improve vision in patients.

BACKGROUND OF THE INVENTION

In many mammalian species including mice and humans, the number of rod photoreceptors that mediate vision under dim light outnumbers greatly that of cone photoreceptors (Curcio et al, 2000). However, in an industrialised world where illumination allows cones to operate throughout the day, rod-mediated vision is less important. Many patients with absent rod function from birth are identified only incidentally and, in fact, cannot recognize their abnormal vision (Dryja, 2000). On the contrary, when cone dysfunction is present, patients are always symptomatic and often suffer visual handicap dependent on the degree of their cone dysfunction. In some conditions, however, only (or mostly) the cones are lost or dysfunctional and rods remain relatively preserved. For example, achromatopsia is a severe hereditary retinal dystrophy with a complete absence of cone function from birth but, presumably, with a normal rod function (Hess et al, 1986; Nishiguchi et al, 2005). Mutations in multiple genes including *CNGA3* (Kohl et al 1998); and *PDE6C* (Chang et al, 2009; Thiadens et al, 2009) have been associated with the disease. Each of the disease causing genes encodes an essential component of the cone phototransduction cascade that translates light into an electric signal by causing hyperpolarization of the photoreceptor cell. In age related macular degeneration (AMD), visual impairment is caused primarily by degeneration of the cone-rich fovea in the central macula. Thus patients lose central vision and acuity, but often have relatively well preserved peripheral macula and thus have some useful residual vision that is limited by the paucity of cones outside the fovea.

Rods are highly sensitive to light, which enables them to perceive a small amount of light in dim conditions. Cones, on the contrary, are less sensitive, but are capable of processing large amounts of light and continuously convey visual signals in daylight. This functional difference is, in part, due to the efficiency of the deactivation machinery of photo-signalling, the GTPase complex composed of RGS9, R9AP (also known as RGS9BP), and Gß5. RGS9 is the catalytic component that hydrolyses the GTP coupled to the G-protein, whereas R9AP and Gß5 are the essential constitutive subunits (Burns et al, 2009; Burns et al, 2010). Importantly, R9AP tethers the complex to the disc membrane at the photoreceptor outer segment where the phototransduction signalling also takes place (Baseler et al, 2002). Expression of R9AP determines the level of GTPase complex such that any RGS9 produced in excess of R9AP is likely quickly degraded (Martyemyanov et al, 2009). Over-expression of R9AP in the murine rods is sufficient to increase the GTPase activity and to substantially speed their deactivation kinetics as evidenced by the single cell recordings (Krispel et al, 2006). In the cones, the RGS9 expression has been estimated to be ~10-fold higher than that of the rods (Cowan et al, 1998; Zhang et al, 2003). This provides a basis for the ability of the cones to recover quickly from light exposure and thus maintain functional to continuous light stimulus. It also allows cones to respond to more rapid stimulation. Indeed, clinically, patients with delayed deactivation of phototransduction cascade caused by genetic defects in *RGS9* or *R9AP*, or *bradyopsia*, have a profound impairment of cone-mediated vision including day blindness and reduced ability to see moving objects Nishiguchi et al, 2004; Michaelides et al, 2010). Meanwhile, the rod-mediated vision is less affected by the same mutation.

Some macular degeneration conditions, such as age-related macular degeneration (AMD) and inherited macular degeneration conditions also exhibit cone dysfunction but normal or less impaired rod function. Macular degeneration is the leading cause of blindness in the developed world and as its prevalence quadruples in each decade of life the instance of AMD is expected to rise in the coming years as life expectancy

increases. Drugs for the treatment of AMD already account for over 1% of the entire drugs budget of the UK's National Health Service. While patients with advanced AMD can be trained to fixate extra-foveally, the low refresh rate and the low bleaching threshold of rod cells limits the quality of resulting vision.

SUMMARY OF THE INVENTION

Using mice with absent cone function, we have demonstrated that AAV-mediated over-expression of Rgs9-anchor protein (R9AP), a critical component of GTPase complex that mediates the deactivation of phototransduction cascade, results in desensitization and "photopic shift" of the rod-driven electroretinogram. The treatment enables the rods to respond to brighter light (up to ~2.0 log) than the untreated cells at the expense of scotopic (lower light level) function. Multi-electrode array measurements using the treated retinas showed that the retinal ganglion cells also reflected the "photopic shift" of the rods, by exhibiting graded responses at photopic light levels. Contrast sensitivity function measured by quantifying the head-tracking movements in response to rotating sinusoidal gratings showed an improvement of the sensitivity by up to 25-fold under room light conditions and faster response to repeated stimuli. Furthermore, biochemical measurement of bleachable rhodopsin levels in these mice indicated that the visual cycle was not limiting rod function.

We have also expressed a fast light-driven proton pump, ArchT (Han et al, 2011) in rod photoreceptors. AAV8 particles carrying ArchT-EGFP under control of the Rhodopsin promoter (Rho) were injected subretinally in adult mice. Expression of Rho-ArchT-EGFP was limited to the membrane of rod photoreceptors. Expression of ArchT allowed extremely rapid light responses, while the intrinsic rod response was preserved and was comparable to that observed in non-transduced rod photoreceptors. Overall, ArchT expression did not alter the ability of rod photoreceptors to respond to scotopic stimuli, but it did confer an additional ability to respond with rapid non-bleaching responses to higher levels of illumination. We also found that the transduced rods were

able reliably to sustain this fast 'cone-like' transmission, in that ArchT-expressing rods drove sustained retinal ganglion cell (RGC) spiking at high light intensities and at frequencies approaching those of cone photoreceptors. Expression of Rho-ArchT-EGFP in CNGA3-/- and PDE6C-/- mice lacking cone-mediated vision also extended the sensitivity of these mice to bright light stimuli and conferred fast vision on these mice. The maximal frequency of stimuli that ArchT-expressing mice could follow was similar to that of cone photoreceptors.

Together, these results show that, after transduction of healthy rod photoreceptors with genes encoding either light sensitive proteins characteristic of cones or genes encoding molecules that increase the speed of the endogenous rod signalling mechanism, rods behave more like cones and hence can compensate for cone dysfunction. This has implications for the treatment of a number of vision disorders in which cone function is reduced, but at least some healthy rods remain. This contrasts with previous approaches (Busskamp et al, 2010; US Patent Publication No. 2012258530) in which the goal was to restore lost function in cones. Altering function in rods in the manner of the present invention is advantageous in that conditions in which cones are dysfunctional but can be repaired (for example in the early stages of retinal degeneration when photoreceptor function is lost but the photoreceptor-to-bipolar synapse may be intact) are rare, whereas conditions in which cone dysfunction is more severe or advanced and cannot be repaired or where cones are lost entirely, but yet at least some healthy rod photoreceptors remain, are common (see above). Furthermore, this invention enables the creation of a 'pseudo-fovea', a small patch of cone-like rods that will improve vision in conditions in which foveal cones have been lost or are dysfunctional.

The invention therefore provides a vector comprising a nucleic acid encoding a gene product that is light-sensitive and/or that modulates endogenous light-sensitive signalling in a photoreceptor cell, for use in a method of improving vision in a patient with cone photoreceptor dysfunction and/or degeneration by introduction of said

nucleic acid into healthy rod photoreceptors in the retina of the patient and expression of said gene product therein, such that the range of light intensities to which the rod photoreceptor responds is extended and/or the speed at which the rod photoreceptor responds to light is increased.

The invention also provides a vector as defined above, a host cell comprising said vector and methods of treatment carried out with such a vector.

BRIEF DESCRIPTION OF THE DRAWINGS

Figure 1: Expression of ArchT in rod photoreceptors leads to fast light-driven currents.

(a), top panels: AAV8-mediated transduction of ArchT-EGFP (green, see left panels) under control of the Rhodopsin promoter. No overlap is observed with cones (purple: Cone arrestin, see middle panels, white: DAPI, see right panels). Lower panels: specificity of expression can also be observed at the level of synapses. (b) ArchT-EGFP is localized to the membrane of rod photoreceptors, including inner and outersegments. (c) Quantification of fluorescence in ArchT-EGFP-expressing rod terminals (green, left peak) and Cone arrestin positive cone terminals (purple, right peak) shows two distinct bands corresponding to the sub-layer where rod and cone synapses localize respectively (n=22). (d) Single-cell recordings from the cell bodies of ArchT-expressing rod photoreceptors. The currents mediated by the intrinsic rod photo-trandsuction (upper trace) in response to 10 ms 530-nm light pulses (green, see vertical bars) were preserved. The ArchT-generated currents were faster (lower trace). Scale bars: (a) upper panels: 50 μm; (a) lower panels and (b): 10 um.

Figure 2: ArchT-expression drives high-frequency responses in rods and fast transmission to Retinal Ganglion Cells.

(a) Intrinsic rod light-evoked currents in uninjected C57BL6 retinas. (b) ArchT-mediated currents are able to follow much higher stimulation frequencies. (c) Responses are time-locked to stimulus presentation (green vertical bars). (d) ArchT-expressing rods respond to frequency stimulation up to 80 Hz without faltering, whereas intrinsic rod responses drop off at ~20 Hz. (e) Summary data showing that ArchT expression does not alter the intrinsic response of rod photoreceptors, while ArchT responses begin at brighter light levels. (f) Multi-electrode array recordings from PDE6C-/- ArchT-expressing retinas. Intrinsic rod responses failed to elicit reliable Retinal Ganglion Cell spiking above 20 Hz.. On the contrary, ArchT-mediated rod activation drove fast spiking of Retinal Ganglion Cells to levels comparable to cone photoreceptors.

Figure 3: ArchT-mediated activation of rods drives behavioural response for fast high light intensity-stimuli.

(a) Top panels: schematic for fear conditioning behaviour. Briefly, a visual stimulus was paired with a shock. 24 hours later freezing behaviour was tested in a new context. Bottom panels: uninjected $CNGA3^{-/-}$ and $PDE6C^{-/-}$ mice failed to learn the task (left sets of bars in each graph). However, ArchT expression successfully drove freezing behaviour in mice (right sets of bars in each graph). (b) Optomotor testing. ArchT-expressing mice are able to follow stimuli at frequencies comparable to those reliably followed by cones.

A. Figure 4: AAV-mediated R9AP over-expression in rods and accelerated a-wave deactivation in *Cnga3-/-* mice.Increased RGS9 expression in a *Cnga3-/-* eye treated with rRAAV2/8.Rho.mR9ap. Over-expression of R9AP results in increased immunoreactivity toward RGS9 (red) throughout the photoreceptor layer in the treated eye (left) compared to the untreated (right). Western blot shows increased expression of RGS9 both in the retina and retinal pigment epithelium (RPE) in the eye over-expressing R9AP (bottom). A small amount of RGS9 protein was also detected in the

RPE of the treated eye. This may reflect "spill over" of the excessive protein contained within the phagocytosed disc membrane. Scale bar indicates 25 μm.

B. Increased speed of a-wave amplitude recovery in the *Cnga3-/-* eye treated with rAAV2/8.Rho.mR9ap and rAAV2/8.CMV.mR9ap. Representative ERG tracings for the probe flash (black traces, see traces with peak in the middle of the timecourse) and for the 2nd flash (red traces) presented at inter-stimulus interval (ISI) of 2 seconds from the treated (top) and untreated (bottom) eyes from the same animal. Note that a second flash yields small a-wave (arrow) is clearly visible in the treated eye, whereas a-wave is not visible (arrow) in the untreated fellow eye. A plot of a-wave recovery at various ISIs in the treated and untreated eyes. The eyes injected with rAAV2/8.CMV.mR9ap (n = 5) or rAAV2/8.Rho.mR9ap (n = 7) have faster recovery kinetics than the untreated eye (n = 5) that is most visible with shorter ISIs. The data is presented as average ± standard error of the mean. OE: over-expression.

Figure 5: Gain of photopic function by rods through over-expression of R9AP in *Cnga3-/-* mice.

A. Elevation of response threshold and photopic shift of 6Hz ERGs through over-expression of R9AP in rods of *Cnga3-/-* mice. Representative 6Hz ERG traces from a *Cnga3-/-* mouse in which one eye was treated with rAAV2/8.CMV.mR9ap and the other eye was left untreated (top panel). ERG traces are aligned from responses against the dimmest flash (-6.0 log cd.s/m^2) to the brightest flash (2.0 log cd.s/m^2; bottom) from the top to the bottom at 0.5 log.cd.s/m^2 step. Note that the lower threshold flash intensity at which the responses emerge is increased, which is coupled with elevated response threshold to brighter flashes. This results in a "photopic shift" of the retinal function in the eye treated with rAAV2/8.CMV.mR9ap. Summary of 6Hz ERG results demonstrating photopic shift of the retinal function following treatment with rAAV2/8.CMV.mR9ap or rAAV2/8.Rho.mR9ap (bottom panel). ERG responses from *Gnat1-/-* mice deficient in rod function represents cone-mediated function. Meanwhile, responses from C57BL6 mice are derived from both rod and cone photoreceptors. The

data is presented as % amplitude relative to the maximal response and is presented as average ± standard error of the mean. ERGs were recorded from *Cnga3-/-* mice treated with rAAV2/8.CMV.mR9ap (Cnga3-/- CMV.R9ap; N = 8), *Cnga3-/-* mice treated with rAAV2/8.Rho.mR9ap (Cnga3-/- Rho.R9ap; N = 6), *Cnga3-/-* mice untreated (Cnga3-/- Untreated; N = 8), *Gnat1-/-* mice untreated (Gnat1-/- Untreated; N = 6), and C57BL6 mice untreated (C57BL6 Untreated; N = 6)

B. Increased retinal responses to long flashes in the *Cnga3-/-* eye treated with rAAV2/8.CMV.mR9ap. Open rectangle denotes the duration of the flash. Note that in the eye treated with rAAV2/8.CMV.mR9ap, responses are detectable with increased duration of light stimulus. Conversely, the untreated contralateral eye shows little or no response when recorded simultaneously at identical conditions.

C. Gain of retinal function under photopic conditions in the *Cnga3-/-* eyes treated with rAAV2/8.CMV.mR9ap. Note that the treated eye shows responses under photopic recording conditions (white background light of 20 cd/m^2) whereas the untreated contralateral eye recorded simultaneously remained unresponsive.

Figure 6: Efficient transmission of the altered photoreceptor signal to the bipolar cells in the eyes over-expressing R9AP

A. Representative ERG traces. ERGs were recorded after rAAV2/8.CMV.mR9ap injection (red trace, lower trace) in a *Cnga3-/-* mouse using a saturating flash (1.9 log cd.s/m^2). The contralateral eye served as an untreated control (black trace, upper trace).

B. Delayed activation of the bipolar cells to a flash. A-wave and b-wave implicit times were measured from an ERG response to a saturating flash (1.9 log cd.s/m^2) in the treated and untreated eyes.

C. Intensity response curve for a-wave and b-wave amplitudes recorded from *Cnga3-/-* mice (N=5) with one eye treated with rAAV2/8.CMV.mR9ap (red curves) and the other eye left untreated (black curves). All data are presented as average ± standard error of the mean. OE: over-expression.

Figure 7: A gain of sustainable visual perception following R9AP over-expression in *Cnga3-/-* mice.

A. Improved contrast sensitivity function measured by optokinetic responses. In the *Cnga3-/-* mice treated with rAAV2/8.Rho.mR9ap in the left eye, the contrast sensitivity function (CSF) was differentially measured for clockwise (representing treated left eye) and counter-clockwise (representing untreated right eye) head tracking movements against sinusoidal gratings. The CSF for the treated eyes (red curve) was better than that for the untreated eyes (blue curve), which was similar to that for the untouched Cnga3-/- mice (black curve; average of both eyes). Note that the CSF for the treated eye was equivalent to, if not slightly better, to that for untouched wild-type controls (green; average of both eyes). N= 5 for all groups. All data are presented as average ± standard error of the mean. OE: over-expression.

B. Sustained rhodopsin levels after prolonged exposure to Optomotry test. A representative recording of optical absorption of ocular sample using scanning spectrophotometer (left panel inside the green dashed box). Subtracting the absorption of ocular samples measured after (blue trace, top trace between 300 and 400nm) from before (red trace) complete photobleaching showed λmin peaking at ~380 nm corresponding to released photoproducts coupled with λmax peaking at ~500 nm representing the amount of bleachable rhodopsin in the sample (right panel inside the green dashed box). Rhodopsin bleaching speed was assessed by measuring the difference spectrum (λmax) in the fully dilated eyes treated or untreated with rAAV2/8.Rho.mR9ap in Cnga3-/- mice after 5 minutes' exposure to 7.0 mW white light (bottom left; average ± standard error of the mean). Rhodopsin levels was measured also after exposure of the *Cnga3-/-* mice to Optomotry test for up to 120 minutes (right bottom; N=3 for each time point) following unilateral injection of rAAV2/8.Rho.mR9ap. The grey area indicates rhodopsin levels (mean ± standard deviation) recorded from untouched *Cnga3-/-* mice (N=8) after an overnight dark-adaptation. Dotted line indicates the average. Note that the level of rhodopsin remains stable for at least 2 hours in both the eyes treated with rAAV2/8.Rho.mR9ap and the

untreated eyes of *Cnga3*-/- mice. Data with error bars were presented as mean ±standard error of the mean.

Figure 8: Over-expression of R9AP increases the recovery speed of rod photoresponse in *Pde6c*-/- mice.

The time constant (σ) for 50% recovery of a-wave amplitude was reduced by ~50% in the *Pde6c*-/- eyes injected with rAAV2/8.CMV.mR9ap (σ = ~ 5.75 sec) compared to the untreated contralateral eyes (σ = ~ 11.46 sec) consistent with accelerated deactivation of phototransduction following the treatment. N = 6. Data with error bars were displayed as mean ±standard error of the mean.

Figure 9: Over-expression of R9AP results in "photopic shift" of the intensity-response curve in *Pde6c*-/- mice.

The eyes injected with rAAV2/8.CMV.mR9ap showed photopic shift of the 6 Hz ERG responses to incremental flash intensities compared to the untreated contralateral eyes in *Pde6c*-/- mice (N = 6). The data is presented as % amplitude relative to maximal response and is displayed as average ± standard error of the mean.

Figure 10: Sustained effect of R9AP over-expression without clear evidence of retinal degeneration at 5 months post-injection of rAAV2/8.CMV.mR9ap in *Cnga3*-/- mice.

Response profile normalized against maximum amplitude confirmed the presence of "photopic shift" of the intensity-response curve to 6Hz flashes (top). The same data without normalization showed no evidence of reduction in amplitudes in the treated eye (bottom). N = 5. The data is presented as average ± standard error of the mean.

Figure 11: Treatment of wild-type mice with rAAV2/8.Rho.mR9ap showed no obvious effect on 6 Hz ERG intensity-response curve.

The eyes treated with rAAV2/8.Rho.mR9ap showed no shift in 6 Hz ERG intensity-response curve compared to that for the untreated contralateral eyes in C57BL6 mice (N = 5). The data is presented as average ± standard error of the mean.

Figure 12: No gain of visual perception following R9AP over-expression in C57BL6 mice.

In the C57BL6 mice treated with rAAV2/8.Rho.mR9ap only in the left eye, the contrast sensitivity function (CSF) was differentially measured for clockwise (representing treated left eye) and counter-clockwise (representing untreated right eye) head tracking movements to rotating sinusoidal gratings. The CSF for both the treated eyes (pink curve) and the untreated eyes (light blue curve) showed similar results, which was similar to that for the untouched C57BL6 mice (green curve; average of both eyes). N= 5 for all groups. All data are presented as average ± standard error of the mean. OE: over-expression.

DETAILED DESCRIPTION OF THE INVENTION

A vector of the invention comprises a nucleic acid whose expression to produce a gene product, typically a protein, which will effect treatment of an ocular condition as described herein, operably linked to a promoter to form an expression cassette.

Nucleic Acids and Gene Products

A vector of the invention comprises a nucleic acid encoding a gene product that is light-sensitive and/or that modulates endogenous light-sensitive signalling in a photoreceptor

cell and makes a rod transduced with the nucleic acid of the invention behave more like a cone by extending the range light intensities to which the rod photoreceptor responds is and/or increasing the speed at which the rod photoreceptor responds to light. Thus, the protein may itself be directly light-sensitive, e.g. it may change membrane conductance in rods in a way that results in hyperpolarisation (outward current flow) upon light stimulation. Such proteins will for example be light-sensitive or light-gated G-coupled membrane proteins, ion channels, ion pumps or ion transporters. Preferred light-sensitive proteins include ArchT, Jaws (cruxhalorhodopsin) (Chuong et al, 2014) and iC1C2. Alternatively, the protein may itself not be directly light-sensitive but may indirectly modulate endogenous light-sensitive signalling in a rod photoreceptor cell. Examples of such proteins are members of the RGS9 complex, notably R9AP (also known as RGS9BP), and Gß5. In the alternative, the nucleic acid may encode any other gene product that increases the speed of the endogenous rod signalling mechanism. In all of these cases, the sequence may encode a wild-type protein or a mutant or variant or truncated version that retains the activity of the wild-type protein. The nucleic acid may also be codon-optimised for expression in the target cell type.

Following expression of the gene product, rods will show stronger and/or faster modulation to light stimuli than non-transduced rods, at higher than usual intensities. Examples include improved modulation strength and/or faster activation/inactivation kinetics. Rods transduced according to the invention will therefore react more strongly and/or quickly to illumination in the mesopic and/or photopic range than non-transduced rods. Preferably, the response of the rods to scotopic illumination conditions is unaffected or not substantially affected, ie the rods gain the ability to respond strongly and/or quickly to brighter light without losing the ability to respond to dim light.

Promoters and other regulatory elements

In the expression construct, the nucleic acid encoding the gene product is typically operably linked to a promoter. The promoter may be constitutive but will preferably

be a photoreceptor-specific or photoreceptor-preferred promoter, more preferably a rod-specific or rod-preferred promoter such as a Rhodopsin (Rho), Neural retina-specific leucine zipper protein (NRL) or Phosphodiesterase 6B (PDE6B) promoter. The promoter region incorporated into the expression cassette may be of any length as long as it is effective to drive expression of the gene product, preferably photoreceptor-specific or photoreceptor-preferred expression or rod-specific or rod- preferred expression.

By a photoreceptor-specific promoter, is meant a promoter that drives expression only or substantially only in photoreceptors, e.g. one that drives expression at least a hundred-fold more strongly in photoreceptors than in any other cell type. By a rod-specific promoter, is meant a promoter that drives expression only or substantially only in photoreceptors, e.g. one that drives expression at least a hundred-fold more strongly in photoreceptors than in any other cell type, including cones. By a photoreceptor-preferred promoter, is meant a promoter that expresses preferentially in photoreceptors but may also drive expression to some extent in other tissues, e.g. one that drives expression at least two-fold, at least five-fold, at least ten-fold, at least 20-fold, or at least 50-fold more strongly in photoreceptors than in any other cell type. By a rod-preferred promoter, is meant a promoter that drives expression preferentially in photoreceptors but may also drive expression to some extent in other tissues, e.g. one that drives expression at least two-fold, at least five-fold, at least ten-fold, at least 20-fold, or at least 50-fold more strongly in photoreceptors than in any other cell type. including cones.

One or more other regulatory elements, such as enhancers, may also be present as well as the promoter.

Vectors

A vector of the invention may be of any type, for example it may be a plasmid vector or a minicircle DNA.

Typically, vectors of the invention are however viral vectors. The viral vector may for example be based on the herpes simplex virus, adenovirus or lentivirus. The viral vector may be an adeno-associated virus (AAV) vector or a derivative thereof. The viral vector derivative may be a chimeric, shuffled or capsid modified derivative.
The viral vector may comprise an AAV genome from a naturally derived serotype, isolate or clade of AAV. The serotype may for example be AAV2, AAV5 or AAV8.

The efficacy of gene therapy is, in general, dependent upon adequate and efficient delivery of the donated DNA. This process is usually mediated by viral vectors. Adeno-associated viruses (AAV), a member of the parvovirus family, are commonly used in gene therapy. Wild-type AAV, containing viral genes, insert their genomic material into chromosome 19 of the host cell. The AAV single-stranded DNA genome comprises two inverted terminal repeats (ITRs) and two open reading frames, containing structural (cap) and packaging (rep) genes.

For therapeutic purposes, the only sequences required *in cis,* in addition to the therapeutic gene, are the ITRs. The AAV virus is therefore modified: the viral genes are removed from the genome, producing recombinant AAV (rAAV). This contains only the therapeutic gene, the two ITRs. The removal of the viral genes renders rAAV incapable of actively inserting its genome into the host cell DNA. Instead, the rAAV genomes fuse via the ITRs, forming circular, episomal structures, or insert into pre-existing chromosomal breaks. For viral production, the structural and packaging genes, now removed from the rAAV, are supplied *in trans*, in the form of a helper plasmid.
AAV is a particularly attractive vector as it is generally non-pathogenic; the majority people have been infected with this virus during their life with no adverse effects.

The immune privilege of ocular tissue, a result of anatomical barriers and immunomodulatory factors, renders the eye largely exempt from the adverse immunological responses that can be triggered in other tissues by AAV (Taylor 2009).

AAV vectors are limited by a relatively small packaging capacity of roughly 4.8kb and a slow onset of expression following transduction. Despite these minor drawbacks, AAV has become the most commonly used viral vector for retinal gene therapy.

Most vector constructs are based on the AAV serotype 2 (AAV2). AAV2 binds to the target cells via the heparin sulphate proteoglycan receptor. The AAV2 genome, like those of all AAV serotypes, can be enclosed in a number of different capsid proteins. AAV2 can be packaged in its natural AAV2 capsid (AAV2/2) or it can be pseudotyped with other capsids (e.g. AAV2 genome in AAV1 capsid; AAV2/1, AAV2 genome in AAV5 capsid; AAV2/5 and AAV2 genome in AAV8 capsid; AAV2/8).

rAAV transduces cells via serotype specific receptor-mediated endocytosis. A major factor influencing the kinetics of rAAV transgene expression is the rate of virus particle uncoating within the endosome. This, in turn, depends upon the type of capsid enclosing the genetic material (Ibid.). After uncoating the linear single-stranded rAAV genome is stabilised by forming a double-stranded molecule via *de novo* synthesis of a complementary strand. The use of self-complementary DNA may bypass this stage by producing double-stranded transgene DNA. Natkunarajah et al (2008) found that self-complementary AAV2/8 gene expression was of faster onset and higher amplitude, compared to single-stranded AAV2/8. Thus, by circumventing the time lag associated with second-strand synthesis, gene expression levels are increased, when compared to transgene expression from standard single-stranded constructs. Subsequent studies investigating the effect of self-complementary DNA in other AAV pseudotypes (e.g. AAV2/5) have produced similar results. One caveat to this technique is that, as AAV has a packaging capacity of approximately 4.8kb, the self-complementary recombinant genome must be appropriately sized (i.e. 2.3kb or less).

In addition to modifying packaging capacity, pseudotyping the AAV2 genome with other AAV capsids can alter cell specificity and the kinetics of transgene expression. AAV2/8 is reported to transduce photoreceptors more efficiently than either AAV2/2 or AAV2/5 (Natkunarajah et al. 2008).

The vector of the invention may therefore comprise an adeno-associated virus (AAV) genome or a derivative thereof.

An AAV genome is a polynucleotide sequence which encodes functions needed for production of an AAV viral particle. These functions include those operating in the replication and packaging cycle for AAV in a host cell, including encapsidation of the AAV genome into an AAV viral particle. Naturally occurring AAV viruses are replication-deficient and rely on the provision of helper functions in *trans* for completion of a replication and packaging cycle. Accordingly and with the additional removal of the AAV *rep* and *cap* genes, the AAV genome of the vector of the invention is replication-deficient.

The AAV genome may be in single-stranded form, either positive or negative-sense, or alternatively in double-stranded form. The use of a double-stranded form allows bypass of the DNA replication step in the target cell and so can accelerate transgene expression. The AAV genome may be from any naturally derived serotype or isolate or clade of AAV. As is known to the skilled person, AAV viruses occurring in nature may be classified according to various biological systems.

Commonly, AAV viruses are referred to in terms of their serotype. A serotype corresponds to a variant subspecies of AAV which owing to its profile of expression of capsid surface antigens has a distinctive reactivity which can be used to distinguish it from other variant subspecies. Typically, a virus having a particular AAV serotype does not efficiently cross-react with neutralising antibodies specific for any other AAV

serotype. AAV serotypes include AAV1, AAV2, AAV3, AAV4, AAV5, AAV6, AAV7, AAV8, AAV9, AAV10 and AAV11, also recombinant serotypes, such as Rec2 and Rec3, recently identified from primate brain. In vectors of the invention, the genome may be derived from any AAV serotype. The capsid may also be derived from any AAV serotype. The genome and the capsid may be derived from the same serotype or different serotypes.

In vectors of the invention, it is preferred that the genome is derived from AAV serotype 2 (AAV2), AAV serotype 4 (AAV4), AAV serotype 5 (AAV5) or AAV serotype 8 (AAV8). It is most preferred that the genome is derived from AAV2 but other serotypes of particular interest for use in the invention include AAV4, AAV5 and AAV8, which efficiently transduce tissue in the eye, such as the retinal pigmented epithelium. It is preferred that the capsid is derived from AAV5 or AAV8, especially AAV8.

Reviews of AAV serotypes may be found in Choi et al (*Curr Gene Ther*. 2005; 5(3); 299-310) and Wu et al (*Molecular Therapy*. 2006; 14(3), 316-327). The sequences of AAV genomes or of elements of AAV genomes including ITR sequences, rep or cap genes for use in the invention may be derived from the following accession numbers for AAV whole genome sequences: Adeno-associated virus 1 NC_002077, AF063497; Adeno-associated virus 2 NC_001401; Adeno-associated virus 3 NC_001729; Adeno-associated virus 3B NC_001863; Adeno-associated virus 4 NC_001829; Adeno-associated virus 5 Y18065, AF085716; Adeno-associated virus 6 NC_001862; Avian AAV ATCC VR-865 AY186198, AY629583, NC_004828; Avian AAV strain DA-1 NC_006263, AY629583; Bovine AAV NC_005889, AY388617.

AAV viruses may also be referred to in terms of clades or clones. This refers to the phylogenetic relationship of naturally derived AAV viruses, and typically to a phylogenetic group of AAV viruses which can be traced back to a common ancestor, and includes all descendants thereof. Additionally, AAV viruses may be referred to in terms of a specific isolate, i.e. a genetic isolate of a specific AAV virus found in nature.

The term genetic isolate describes a population of AAV viruses which has undergone limited genetic mixing with other naturally occurring AAV viruses, thereby defining a recognisably distinct population at a genetic level.

Examples of clades and isolates of AAV that may be used in the invention include:

Clade A: AAV1 NC_002077, AF063497, AAV6 NC_001862, Hu. 48 AY530611, Hu 43 AY530606, Hu 44 AY530607, Hu 46 AY530609

Clade B: Hu. 19 AY530584, Hu. 20 AY530586, Hu 23 AY530589, Hu22 AY530588, Hu24 AY530590, Hu21 AY530587, Hu27 AY530592, Hu28 AY530593, Hu 29 AY530594, Hu63 AY530624, Hu64 AY530625, Hu13 AY530578, Hu56 AY530618, Hu57 AY530619, Hu49 AY530612, Hu58 AY530620, Hu34 AY530598, Hu35 AY530599, AAV2 NC_001401, Hu45 AY530608, Hu47 AY530610, Hu51 AY530613, Hu52 AY530614, Hu T41 AY695378, Hu S17 AY695376, Hu T88 AY695375, Hu T71 AY695374, Hu T70 AY695373, Hu T40 AY695372, Hu T32 AY695371, Hu T17 AY695370, Hu LG15 AY695377,

Clade C: Hu9 AY530629, Hu10 AY530576, Hu11 AY530577, Hu53 AY530615, Hu55 AY530617, Hu54 AY530616, Hu7 AY530628, Hu18 AY530583, Hu15 AY530580, Hu16 AY530581, Hu25 AY530591, Hu60 AY530622, Ch5 AY243021, Hu3 AY530595, Hu1 AY530575, Hu4 AY530602 Hu2, AY530585, Hu61 AY530623

Clade D: Rh62 AY530573, Rh48 AY530561, Rh54 AY530567, Rh55 AY530568, Cy2 AY243020, AAV7 AF513851, Rh35 AY243000, Rh37 AY242998, Rh36 AY242999, Cy6 AY243016, Cy4 AY243018, Cy3 AY243019, Cy5 AY243017, Rh13 AY243013

Clade E: Rh38 AY530558, Hu66 AY530626, Hu42 AY530605, Hu67 AY530627, Hu40 AY530603, Hu41 AY530604, Hu37 AY530600, Rh40 AY530559, Rh2 AY243007, Bb1 AY243023, Bb2 AY243022, Rh10 AY243015, Hu17 AY530582, Hu6 AY530621, Rh25 AY530557, Pi2 AY530554, Pi1 AY530553, Pi3 AY530555, Rh57

AY530569, Rh50 AY530563, Rh49 AY530562, Hu39 AY530601, Rh58 AY530570, Rh61 AY530572, Rh52 AY530565, Rh53 AY530566, Rh51 AY530564, Rh64 AY530574, Rh43 AY530560, AAV8 AF513852, Rh8 AY242997, Rh1 AY530556 Clade F: Hu14 (AAV9) AY530579, Hu31 AY530596, Hu32 AY530597, Clonal Isolate AAV5 Y18065, AF085716, AAV 3 NC_001729, AAV 3B NC_001863, AAV4 NC_001829, Rh34 AY243001, Rh33 AY243002, Rh32 AY243003/

The skilled person can select an appropriate serotype, clade, clone or isolate of AAV for use in the present invention on the basis of their common general knowledge. It should be understood however that the invention also encompasses use of an AAV genome of other serotypes that may not yet have been identified or characterised. The AAV serotype determines the tissue specificity of infection (or tropism) of an AAV virus. Accordingly, preferred AAV serotypes for use in AAV viruses administered to patients in accordance with the invention are those which have natural tropism for or a high efficiency of infection of rod photoreceptors.

Typically, the AAV genome of a naturally derived serotype or isolate or clade of AAV comprises at least one inverted terminal repeat sequence (ITR). Vectors of the invention typically comprise two ITRs, preferably one at each end of the genome. An ITR sequence acts in *cis* to provide a functional origin of replication, and allows for integration and excision of the vector from the genome of a cell. Preferred ITR sequences are those of AAV2 and variants thereof. The AAV genome typically comprises packaging genes, such as *rep* and/or *cap* genes which encode packaging functions for an AAV viral particle. The *rep* gene encodes one or more of the proteins Rep78, Rep68, Rep52 and Rep40 or variants thereof. The *cap* gene encodes one or more capsid proteins such as VP1, VP2 and VP3 or variants thereof. These proteins make up the capsid of an AAV viral particle. Capsid variants are discussed below.

Preferably the AAV genome will be derivatised for the purpose of administration to patients. Such derivatisation is standard in the art and the present invention

encompasses the use of any known derivative of an AAV genome, and derivatives which could be generated by applying techniques known in the art. Derivatisation of the AAV genome and of the AAV capsid are reviewed in, for example, Choi et al and Wu et al, referenced above.

Derivatives of an AAV genome include any truncated or modified forms of an AAV genome which allow for expression of a Rep-1 transgene from a vector of the invention *in vivo*. Typically, it is possible to truncate the AAV genome significantly to include minimal viral sequence yet retain the above function. This is preferred for safety reasons to reduce the risk of recombination of the vector with wild-type virus, and also to avoid triggering a cellular immune response by the presence of viral gene proteins in the target cell.

Typically, a derivative will include at least one inverted terminal repeat sequence (ITR), preferably more than one ITR, such as two ITRs or more. One or more of the ITRs may be derived from AAV genomes having different serotypes, or may be a chimeric or mutant ITR. A preferred mutant ITR is one having a deletion of a *trs* (terminal resolution site). This deletion allows for continued replication of the genome to generate a single-stranded genome which contains both coding and complementary sequences i.e. a self-complementary AAV genome. This allows for bypass of DNA replication in the target cell, and so enables accelerated transgene expression.

The one or more ITRs will preferably flank the expression construct cassette containing the promoter and transgene of the invention. The inclusion of one or more ITRs is preferred to aid packaging of the vector of the invention into viral particles. In preferred embodiments, ITR elements will be the only sequences retained from the native AAV genome in the derivative. Thus, a derivative will preferably not include the *rep* and/or *cap* genes of the native genome and any other sequences of the native genome. This is preferred for the reasons described above, and also to reduce the possibility of integration of the vector into the host cell genome. Additionally, reducing the size of

the AAV genome allows for increased flexibility in incorporating other sequence elements (such as regulatory elements) within the vector in addition to the transgene. With reference to the AAV2 genome, the following portions could therefore be removed in a derivative of the invention: One inverted terminal repeat (ITR) sequence, the replication (rep) and capsid (cap) genes. However, in some embodiments, including *in vitro* embodiments, derivatives may additionally include one or more *rep* and/or *cap* genes or other viral sequences of an AAV genome.

A derivative may be a chimeric, shuffled or capsid-modified derivative of one or more naturally occurring AAV viruses. The invention encompasses the provision of capsid protein sequences from different serotypes, clades, clones, or isolates of AAV within the same vector. The invention encompasses the packaging of the genome of one serotype into the capsid of another serotype i.e. pseudotyping.

Chimeric, shuffled or capsid-modified derivatives will be typically selected to provide one or more desired functionalities for the viral vector. Thus, these derivatives may display increased efficiency of gene delivery, decreased immunogenicity (humoral or cellular), an altered tropism range and/or improved targeting of a particular cell type compared to an AAV viral vector comprising a naturally occurring AAV genome, such as that of AAV2. Increased efficiency of gene delivery may be effected by improved receptor or co-receptor binding at the cell surface, improved internalisation, improved trafficking within the cell and into the nucleus, improved uncoating of the viral particle and improved conversion of a single-stranded genome to double-stranded form. Increased efficiency may also relate to an altered tropism range or targeting of a specific cell population, such that the vector dose is not diluted by administration to tissues where it is not needed.

Chimeric capsid proteins include those generated by recombination between two or more capsid coding sequences of naturally occurring AAV serotypes. This may be performed for example by a marker rescue approach in which non-infectious capsid

sequences of one serotype are cotransfected with capsid sequences of a different serotype, and directed selection is used to select for capsid sequences having desired properties. The capsid sequences of the different serotypes can be altered by homologous recombination within the cell to produce novel chimeric capsid proteins. Chimeric capsid proteins also include those generated by engineering of capsid protein sequences to transfer specific capsid protein domains, surface loops or specific amino acid residues between two or more capsid proteins, for example between two or more capsid proteins of different serotypes.

Shuffled or chimeric capsid proteins may also be generated by DNA shuffling or by error-prone PCR. Hybrid AAV capsid genes can be created by randomly fragmenting the sequences of related AAV genes e.g. those encoding capsid proteins of multiple different serotypes and then subsequently reassembling the fragments in a self-priming polymerase reaction, which may also cause crossovers in regions of sequence homology. A library of hybrid AAV genes created in this way by shuffling the capsid genes of several serotypes can be screened to identify viral clones having a desired functionality. Similarly, error prone PCR may be used to randomly mutate AAV capsid genes to create a diverse library of variants which may then be selected for a desired property.

The sequences of the capsid genes may also be genetically modified to introduce specific deletions, substitutions or insertions with respect to the native wild-type sequence. In particular, capsid genes may be modified by the insertion of a sequence of an unrelated protein or peptide within an open reading frame of a capsid coding sequence, or at the N- and/or C-terminus of a capsid coding sequence.

The unrelated protein or peptide may advantageously be one which acts as a ligand for a particular cell type, thereby conferring improved binding to a target cell or improving the specificity of targeting of the vector to a particular cell population.

The unrelated protein may also be one which assists purification of the viral particle as part of the production process i.e. an epitope or affinity tag. The site of insertion will typically be selected so as not to interfere with other functions of the viral particle e.g. internalisation, trafficking of the viral particle. The skilled person can identify suitable sites for insertion based on their common general knowledge. Particular sites are disclosed in Choi et al, referenced above.

The invention additionally encompasses the provision of sequences of an AAV genome in a different order and configuration to that of a native AAV genome. The invention also encompasses the replacement of one or more AAV sequences or genes with sequences from another virus or with chimeric genes composed of sequences from more than one virus. Such chimeric genes may be composed of sequences from two or more related viral proteins of different viral species.

The vector of the invention takes the form of a viral vector comprising the promoters and expression constructs of the invention.

The invention also provides an AAV viral particle comprising a vector of the invention. The AAV particles of the invention include transcapsidated forms wherein an AAV genome or derivative having an ITR of one serotype is packaged in the capsid of a different serotype. The AAV particles of the invention also include mosaic forms wherein a mixture of unmodified capsid proteins from two or more different serotypes makes up the viral envelope. The AAV particle also includes chemically modified forms bearing ligands adsorbed to the capsid surface. For example, such ligands may include antibodies for targeting a particular cell surface receptor.

The invention additionally provides a host cell comprising a vector or AAV viral particle of the invention.

Vectors of the invention may be prepared by standard means known in the art for provision of vectors for gene therapy. Thus, well established public domain transfection, packaging and purification methods can be used to prepare a suitable vector preparation.

As discussed above, a vector of the invention may comprise the full genome of a naturally occurring AAV virus in addition to a promoter of the invention or a variant thereof. However, commonly a derivatised genome will be used, for instance a derivative which has at least one inverted terminal repeat sequence (ITR), but which may lack any AAV genes such as *rep* or *cap*.

In such embodiments, in order to provide for assembly of the derivatised genome into an AAV viral particle, additional genetic constructs providing AAV and/or helper virus functions will be provided in a host cell in combination with the derivatised genome. These additional constructs will typically contain genes encoding structural AAV capsid proteins i.e. *cap*, VP1, VP2, VP3, and genes encoding other functions required for the AAV life cycle, such as *rep*. The selection of structural capsid proteins provided on the additional construct will determine the serotype of the packaged viral vector.

A particularly preferred packaged viral vector for use in the invention comprises a derivatised genome of AAV2 in combination with AAV5 or AAV8 capsid proteins.
As mentioned above, AAV viruses are replication incompetent and so helper virus functions, preferably adenovirus helper functions will typically also be provided on one or more additional constructs to allow for AAV replication.

All of the above additional constructs may be provided as plasmids or other episomal elements in the host cell, or alternatively one or more constructs may be integrated into the genome of the host cell.

Pharmaceutical Compositions, Dosages and Treatments

The vector of the invention can be formulated into pharmaceutical compositions. These compositions may comprise, in addition to the vector, a pharmaceutically acceptable excipient, carrier, buffer, stabiliser or other materials well known to those skilled in the art. Such materials should be non-toxic and should not interfere with the efficacy of the active ingredient. The precise nature of the carrier or other material may be determined by the skilled person according to the route of administration, i.e. here direct retinal, subretinal or intravitreal injection.

The pharmaceutical composition is typically in liquid form. Liquid pharmaceutical compositions generally include a liquid carrier such as water, petroleum, animal or vegetable oils, mineral oil or synthetic oil. Physiological saline solution, magnesium chloride, dextrose or other saccharide solution or glycols such as ethylene glycol, propylene glycol or polyethylene glycol may be included. In some cases, a surfactant, such as pluronic acid (PF68) 0.001% may be used.

For injection at the site of affliction, the active ingredient will be in the form of an aqueous solution which is pyrogen-free and has suitable pH, isotonicity and stability. Those of relevant skill in the art are well able to prepare suitable solutions using, for example, isotonic vehicles such as Sodium Chloride Injection, Ringer's Injection, Lactated Ringer's Injection, Hartmann's solution. Preservatives, stabilisers, buffers, antioxidants and/or other additives may be included, as required.

For delayed release, the vector may be included in a pharmaceutical composition which is formulated for slow release, such as in microcapsules formed from biocompatible polymers or in liposomal carrier systems according to methods known in the art.
The vectors and/or pharmaceutical compositions of the invention can be packaged into a kit.

In general, direct retinal, subretinal or intravitreal delivery of vectors of the invention, typically by injection, is preferred. Delivery to the retinal, subretinal space or intravitreal space is thus preferred. Vectors may also be introduced into rod photoreceptors *in vitro* followed by cell transplantation into the retina

The vectors and/or pharmaceutical compositions of the invention can also be used in combination with any other therapy for the treatment or prevention of vision disorders. For example, they may be used in combination with known treatments that employ VEGF antagonists, eg anti-VEGF antibodies such as Bevacizumab or Ranibizumab or soluble receptor antagonists such as Aflibercept, for the treatment of AMD or other eye disorders as discussed herein.

Dosages and dosage regimes can be determined within the normal skill of the medical practitioner responsible for administration of the composition. The dose of a vector of the invention may be determined according to various parameters, especially according to the age, weight and condition of the patient to be treated; the route of administration; and the required regimen. Again, a physician will be able to determine the required route of administration and dosage for any particular patient.

A typical single dose is between 10^{10} and 10^{12} genome particles, depending on the amount of retinal tissue that requires transduction. A genome particle is defined herein as an AAV capsid that contains a single stranded DNA molecule that can be quantified with a sequence specific method (such as real-time PCR). That dose may be provided as a single dose, but may be repeated for the fellow eye or in cases where vector may not have targeted the correct region of retina for whatever reason (such as surgical complication). The treatment is preferably a single permanent treatment for each eye, but repeat injections, for example in future years and/or with different AAV serotypes may be considered.

Treatments

Vectors of the invention may be used to treat any ocular condition in which there is dysfunction, degeneration or absence of cones but at least some healthy rods remain. Cone function may be wholly or partially missing, e.g. at least 10%, at least 25%, at least, at least 50%, at least 75%, at least 80%, at least 90% or more missing. Healthy rods are rods that are capable of performing normal or partial, e.g. at least 10%, at least 25%, at least, at least 50%, at least 75% or at least 90% of normal rod function in terms of perception of light at scotopic levels.

Conditions that can be treated using vectors of the invention thus include macular degeneration, achromatopsia and Leber congenital amaurosis. The macular degeneration may be age-related macular degeneration (AMD), for example wet or neovascular AMD or geographic atrophy, an inherited macular degeneration condition or an inherited cone dystrophy. In some embodiments, the invention will result in the creation of a 'pseudo-fovea', a small patch of cone-like rods that improves vision in conditions in which foveal cones have been lost or are dysfunctional.
In general, patients to be treated with vectors of the invention will be human patients. They may be male or female and of any age.

The following Examples illustrate the invention.

EXAMPLES

Example 1 - Methods for ArchT experiments.

Animals

Wild-type mice (C57BL/6J) were purchased from Harlan Laboratories (Blackthorn, UK). CNGA3-/- and PDE6C-/- mice were bred in house. All mice were maintained under cyclic light (12 h light-dark) conditions; cage illumination was 7 foot-candles

during the light cycle. All experiments were approved by the local Institutional Animal Care and Use Committees (UCL, London, UK) and conformed to the guidelines on the care and use of animals adopted by the Society for Neuroscience and the Association for Research in Vision and Ophthalmology (Rockville, MD).

Plasmid constructions, viral production and injection procedure

The transgene construct (ArchT-EGFP) was kindly provided by Prof Ed Boyden (MIT, USA) and contains the cDNA sequence of the ArchT gene fused to the fluorescent protein EGFP. The plasmids were packaged into AAV8 to generate recombinant AAV viral vectors, AAV8.hRho.ArchT-EGFP. Recombinant AAV8 vector was produced through a triple transient transfection method as described previously. The plasmid construct, AAV serotype-specific packaging plasmid and helper plasmid were mixed with Polyethylenimine (Polysciences Inc.) to form transfection complexes, which were then added to 293T cells and left for 72h. The cells were harvested, concentrated and lysed to release the vector. AAV8 was purified using AVB Sepharose columns (GE Healthcare). Both were washed in 1X PBS and concentrated to a volume of 100–150 μL. Viral particle titres were determined by comparative dot-blot DNA prepared from purified viral stocks and defined plasmid controls. Purified vector concentrations used for all experiments were 5×10^{12} viral particles/ml. Subretinal injections were performed as described previously by our group and consisted of double injections of 2ul each.

Immunohistochemistry

Animals were euthanized, the eyeballs enucleated and cornea, lens and iris removed. For retinal sections, the eyecups were fixed in 4% paraformaldehyde (PFA) for 1 hour at room temperature, before embedding in optimal cutting temperature (OCT) medium. 30μm cryosections were cut in sagittal orientation, rinsed with PBS and blocked in 10% normal goat serum (NGS), 3% bovine serum albumin (BSA) and 0.1% Triton-X100.

The respective samples were incubated with primary antibodies in block solution at 4°C overnight using rabbit anti-cone arrestin (diluted 1:500). Following PBS washes, the respective combination of secondary antibodies (all diluted 1:500, life technologies) including goat anti rabbit Alexa Fluor 546 (#A11035), goat anti mouse Alexa Fluor 633 (#A21052) and streptavidin, Alexa Fluor 633 conjugate (#S21375) were used to label the samples before these were counterstained with DAPI and mounted with DAKO fluorescent mounting media (DAKO, S3023, Denmark). Images were acquired by confocal microscopy (Leica DM5500Q).

Single photoreceptor suction recordings

Animals were dark adapted for 12h prior to the start of experiments. Mice were administered an overdose of ketamine-dormitor anaesthetic mix via the intra- peritoneal cavity, to induce terminal surgical-plane anaesthesia. Mice were then sacrificed by cervical dislocation and enucleated. Eyes were dissected under dim, far-red illumination. Isolated retinas were imbedded in 1% low melting agarose solution and then cut using a vibrotome (leica) into 230um thick en face slices. Slices were mounted in a recording chamber and perfused with carbogen (95% O_2 5% CO_2) saturated Ames medium containing 100µm 9-cis retinal (Sigma) and 0.2% BSA (Sigma). The temperature of the perfusion solution was maintained at 37°C using an in-line heating element under feedback control (Scientifica). Very low resistance (1-2MΩ) patch pipettes were made from filamented boroscilicate glass capillaries (Harvard Apparatus Ltd) using a Narishige PC-10 vertical puller. Pipettes were filled with external solution, mounted onto the headstage and a small pressure applied across the tip (~30mbar). Using infrared illumination and a microscope to aid visualisation the pipette was placed onto the surface of the retina, and then lowered ~50um into the slice, until photoreceptor segments appeared intact and neatly arranged. Slight negative pressure was applied across the pipette tip as it was advanced slowly through the retinal tissue, using a 100ms, 10mV test pulse to monitor resistance across the pipette tip. When resistance increased to ~20-30MΩ light evoked responses were tested. Light stimuli from an LED

light-source (peak wavelength 530nm) coupled to a liquid light guide, were delivered through the microscope objective (Olympus). Neutral density filters were used to precisely control the intensity of the light stimulus. Light stimuli consisted of square wave pulses programmed using P-Clamp software (Molecular Devices), and delivered via a DAC board (Axon Instruments) in conjunction with an LED driver (Thorlabs). Electrophysiological recordings were carried out using a Multiclamp 700B amplifier (Molecular Devices). Data was digitized at 20kHz.

MEA recordings

Animals were dark adapted for 12h prior to the start of experiments. Mice were administered an overdose of ketamine-dormitor anaesthetic mix via the intra- peritoneal cavity, to induce terminal surgical-plane anaesthesia. Mice were then sacrificed by cervical dislocation and enucleated. Eyes were dissected in carbogen (95% Oxygen, 5% Carbon Dioxide) saturated Ames medium (Sigma), under dim red light. The cornea and lens were removed, with care taken to remove as much vitreous from the surface of the retina as possible. The RPE was separated from the retina and a flat petal 1-3 mm across was cut away from the retinal 'cup'. This retinal petal was placed ganglion-cell side down on the surface of the multielectrode array, and a circular harm constructed from unreactive platinum wire (Sigma) and nylon was used to keep the petal in position. Throughout recordings, the tissue was perfused with carbogen saturated Ames medium (Sigma), maintained at a temperature of 36.5 degrees Celsius. For recordings that included scotopic or mesopic conditions, the perfusion medium was made up to include 9-cis retinal (Sigma), at a concentration of 100μM, in 0.2% BSA (Sigma). A perforated 60-electrode recording array, consisting of tungsten electrodes spaced 100 μm apart (Multi Channel Systems) was used to record ganglion cell extracellular potentials. Voltage changes were amplified and digitized at 50kHz by an MC Card system, using MC Rack software (MultiChannel Systems).

Electrophysiological data analysis

Electrophysiological data was analysed using custom-written macros in IgorPro 6. Synaptic currents and potentials were detected using an amplitude threshold algorithm where the threshold for event detection was set at 2 times the standard deviation of the baseline noise (typically about 10pA). Detected currents and potentials were verified manually through careful inspection of all electrophysiological data.

Fear conditioning

Mice were trained and tested using a commercially available fear conditioning system (Med Associates). To ensure blind conditions, the experimenter performing the training and testing was always blind to the strain of mouse and treatment conditions. Briefly, the setup consisted of a conditioning chamber (20x30 cm) with a stainless steel grid floor placed inside a sound-attenuating cubicle. Mouse behaviour was monitored constantly during training and testing by means of a built-in infrared digital video camera (30 frames/s acquisition rate) and infrared illumination. Video Freeze software (Med Associates) was used to control delivery of the light stimulus and shock. The light stimulus consisted of a single LED (530 nm, Thorlabs) 5 Hz 50ms full-brightness flicker generated via an Arduino interface (Arduino Software) positioned on a side panel of the conditioning chamber. To ensure that the context in which training and testing took place were different, floor and curved wall panels were inserted into the chamber for the testing session. A background white light was used to reduce chances of rod activation and pupils were dilated with Tropicamide drops to increase the amount of light reaching the mouse retina.

Mice were placed inside the chamber and underwent one conditioning session, consisting of 6 pairings of a 5 s, light stimulus that co-terminated with a 2 s, 0.65 mA foot shock. Inter-trial interval was pseudo-randomized (average interval 90 s). Following the training session mice were returned to the home cage. 24 hours after training, mice were tested for visually cued memory recall. Mice were placed in the test

chamber and monitored for a total of 360 s. The conditioning light stimulus was presented continuously for the last 120 s of the test session. All data was acquired and scored automatically by VideoFreeze software (Med Associates). Briefly, the software is calibrated before placing the animal in the chamber. The software then measures the pixel changes that take place between every video frame. The motion threshold was set to be as low as possible (20 motion index units), and the continuous freezing count was set to the frame rate to ensure the most sensitive read-out of motion. To assess light cued memory recall the percentage time of freezing behaviour was averaged for the two minutes immediately prior to and following the light stimulus onset. Statistical significance was assessed with a one-way ANOVA. Results are presented as mean ± S.E.M.

Optomotry

Visual acuities were measured by observing the optomotor responses of mice to rotating sinusoidal gratings (OptoMotry, Cerebral Mechanics). The protocol used yields independent measures of the acuities of right and left eyes based on the unequal sensitivities of the two eyes to pattern rotation as only motion in the temporal-to-nasal direction evokes the tracking response. As a result, the right and the left eyes are most sensitive to counter-clockwise (CCW) and clockwise (CW) rotations, respectively. Stimuli of different temporal frequency were used to determine the threshold at which a response was present. A double-blind two-alternative forced choice procedure was employed, in which the observer was 'blind' to the direction of pattern rotation, to whether it was an ArchT-treated or untreated *CNGA3-/- or PDE6C-/-* mouse or age-matched wild-type control animal (C57BL6). Visual acuity was measured in both eyes of the tested animal and averaged or separately analyzed for each eye after 4 trials were conducted on 4 separate days. The measurement was carried out on injected mice 3-10 weeks after treatment together with age-matched isogenic controls.

Example 2 - ArchT expression in rod photoreceptors confers the ability to respond with rapid non-bleaching responses

Rod-mediated vision is optimized for low light levels, including single photon detection. However, rods cannot match the rapid onset and recovery of cone responses to light (Fu et al., 2007, Pugh et al., 1999). This functional difference, useful to ensure reliable vision in different environments, becomes debilitating when cone-mediated vision is lost in conditions such as in age-related macular degeneration, when the densely packed cones in the fovea degenerate (de Jong 2006). It was investigated whether if rods could respond and recover more quickly to stimuli, this would help alleviate the functional impairment caused by the loss of cones.

A fast light-driven proton pump (ArchT) (Han et al., 2011) was expressed in rod photoreceptors. AAV8 particles carrying ArchT-EGFP under control of the Rhodopsin promoter (Rho) were injected subretinally in adult mice. Expression of Rho-ArchT-EGFP was limited to the membrane of rod photoreceptors (Figures1a-b). Synaptic terminals of rods expressing Rho-ArchT-EGFP and cones could be easily distinguished following immunohistochemistry (Figure 1c). Quantitative PCR on a sorted population of cones confirmed that Rho-ArchT-EGFP expression was specific to the rod population and no evident sign of toxicity was observed up to 6 months following AAV8 injection. Expression of ArchT allowed extremely rapid light responses, while the intrinsic rod response was preserved and was comparable to that observed in non-transduced rod photoreceptors (Figure 1d). Light-evoked currents recorded from ArchT-expressing rods demonstrated considerably faster kinetics than the intrinsic rod currents in all mouse models tested (Figure 2a-b). These kinetics allowed light evoked currents to be modulated up to 80 Hz, far above the limits of both rods, which faltered at ~20 Hz (Figure 2a-c), and of cones (Fu et al., 2007).

Surprisingly, ArchT expression did not alter the properties of rod photoreceptors while conferring the ability to respond with rapid non-bleaching responses (Figure 2e).

Example 3 - ArchT-expressing rods drive sustained RGC spiking at high light intensities and at frequencies approaching those of cone photoreceptors

It was next investigated whether the circuitry driven by rods would be able to follow faster-than-normal rod-driven vision. Rod and cone pathways present some similarities and some striking differences and it is therefore not clear whether the rod circuitry can reliably sustain fast 'cone-like' transmission (Wässle et al., 2004). Rods have been shown to contact OFF 'cone' bipolar cells directly (Soucy et al., 1998 and Hack et al., 1999) and paired-pulse stimulation suggests that this alternative pathway may be as fast as the cone-to-OFF-bipolar one (Li et al., 2010). However, it is not clear how sustained this response can be and whether rod (ON) bipolar cells can also sustain fast transmission. Furthermore, rod synaptic terminals have different size and ultra-structural organization compared to cones and rod bipolar cells do not contact Retinal Ganglion Cells (RGCs) directly but only through a pathway involving AII amacrine cells (Wässle et al., 2004). To investigate the maximal speed that the rod pathway can achieve, multi-electrode recordings from RGCs in mouse models lacking cone function were performed, to isolate rod-mediated RGC output. Rod-driven responses in RGCs in non-transduced retinas were bleached at high light levels and could not follow stimulation frequencies higher than ~20 Hz (Figure 2f).

On the contrary, ArchT-expressing rods drove sustained RGC spiking at high light intensities and at frequencies approaching those of cone photoreceptors (Figure 2f).

Example 4 - expression of Rho-ArchT-EGFP extended the sensitivity of mice lacking cone-mediated vision to bright light stimuli

For this faster-than-normal rod vision to be useful, it was reasoned that mice should be able to use ArchT-mediated currents to reliably respond to bright and fast stimuli. CNGA3$^{-/-}$ and PDE6C$^{-/-}$ mice lacking cone-mediated vision (Biel et al., 1999 and

Change et al., 2009) failed to learn a fear conditioning paradigm where bright light stimuli were paired and co-terminated with a mild foot shock (Figure 3a). However, expression of Rho-ArchT-EGFP extended the sensitivity of these mice to bright light stimuli, allowing learning of the association between visual stimulus and shock (Figure 3a). Finally, it was tested whether ArchT expression conferred fast vision to CNGA3$^{-/-}$ and PDE6C$^{-/-}$ mice. Assessment of the speed of vision by means of Optomotor testing (Umino et al., 2008) showed that ArchT-expressing mice were able to follow stimuli faster than mice that did not undergo subretinal viral injections and mice that received a GFP-only vector (Figure 3b). The maximal frequency of stimuli that ArchT-expressing mice could follow was similar to that of cone photoreceptors (Figure 3b).

Together, these results show that rods can be driven faster than by their intrinsic photo-transduction cascade and that rod-driven circuits can sustain a faster signalling. Importantly, synaptic release from rods does not require large voltage fluctuations, but small currents can instead cause sufficient voltage variations to significantly alter their synaptic transmission (Cangiano et al., 2012). This extends the use of the Invention to light levels several-fold lower than the average light levels required for optogenetic manipulation of activity in most other neurons (Han et al., 2011).

Example 5 - Methods for RPAP experiments

Animals

C57BL6 (Harlan, UK), *Cnga3-/-* (J.R. Heckenlively, University of Michigan), *Pde6c-/-* (J.R. Heckenlively, University of Michigan, MI) (Chang et al., 2009), and *Gnat1-/-* (J. Lem, Tufts University School of Medicine, MA) (Calvert et al., 2000) mice were maintained in the animal facility at University College London. Adult male and female animals were 6-12 weeks old at the time of viral injection and were used for experiments at least 2 weeks after the injection to allow for a sufficient expression of

R9AP. All the mice used were between ages of 2 to 6 months and were age matched between groups of a given experiment. All experiments have been conducted in accordance with the Policies on the Use of Animals and Humans in Neuroscience Research and with the ARVO Statement for the Use of Animals in Ophthalmic and Vision Research. Animals were kept on a standard 12/12 hour light-dark cycle

Plasmid constructions and production of recombinant AAV8

The murine *R9ap* cDNA was PCR amplified from murine retinal cDNA using primers which have been designed to encompass the whole of the coding region. The *R9ap* cDNA was cloned between the promoter (CMV promoter or bovine rhodopsin promoter) and the SV40 polyadenylation site. These plasmids were used to generate two pseudotyped AAV2/8 viral vectors, rAAV2/8.CMV.mR9ap and rAAV2/8.Rho.mR9ap, as described below.

Recombinant AAV2/8 vector was produced through a triple transient transfection method as described previously (Gao et al., 2002). The plasmid construct, AAV serotype-specific packaging plasmid and helper plasmid were mixed with polyethylenimine to form transfection complexes which was then added to 293T cells and left for 72 h. The cells were harvested, concentrated and lysed to release the vector. The AAV2/8 was purified by affinity chromatography and concentrated using ultrafiltration columns (Sartorius Stedim Biotech, Goettingen, Germany), washed in PBS and concentrated to a volume of 100–150 µl. Viral particle titres were determined by dot-blot or by real-time PCR. Purified vector concentrations used were 1-2 $\times$ 10^{12} viral particles/ml.

Electroretinogram (ERG)

ERGs were recorded from both eyes after mice were dark adapted overnight using a commercially available system (Espion E2, Diagnosys LLC, Lowell, MA). The animals

were anesthetized with an intraperitoneal injection of a 0.007 ml/g mixture of medetomidine hydrochloride (1 mg/ml), ketamine (100 mg/ml), and water at a ratio of 5:3:42 before recording. Pupils were fully dilated using 2.5% phenylephrine and 1.0% tropicamide. Midline subdermal ground and mouth reference electrodes were first placed, followed by positive silver electrodes that were allowed to lightly touch the center of the corneas under dim red illumination. A drop of Viscotears 0.2% liquid gel (Dr. Robert Winzer Pharma/OPD Laboratories, Watford, UK) was placed on top of the positive electrodes to keep the corneas moistened during recordings and the mouse was allowed to further dark-adapt for 5 minutes. Bandpass filter cutoff frequencies were 0.312 Hz and 1000 Hz. Recovery speed of photoresponse was measured using paired flash paradigm where pairs of flashes with identical saturating intensity (1.8 log.cd.s/m^2) separated by various inter-stimulus intervals (ISI; 0.5, 1, 2, 4, 8, 16, 32, 64 sec) were presented. In this paradigm, the 1st flash would completely suppress the electric responses of rod mechanisms which allow observation of the speed of functional recovery of the rod function by presenting 2nd flash with different ISI. Sufficient amount of time (150 sec) were provided between pairs of flashes to allow full recovery of the 1st flash. Then the recovery of a-wave amplitude observed should reflect the speed of deactivation of the rods in animals devoid of cone function since the flash should only bleach a fraction (0.02%) of the rhodopsin (Lyubarsky et al., 2004 and Weymouth, A.E. & Vingrys 2008). Scotopic 6 Hz flicker intensity series were performed as previously reported with a few modifications (Seeliger et al., 2001). 17 steps of flash intensities were used ranging from -6 to 2 log.cd.s/m^2 each separated by 0.5 log unit. For each step, after 10 seconds of adaptation, 600 msec sweeps were averaged 20 times using the same flash condition. Series of dark-adapted responses were also obtained using longer flashes with durations of 20, 100, and 200 msec all at 83.3 cd/m^2. Standard single flash scotopic recordings were obtained from dark-adapted animals at the following increasing light intensities: -6, -5, -4, -3, -2, -1, 0, 1.0, 1.5, and 1.9 log.cd.s/m^2. Photopic flash recordings were performed following 5 min light adaptation intervals on a background light intensity of 20 cd/m^2, which was also used

as the background light for the duration of the recordings. Photopic light intensities used were -2, -1, 0, 1, 1.5, and 1.9 log.cd.s/m^2.

Histology

Six weeks after unilateral subretinal injection of rAAV2/8.Rho.mR9ap, both eyes from a *Cnga3-/-* mouse were quickly removed and snap frozen in liquid nitrogen. After cryoembedding the eye in OCT (RA Lamb, Eastborne, UK), the eyes were cut as transverse sections 15 μm thick and were air-dried for 15 - 30 min. For immunohistochemistry, sections were pre-blocked in PBS containing normal donkey serum (2%), bovine serum albumin (2 %) 1 hr before being incubated with anti-RGS9 antibody (1:500; Santa Cruz Biotechnology, SantaCruz, CA) for 2 hours at room temperature. After rinsing 2 x 15 min with PBS, sections were incubated with the appropriate Alexa 546-tagged secondary antibody (Invitrogen, Carlsbad, CA) for 2 hrs at room temperature (RT), rinsed and counter-stained with Hoechst 33342 (Sigma-Aldrich, Gillingham, UK). Retinal sections were viewed on a confocal microscope (Leica TCS SP2, Leica Microsystems; Wetzlar, Germany).

Western blotting

The eyes from a *Cnga3-/-* mouse 4 weeks after unilateral subretinal injection of rAAV2/8.Rho.mR9ap were collected. After separating the neural retina from the RPE/choroid/sclera complex, tissues were homogenized in RIPA buffer and left on ice for 20 minutes. The samples were centrifuged at 16,000 g for 30 minutes at 4 °C and stored in -20°C until use. Western blotting was carried out using known protocols.

Optomotor responses and contrast sensitivity function

Contrast sensitivities and visual acuities of treated and untreated eyes were measured by observing the optomotor responses of mice to rotating sinusoidal gratings

(OptoMotry™, Cerebral Mechanics, Lethbridge, AB Canada). The protocol used yields independent measures of the acuities of the right and the left eyes based on unequal sensitivities of the two eyes to pattern rotation: the right and the left eyes are driven primarily by counter-clockwise and clockwise rotations, respectively (Douglas et al., 2005). A mouse was placed on a small island isolated from the floor in a closed space surrounded by 4 monitors with rotating sinusoidal grating with a mean illuminance of 62 cd/m^2. A double-blind two-alternative forced choice procedure was employed, in which the observer was 'blind' to the direction of pattern rotation, to whether it was a treated or untreated *Cnga3-/-* mouse or age-matched wild-type control animal (C57BL6). The contrast sensitivity measured at 0.128, 0.256, 0.383, 0.511 cycles/degree presented at 6 Hz was defined as 100 divided by the lowest percent contrast yielding a threshold response. Both eyes of each mouse were tested four times on independent days. The data was projected on to a Campbell-Robson Contrast Sensitivity Chart with sinusoidal gratings representing relative spatial frequencies.

Rhodopsin measurement

After fully dark-adapting the mice overnight, the mice were anaesthetized and the pupils were fully dilated to assess the speed of visual pigment bleaching. Then the mice were placed in a light box with a light source (7.0 mW) directly illuminating the eye for 5 minutes before the eyes were collected. In another experiment, mice were exposed to an identical condition as that for measuring contrast sensitivity for various durations (0, 30 60, 120 minutes). The mouse eyes were removed at each time point and placed in 250 µl of phosphate buffered saline and snap frozen in liquid nitrogen in a light tight tube and kept at -20 °C until use. Some eyes were collected in the dark under red illumination after overnight dark-adaptation of the mice. Spectrophotometric measurement of rhodopsin were performed as previously reported with minor modifications (Douglas et al., 1995). In brief, the samples were thawed at room temperature and homogenized. This and all subsequent operations were performed under dim red illumination that bleaches the visual pigments minimally. Fifty

microliters of n-dodecyl β-D-maltoside (200 mM; Sigma-Aldrich, St. Louis, MO) was added to every sample and the resulting mixture rotated for 2 h at room temperature, followed by 10 min centrifugation (23,000 g) at 4°C. The supernatant was removed and placed in a quartz cuvette in a Shimadzu UV-2101PC spectrophotometer (Shimadzu, Kyoto, Japan). After an initial scan of the unbleached extract from 300 nm to 700 nm, the sample was exposed to monochromatic light (502 nm) for 3 minutes, shown to be enough to completely bleach rhodopsin (Longbottom et al., 2009), and rescanned. All absorption spectra were zeroed at 700 nm. Difference spectra were constructed using the pre- and post-bleach curves and the maximum optical densities at ~ 500 nm determined, representing the amount of the extracted visual pigment.

Example 6 - R9AP over-expression in rods and increased speed of photoreceptor deactivation

RGS9, Gβ5, and R9AP are obligate members of the regulatory GTPase complex. To study the effect of AAV-mediated R9AP over-expression on the GTPase complex in the rods, the level and distribution of RGS9 was examined following subretinal injection of rAAV2/8.Rho.mR9ap in *Cnga3-/-* mice. These mice have normal rod function but absent cone function and serve as a model of achromatopsia. Four weeks later, treated retina showed increased immunoreactivity against RGS9 throughout the photoreceptor layer in the treated compared to the untreated retinas (Figure 4A). Westernblot analysis further confirmed the increased RGS9 protein expression in the treated retina (Figure 4B). These results indicated that the over-expression of R9AP using AAV2/8 effectively increased the level of catalytic component RGS9 and the GTPase complex.

Next the functional effect of AAV2/8-mediated R9AP over-expression on rod phototransduction was studied by applying paired-flash ERG (Lyubarsky and Pugh 1996). In this paradigm, a pair of identical flash intensity is delivered with a variable inter-stimulus interval and the recovery of the second response relative to the first is

measured. In the rod photoreceptor pathway, the speed of the a-wave (originating from photoreceptors) recovery is dependent on the speed of the deactivation. It was found that the time constant (σ) for 50% recovery of a-wave amplitude was reduced by ~60% in the *Cnga3-/-* eyes injected with rAAV2/8.CMV.mR9ap (σ = ~ 2.99 sec) compared to the untreated eyes (σ = ~ 7.38 sec; Figure 4C). Similarly, an increased speed of a-wave recovery was observed using rhodopsin promoter (rAAV2/8.Rho.mR9ap; σ = ~ 2.74 sec; Figure 4C) in the same mouse line (*Cnga3-/-*) or the same virus (rAAV2/8.CMV.mR9ap) in another cone-defective mouse line (Pde6c-/-; Figure 8). These observations indicated that the subretinal injection of rRAAV2/8.CMV.mR9ap or rAAV2/8.Rho.mR9ap can significantly increase the deactivation speed of the rod phototransduction through increasing the level of RGS9 and GTPase complex.

Example 7 - "Photopic shift" of rod function by over-expression of R9AP

To investigate if an increased deactivation speed achieved by overexpression of R9AP and GTPase complex in the rods could alter the operating range of the photoreceptor function, dark-adapted 6 Hz flicker ERGs were recorded using incremental flash intensities. The eyes treated with rAAV2/8.CMV.mR9ap or rAAV2/8.Rho.mR9ap showed increased responses to brighter flashes compared to the untreated eyes. This resulted in an elevation the upper threshold of the response by up to ~2 log units (Figure 5A), with little effect on the maximal photoresponse (151 ± 17 μV in the treated vs 162 ± 29 μV in the untreated eyes; average ± standard error of the mean). As expected, this "photopic shift" in the operating range of the rods was accompanied by a reciprocal elevation the lower threshold of the response by up to ~1.5 log units. Meanwhile, upper threshold of ERG responses of wild-type eyes and *Gnat1-/-* eyes, both with functional cones, were elevated by ~4.0 log units compared to that of the untreated *Cnga3-/-* eyes. Similar results were obtained when rAAV2/8.Rho.mR9ap was injected into *Pde6c-/-* mice (Figure 9). As a consequence, the treatment allowed the rods to respond to flashes of longer durations (Figure 5B) and to flashes under a cone-isolating background

illumination (Figure 5C). These include conditions where the untreated rods showed virtually no response.

Taken together, these results established that R9AP-over expression in rods results in their desensitization and endows the cells to gain photopic function in exchange for scotopic function. This therapeutic induction of "photopic shift" of the rod function lasted at least for 5 months without overt evidence of retinal degeneration (Figure 10). Meanwhile, the treatment of wildtype mice using the same viral vectors failed to show a measurable change in retinal function (Figure 11).

Example 8 - Rod bipolar pathway accommodates the transmission of altered rod function.

This work has established that an overexpression of R9AP in rods results in faster photoreceptor deactivation kinetics and allows the neuron to respond to larger amount of photons. Meanwhile, the accelerated deactivation should also result in a shorter duration of the neurotransmitter release at the photoreceptor synaptic terminal. Therefore, it was assessed whether the down-stream rod bipolar signaling is affected by the treatment. First the speed and the extent of transmission of signals from the photoreceptors to the bipolar cells to a short single flash was studied by measuring the implicit time and amplitudes of the a-wave (originating from the photoreceptors) and b-wave (originating from the bipolar cells) using ERG (Figure 6a). Overall, slightly smaller but a nearly identical intensity-response curve was observed for the treated and the untreated eyes for both a-wave and b-wave. The small difference observed may reflect either the true consequence of accelerated photoreceptor deactivation or merely the neural damage induced by the subretinal injection. The a-wave implicit time marks the point at which the bipolar cell-driven b-wave becomes detectable. We also observed a small delays in the a-wave and the b-wave implicit times, indicating a modest delay exists in the transmission of neural signals from photoreceptors to bipolar cells. Nevertheless, a relatively large variation of ERG responses between individuals

indicate a small delay or reduction in rod response do not necessarily translate into visual dysfunction (Birch and Anderson 1992).

Therefore, these results indicated that, in principle, the bipolar cells almost fully accommodate the alteration of photoreceptor function and, importantly, display an appropriate dose-response relationship.

Example 9 - R9ap over-expression results in improved Contrast Sensitivity Function

Next, it was asked if the "photopic shift" of the rod function by R9AP over-expression were consequently translated into improved visual performance under light by measuring optokinetic response to rotating sinusoidal gratings under the brightest recording condition possible with a standard computer monitor (62 cd/m^2) (Carvalho et al., 2011). The unique advantage of this behavioral test is that visual function of each eye can be studied separately; the function of the right eye can be probed by responses to counterclockwise (CCW) gratings and the left eye by clockwise (CW) stimuli (Douglas et al., 2005). The spatial contrast sensitivity function (CSF) was studied with a fixed temporal frequency of 6.0 Hz and found that *Cnga3-/-* mice had reduced CSF compared to the wildtype mice (Figure 7). CSF, a function of contrast sensitivity and visual acuity, displayed the estimate range of visual perception (animals could presumably perceive the gratings under the curve but not above; Figure 7A). Intriguingly, an 8.0-fold (P = 0.005) and 5.4-fold (P = 0.011) increase in the sensitivity using gratings of both 0.128 and 0.256 cycles/degree (c/d), respectively, was observed when contrast sensitivity of the treated and the untreated eyes were compared (Figure 7A left panel). No clear alteration of contrast sensitivity was observed for gratings of 0.383 (P = 0.056) and 0.511 (P = 0.111) c/d. Interestingly, the average sensitivity of the treated eye in *Cnga3-/-* mice exceeded that of the wild-type controls with normal cone function. However, when wild-type mice were treated with the same viral

construct, CSFs were not different between the treated and the untreated eyes (Figure 12).

Having established that R9AP overexpression results in gain of visual performance when viewing maximally bright monitor settings, it was sought to determine if this gain-of-vision is sustainable. This is of a valid concern considering that the regeneration of visual pigment in rods is known to be considerably slower than that of the cones (Wang and Kefalov 2011). First, it was assessed if the treatment results in alteration in the speed of visual pigment bleaching. It was found that an exposure of the treated and untreated eyes to a bright light for 5 minutes did not yield any difference in the levels of residual bleachable visual pigment (Figure 7B lower left panel). Second, the amount of bleachable rhodopsin in the eye was studied after exposing the *Cnga3-/-* mice for a variable amount of time to the same experimental condition carried out for CSF measurement. The results showed that visual pigment level remained stable without evidence of reduction throughout 2 hours' exposure to the visual stimuli similarly for the treated and the untreated eyes (Figure 7B lower right panel). These results indicated that the gain of visual perception in the treated *Cnga3-/-* mice is supported by sufficient supply of rhodopsin molecules and is sustainable.

REFERENCES

Curcio, C.A., *et al. The Journal of comparative neurology* **292**, 497-523 (1990).

Dryja, T.P. *American journal of ophthalmology* **130**, 547-563 (2000).

Hess, R.F. & Nordby, K. *The Journal of physiology* **371**, 365-385 (1986).

Nishiguchi, K.M., *et al. Human mutation* **25**, 248-258 (2005).

Kohl, S., *et al. Nature genetics* **19**, 257-259 (1998).

Chang, B. *et al. P.N.A.S* **106**, 19581-19586 (2009).

Thiadens, A.A., *et al. American journal of human genetics* **85**, 240-247 (2009).

Burns, M.E. & Pugh, E.N. *Biophys J* **97**, 1538-1547 (2009).

Burns, M.E. & Pugh, E.N. *Physiology* **25**, 72-84 (2010).

Baseler, H.A., *et al. Nature neuroscience* **5**, 364-370 (2002).

Martemyanov, K.A. & Arshavsky, V.Y. *Prog Mol Biol Transl* **86**, 205-227 (2009).

Krispel, C.M., *et al. Neuron* **51**, 409-416 (2006).

Cowan, C.W., *et al. P.N.A.S.* **95**, 5351-5356 (1998).

Zhang, X., Wensel, T.G. & Kraft, T.W. *The Journal of neuroscience: the official journal of the Society for Neuroscience* **23**, 1287-1297 (2003).

Nishiguchi, K.M., *et al. Nature* **427**, 75-78 (2004).

Michaelides, M., *et al. Ophthalmology* **117**, 120-127 e121 (2010).

Han, X. *et al. Front Syst Neurosci.* **5**, 18 (2011).

Busskamp, V., *et al. Science* **329**, 413-417 (2010).

Fu, Y., Yau, K.W. *Pflugers Arch.* **454**, 805-819 (2007).

Pugh, E.N. Jr *et al. Curr Opin Neurobiol.* **9**, 410-418 (1999).

de Jong, P.V.T.M. *N Engl J Med* **355**, 1474-1485 (2006).

Wässle, H. *Nat Rev Neurosci.* **5**, 747-757 (2004).

Soucy, E. *et al. Neuron* **21**, 481-493 (1998).

Hack, I. *et al. P.N.A.S.* **96**, 14130-14135 (1999).

Li, W. *et al. Nat Neurosci* **13**, 414-416 (2010).

Biel, M. *et al. P.N.A.S.* **96**, 7553-7557 (1999).

Umino, Y. *et al. J Neurosci* **28**, 189-198 (2008).

Cangiano, L. *et al. J Physiol.* **590**, 3841-3855 (2012).

Berndt, A. *et al. Science* **344**, 420-424 (2014).

Wietek, J. *et al. Science* **344**, 409-412 (2014).

Calvert, P.D. *et al. P.N.A.S* **97**, 13913-13918 (2000).

Gao, G.P. *et al. P.N.A.S* **99**, 11854-11859 (2002).

Lyubarsky, A.L., *et al. Vision research* **44**, 3235-3251 (2004).

Weymouth, A.E. & Vingrys, A.J. *Progress in retinal and eye research* **27**, 1-44 (2008).

Seeliger, M.W., *et al. Nature genetics* **29**, 70-74 (2001).

Douglas, R.M., *et al. Visual neuroscience* **22**, 677-684 (2005).

Douglas, R.H., *et al. Journal of Comparative Physiology a-Sensory Neural and Behavioral Physiology* **177**, 111-122 (1995).

Longbottom, R., *et al. P.N.A.S.* **106**, 18728-18733 (2009).

Lyubarsky, A.L. & Pugh, E.N., Jr. *The Journal of neuroscience : the official journal of the Society for Neuroscience* **16**, 563-571 (1996).

Birch, D.G. & Anderson, J.L. *Archives of ophthalmology* **110**, 1571-1576 (1992).

Carvalho, L.S., *et al. Human molecular genetics* **20**, 3161-3175 (2011).

Wang, J.S. & Kefalov, V.J. Progress in retinal and eye research 30, 115-128 (2011).

Taylor, A. W., Ocular immune privilege, Eye, 23, 1885-1889 (2009).

Natkunarajah, M. et al., Assessment of ocular transduction using single-stranded and self-complementary recombinant adeno-associated virus serotype 2/8, Gene Ther. 15, 463-467 (2008).

Choi, V. W. *et al.,* AAV hybrid serotypes: improved vectors for gene delivery, *Curr. Gene Ther.*, **5,** 299-310 (2005).

Wu, Z. *et al.,* Adeno-associated virus serotypes: vector toolkit for human gene therapy, *Mol. Ther.,* **14,** 316-327 (2006).

Chuong, A.S. *et al.,* Non-invasive optical inhibition with a red-shifted microbial rhodopsin, *Nat Neurosci.,* **17**, 1123-1129 (2014).

CLAIMS

1. A vector comprising a nucleic acid encoding a gene product that is light-sensitive and/or that modulates endogenous light-sensitive signalling in a photoreceptor cell, for use in a method of improving vision in a patient with cone photoreceptor dysfunction and/or degeneration by introduction of said nucleic acid into healthy rod photoreceptors in the retina of the patient and expression of said gene product therein, such that the range of light intensities to which the rod photoreceptor responds is extended and/or the speed at which the rod photoreceptor responds to light is increased.

2. A vector for use according to claim 1 wherein the nucleic acid encodes a protein that changes membrane conductance in a way that results in rod hyperpolarisation (outward current flow) upon light stimulation.

3. A vector for use according to claim 2 wherein the nucleic acid encodes (a) a light-sensitive or light-gated G-coupled membrane protein, ion channel, ion pump or ion transporter (b) a member of the RGS9 complex, or (c) another protein that increases the speed of the endogenous rod signalling mechanism.

4. A vector for use according to claim 3 wherein the light-gated molecule is ArchT, Jaws (cruxhalorhodopsin), iC1C2, or the member of the RGS9 complex is R9AP.

5. A vector for use according to any one of the preceding claims which is a viral vector.

6. A vector for use according to claim 5 which is an adeno associated virus (AAV) vector.

7. An AAV vector for use according to claim 6 whose capsid is derived from AAV8.

8. An AAV vector for use according to claim 6 or 7 whose genome is derived from AAV2.

9. A vector for use according to any of the preceding claims wherein the patient suffers from macular degeneration, achromatopsia or Leber congenital amaurosis.

10. A vector for use according to claim 9 wherein the macular degeneration is age-related macular degeneration (AMD), an inherited macular degeneration condition or an inherited cone dystrophy.

11. A vector for use according to claim 10 wherein the AMD is wet or neovascular AMD or geographic atrophy.

12. A vector for use according to any of the preceding claims wherein rod photoreceptor signalling is extended into the mesopic and/or photopic illumination range.

13. A vector for use according to any of the preceding claims wherein the rods exhibit improved modulation strength and/or faster activation/inactivation kinetics.

14. A vector for use according to any of the preceding claims wherein the vector is introduced into rod photoreceptors in vitro followed by transplantation into the retina.

15. A vector for use according to any of the preceding claims wherein the mesopic and/or photopic vision of the patient is improved.

16. A vector for use according to any of the preceding claims wherein the nucleic acid is expressed under the control of a photoreceptor-specific or photoreceptor-preferred promoter.

17. A vector for use according to claim 16, wherein said photoreceptor-specific or photoreceptor-preferred promoter is a rod-specific or rod-preferred promoter.

18. A vector for use according to claim 17 wherein the nucleic acid is expressed under the control of a Rhodopsin (Rho), Neural retina-specific leucine zipper protein (NRL) or Phosphodiesterase 6B (PDE6B) promoter.

19. An expression cassette comprising a nucleic acid as defined in any one of claims 1 to 4, operably linked to a rod-specific or rod-preferred promoter as defined in claim 17 or 18.

20. A vector comprising an expression cassette according to claim 19.

21. A vector according to claim 20 which is a viral vector as defined in any one of claims 5 to 8.

22. A host cell comprising a vector according to claim 20 or 21.

23. Use of a vector as defined in any one of claims 1 to 8, 16, 17, 19 or 20 in the manufacture of a medicament for the improvement of vision as defined in any one of claims 1 or 9 to 15.

24. A method of improving vision in a patient with cone photoreceptor dysfunction by introducing into healthy rod photoreceptors in the retina of the patient a nucleic acid encoding a light-sensitive gene product and expression of said gene product therein, such that the range of light intensities to which the rod photoreceptor responds is extended and/or the speed at which the rod photoreceptor responds to light is increased.

25. A method according to claim 24 wherein the vector is as defined in any one of claims 1 to 8, 16, 17, 19 or 20.

26. A method according to claim 23 or 24 wherein vision is improved as defined in any one of claims1 or 9 to 15.

Fig. 1a

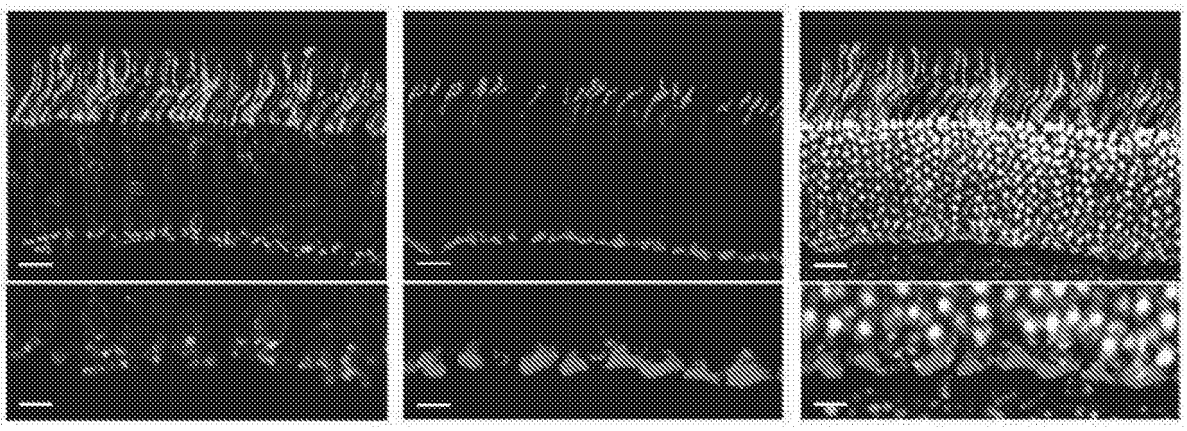

Fig. 1b

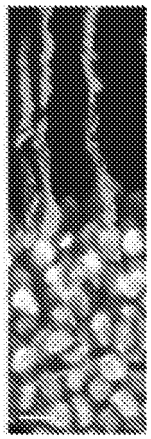

Fig. 1c

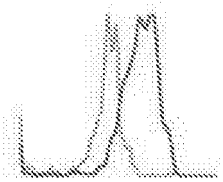

Fig. 1d

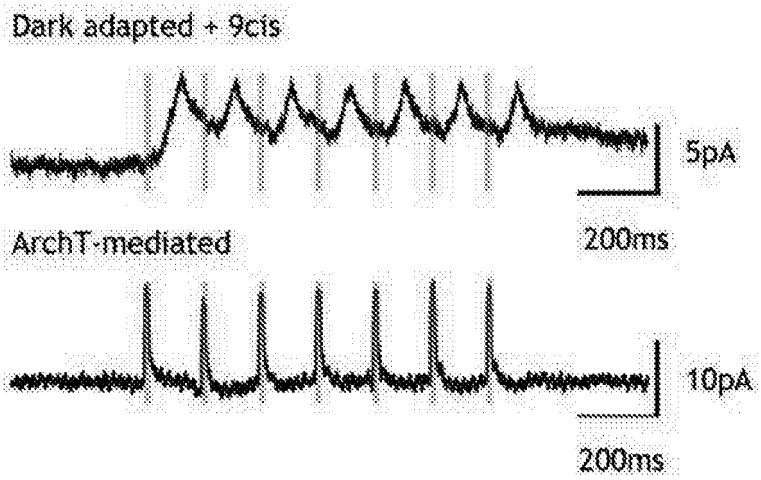

Fig. 2a

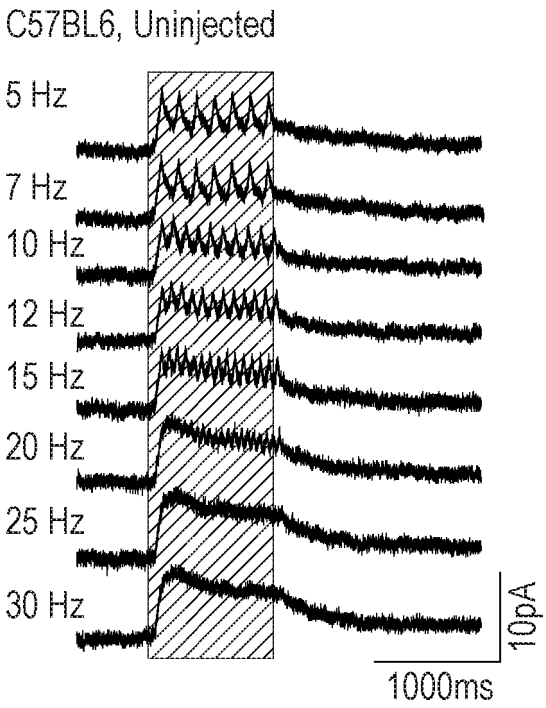

Fig. 2b

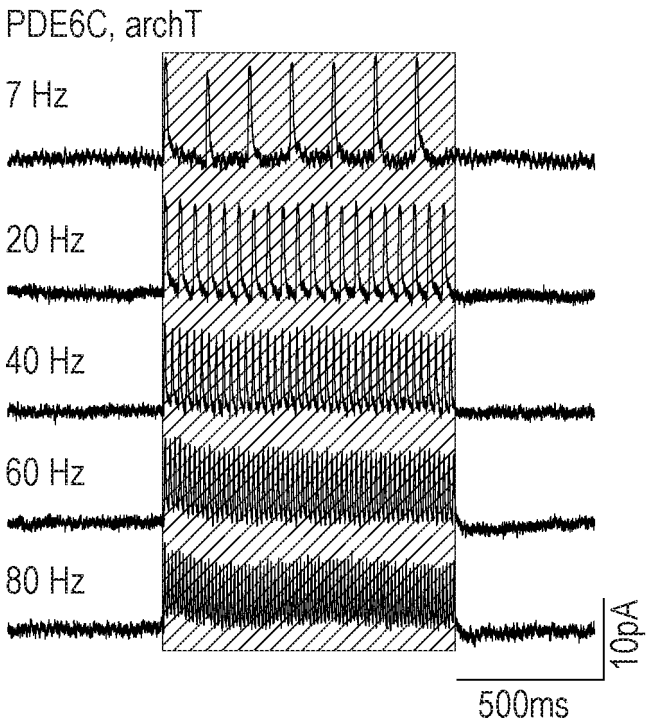

Fig. 2c

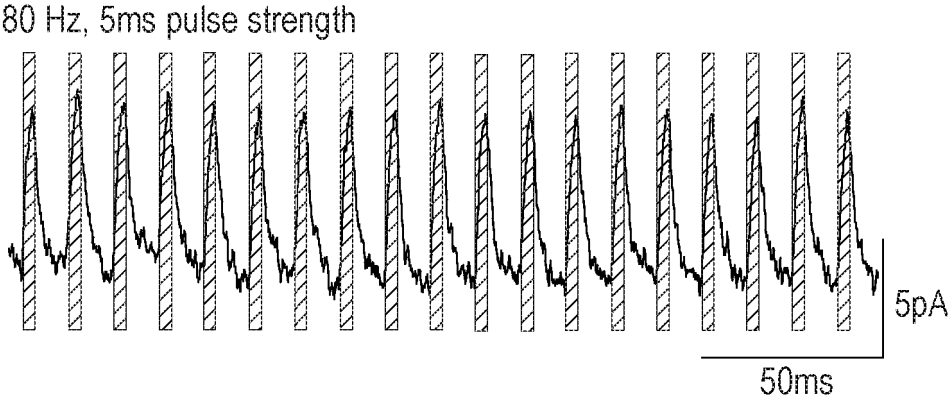

Fig. 2d

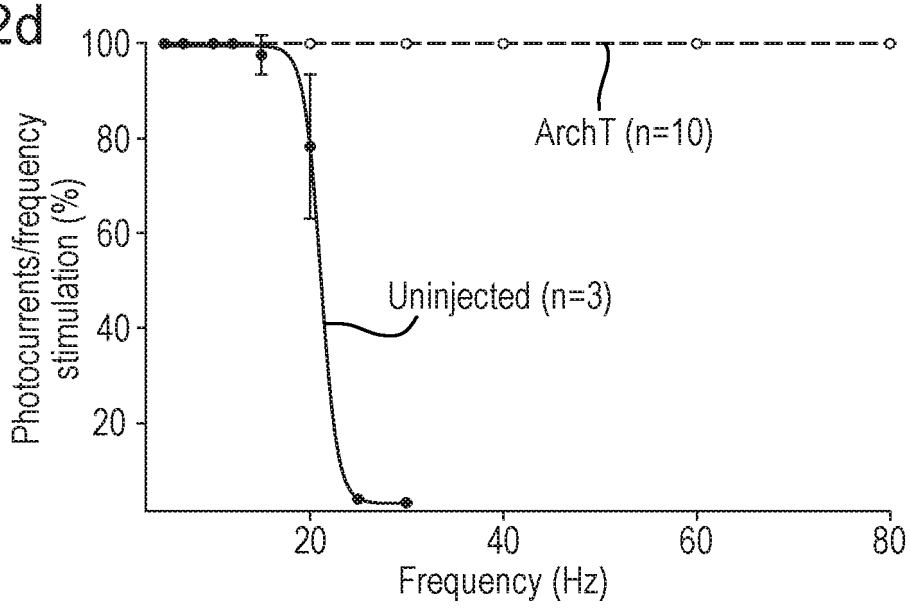

Fig. 2e

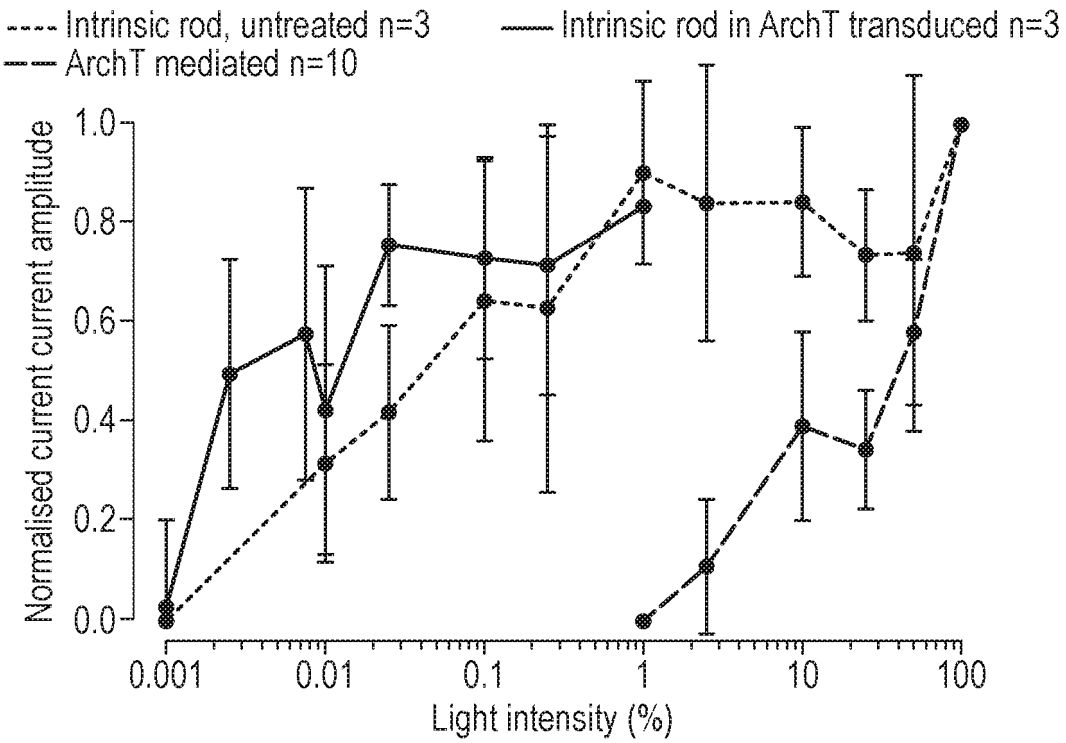
Intrinsic rod, untreated n=3
Intrinsic rod in ArchT transduced n=3
ArchT mediated n=10
Normalised current current amplitude
1.0
0.8
0.6
0.4
0.2
0.0
0.001
0.01
0.1
1
10
100
Light intensity (%)

Fig. 2f

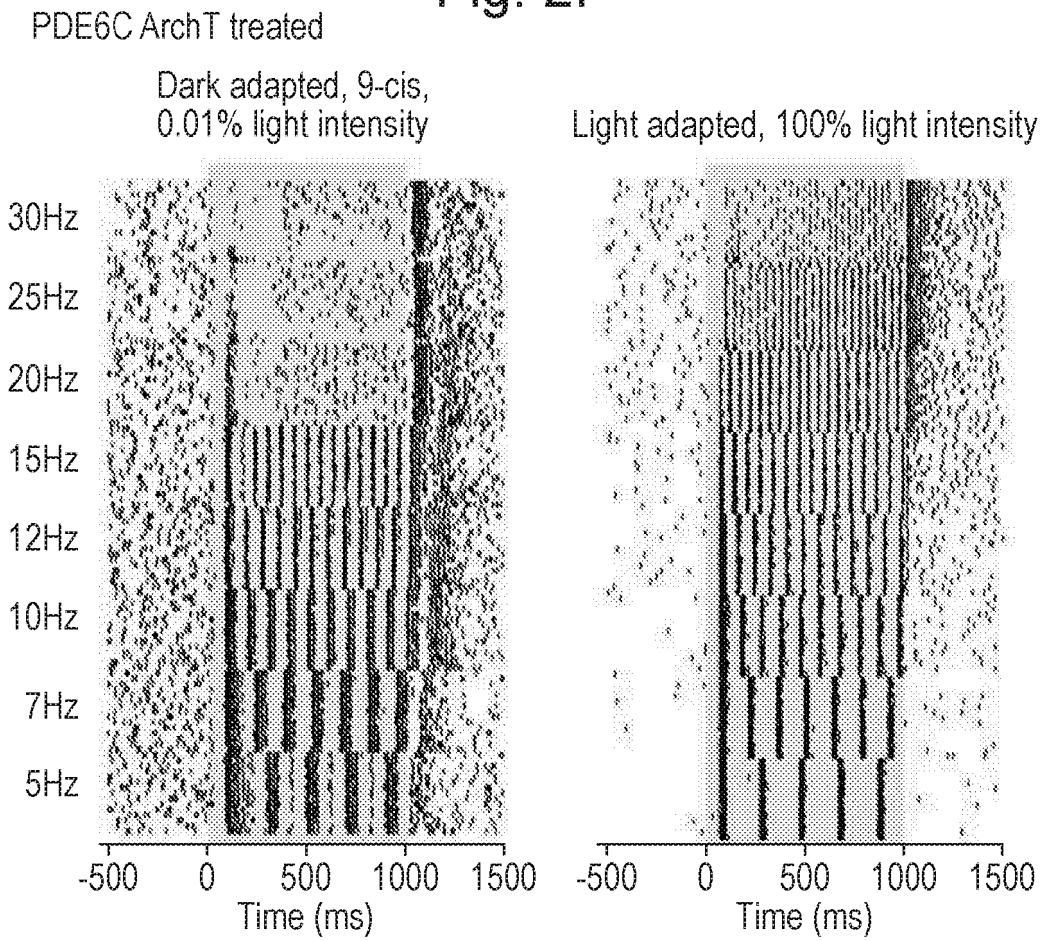
PDE6C ArchT treated
Dark adapted, 9-cis,
0.01% light intensity
Light adapted, 100% light intensity
30Hz
25Hz
20Hz
15Hz
12Hz
10Hz
7Hz
5Hz
-500
0
500
1000
1500
Time (ms)
-500
0
500
1000
1500
Time (ms)

Fig. 3a

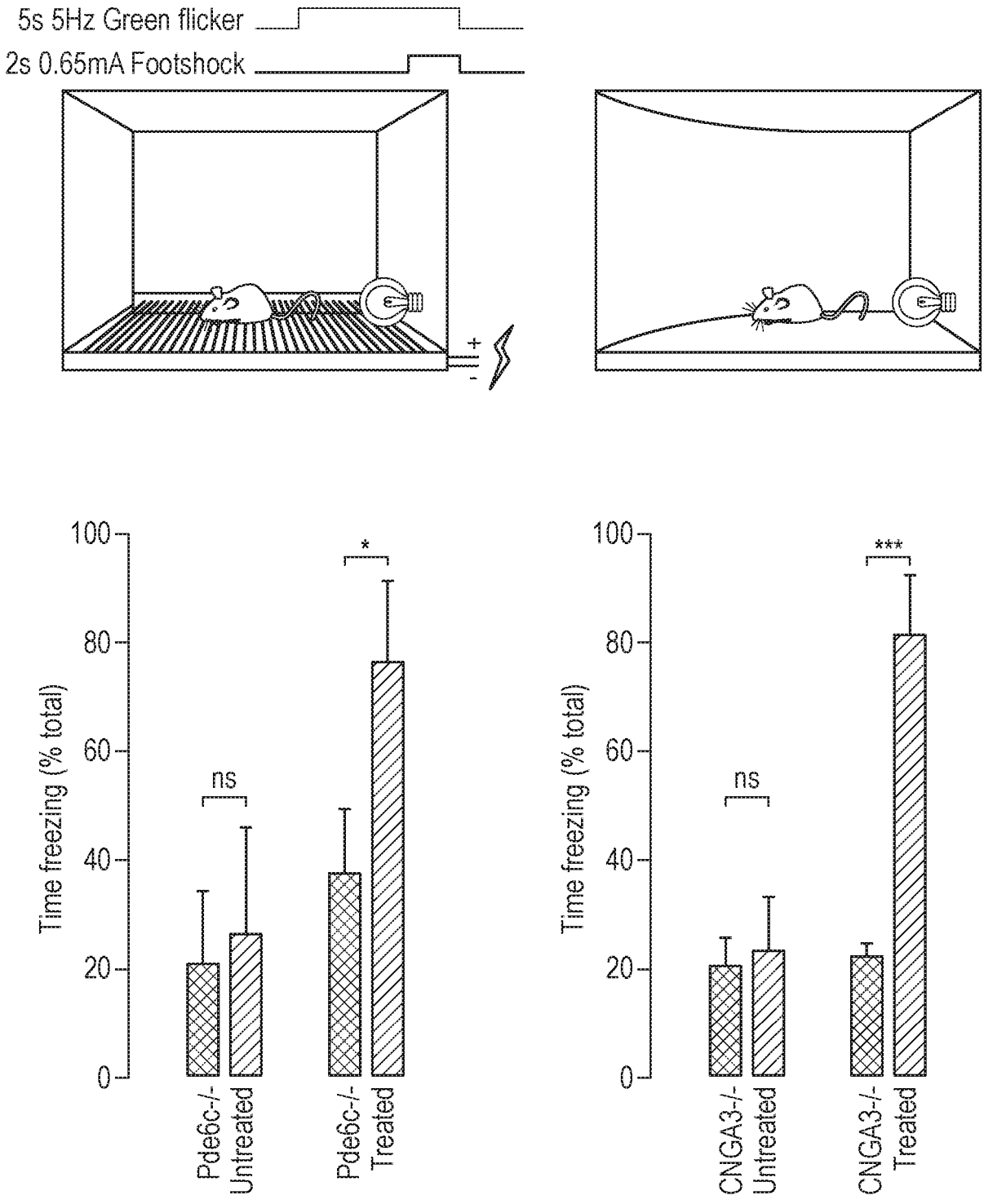
5s 5Hz Green flicker
2s 0.65mA Footshock
+
-
Time freezing (% total)
100
80
60
40
20
0
ns
*
Pde6c-/-
Untreated
Pde6c-/-
Treated
Time freezing (% total)
100
80
60
40
20
0
ns
***
CNGA3-/-
Untreated
CNGA3-/-
Treated

Fig. 3b

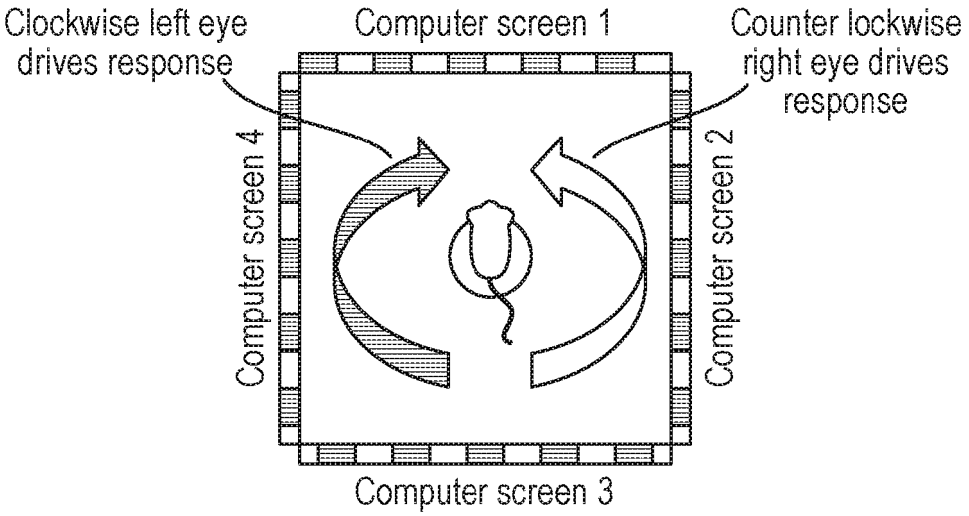
Clockwise left eye drives response
Computer screen 1
Counter lockwise right eye drives response
Computer screen 4
Computer screen 2
Computer screen 3

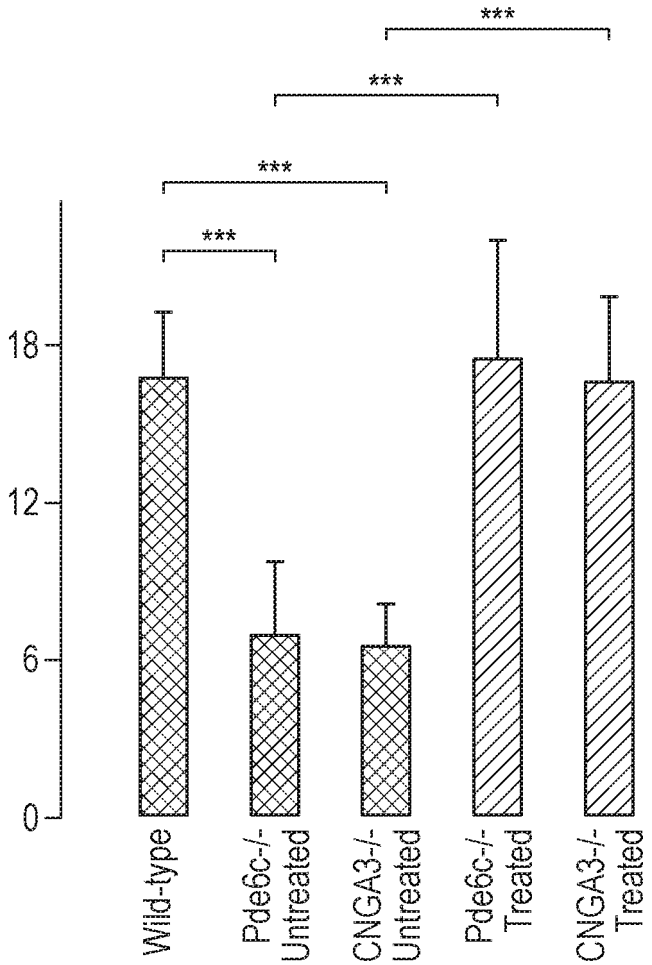
***
***
***
***
18
12
6
0
Wild-type
Pde6c-/- Untreated
CNGA3-/- Untreated
Pde6c-/- Treated
CNGA3-/- Treated

Fig. 4a

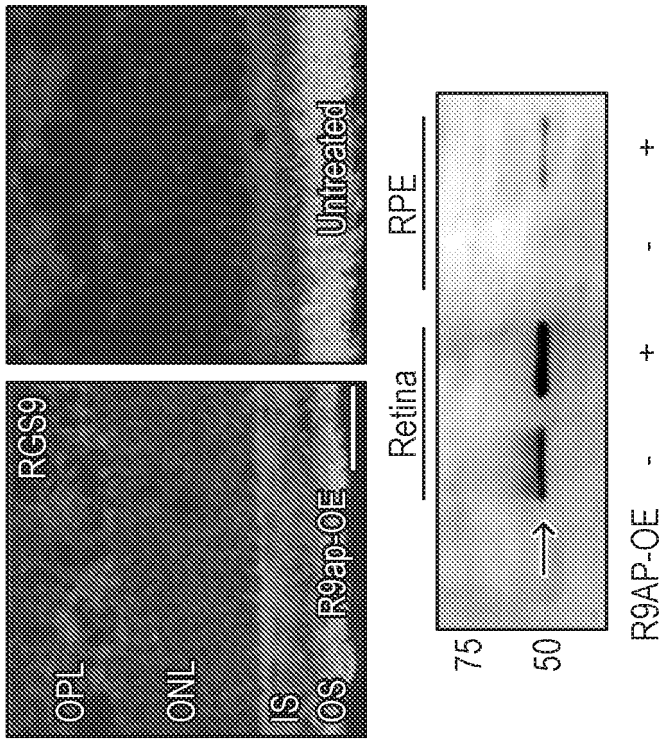
RGS9
R9ap-OE
Untreated
OPL
ONL
IS
OS
Retina
RPE
75
50
R9AP-OE - + - +

Fig. 4b

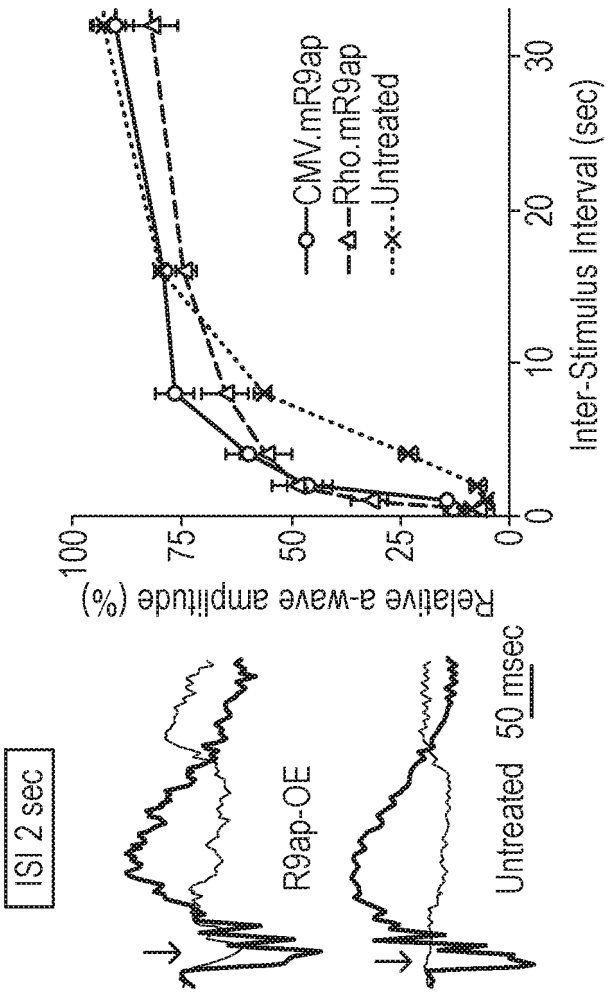
ISI 2 sec
R9ap-OE
Untreated
50 msec
Relative a-wave amplitude (%)
100
75
50
25
0
0
10
20
30
Inter-Stimulus Interval (sec)
CMV.mR9ap
Rho.mR9ap
Untreated

Fig. 5a

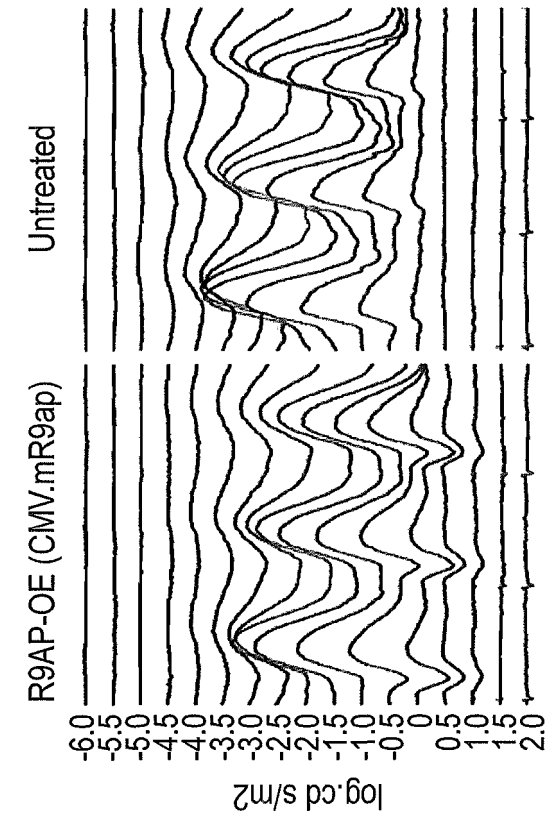

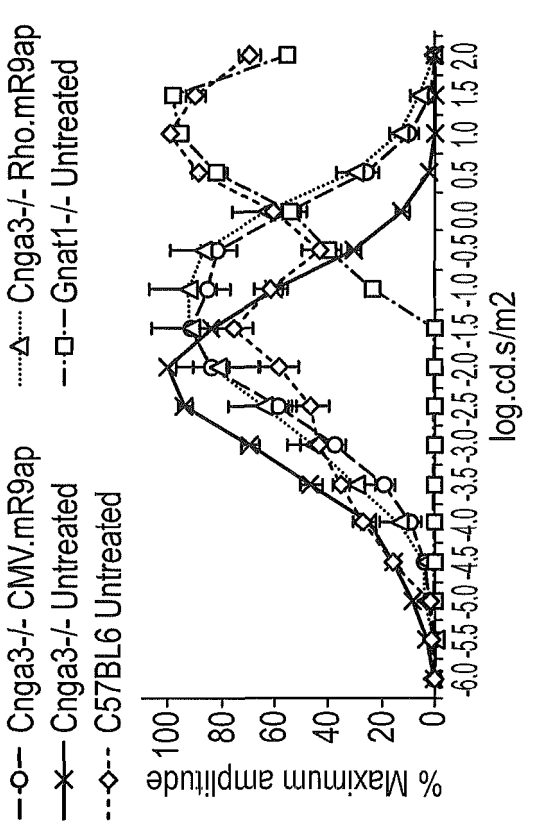

Fig. 5b

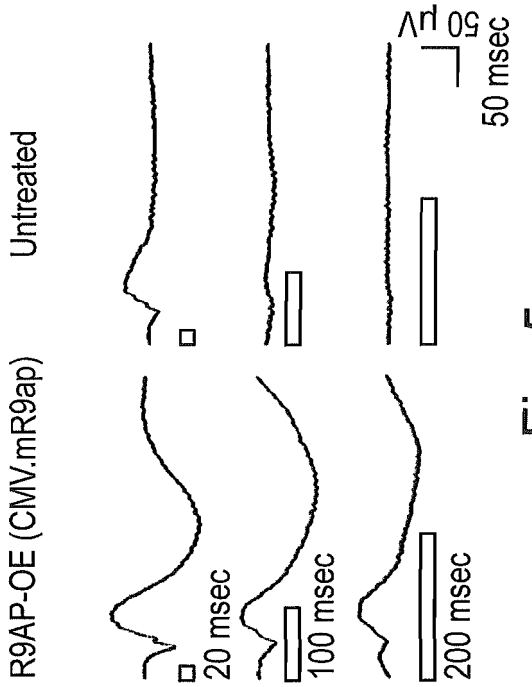

Fig. 5c

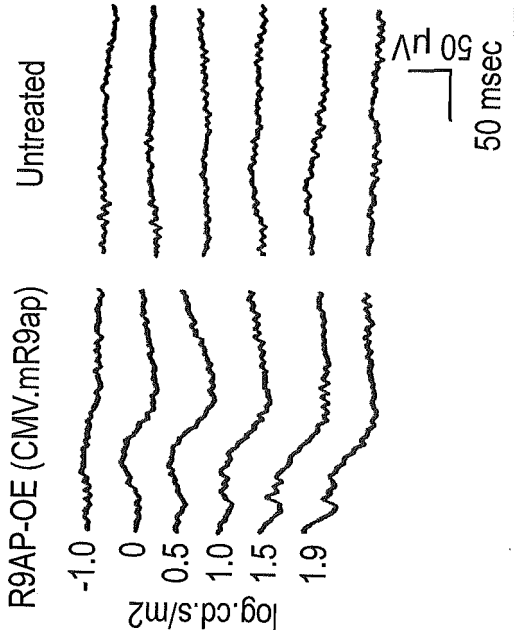

Fig. 6a

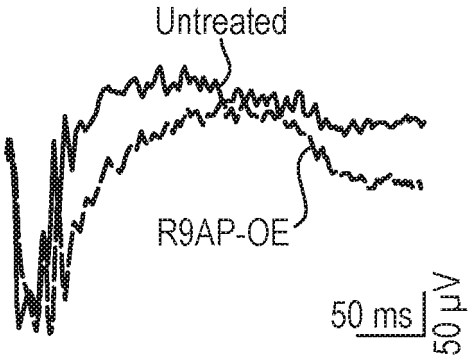

Fig. 6b

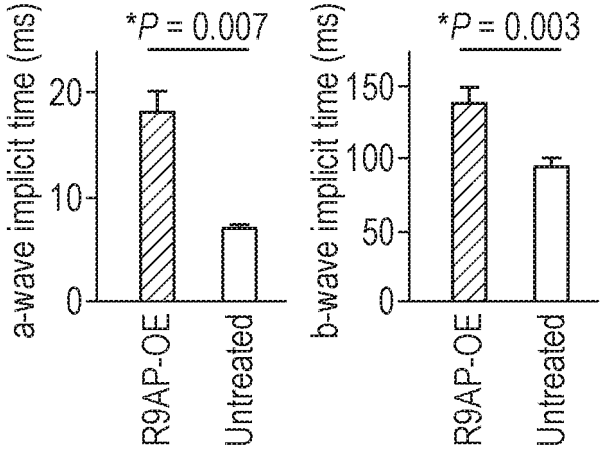

Fig. 6c

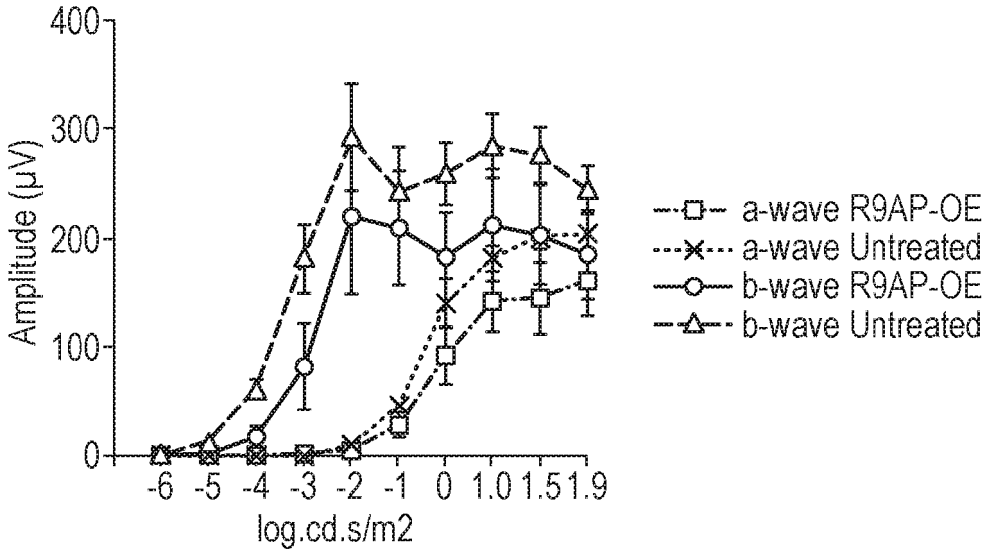

Fig. 7a

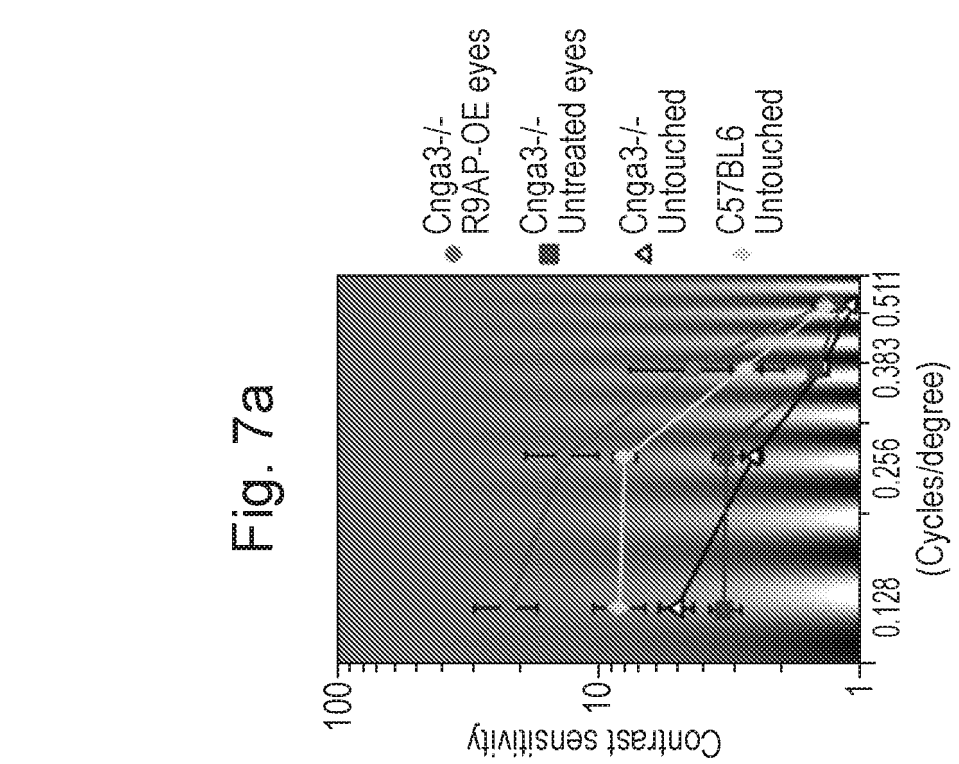
Contrast sensitivity
100
10
1
0.128
0.256
0.383
0.511
(Cycles/degree)
Cnga3-/- R9AP-OE eyes
Cnga3-/- Untreated eyes
Cnga3-/- Untouched
C57BL6 Untouched

Fig. 7b

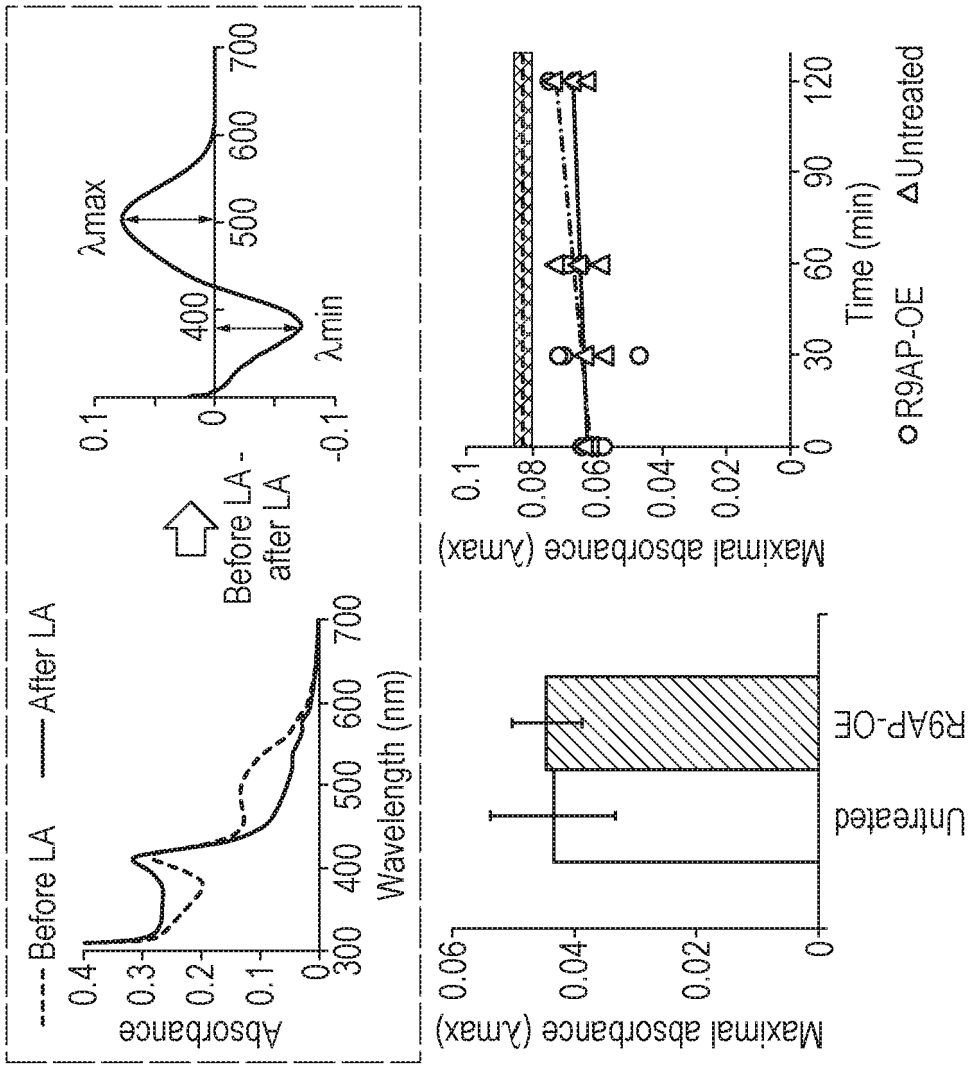
Before LA
After LA
Absorbance
0.4
0.3
0.2
0.1
0
300
400
500
600
700
Wavelength (nm)
Before LA - after LA
λmax
λmin
0.1
0
-0.1
400
500
600
700
Maximal absorbance (λmax)
0.1
0.08
0.06
0.04
0.02
0
0
30
60
90
120
Time (min)
R9AP-OE
Untreated
Maximal absorbance (λmax)
0.06
0.04
0.02
0
Untreated
R9AP-OE

Fig. 8

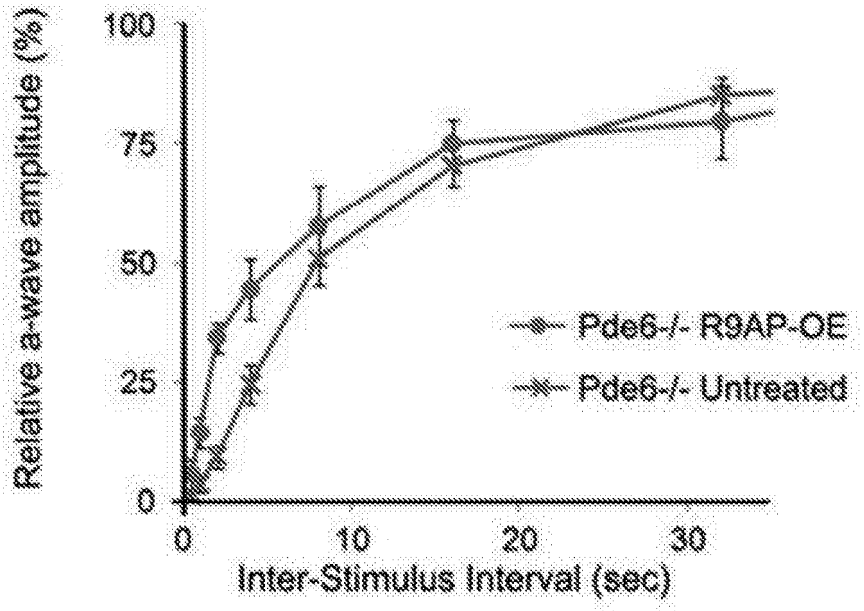
Relative a-wave amplitude (%)
100
75
50
25
0
0
10
20
30
Inter-Stimulus Interval (sec)
Pde6-/- R9AP-OE
Pde6-/- Untreated

Fig. 9

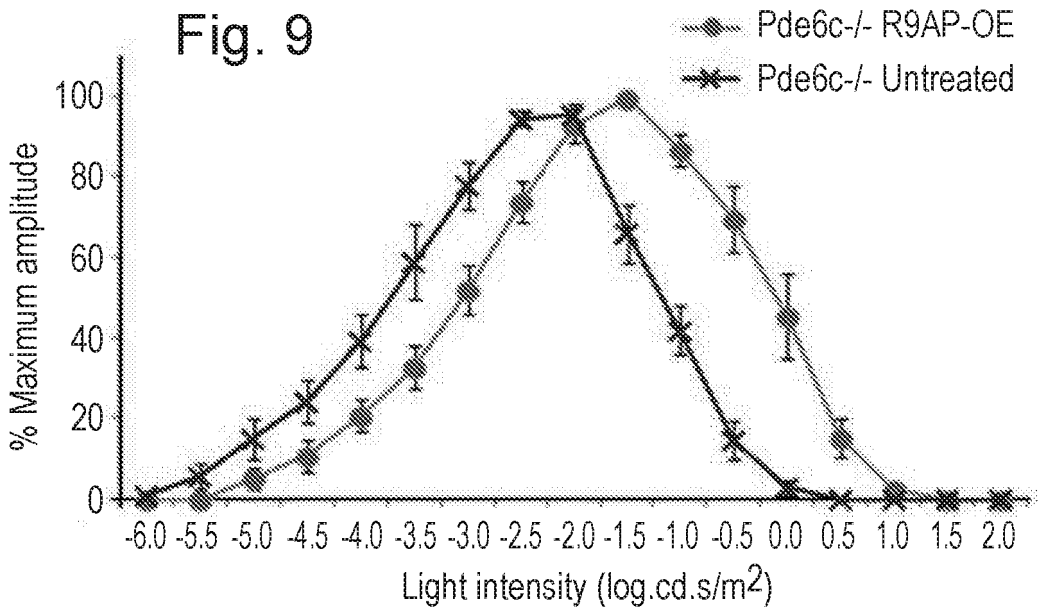
Pde6c-/- R9AP-OE
Pde6c-/- Untreated
% Maximum amplitude
100
80
60
40
20
0
-6.0 -5.5 -5.0 -4.5 -4.0 -3.5 -3.0 -2.5 -2.0 -1.5 -1.0 -0.5 0.0 0.5 1.0 1.5 2.0
Light intensity (log.cd.s/m2)

Fig. 10

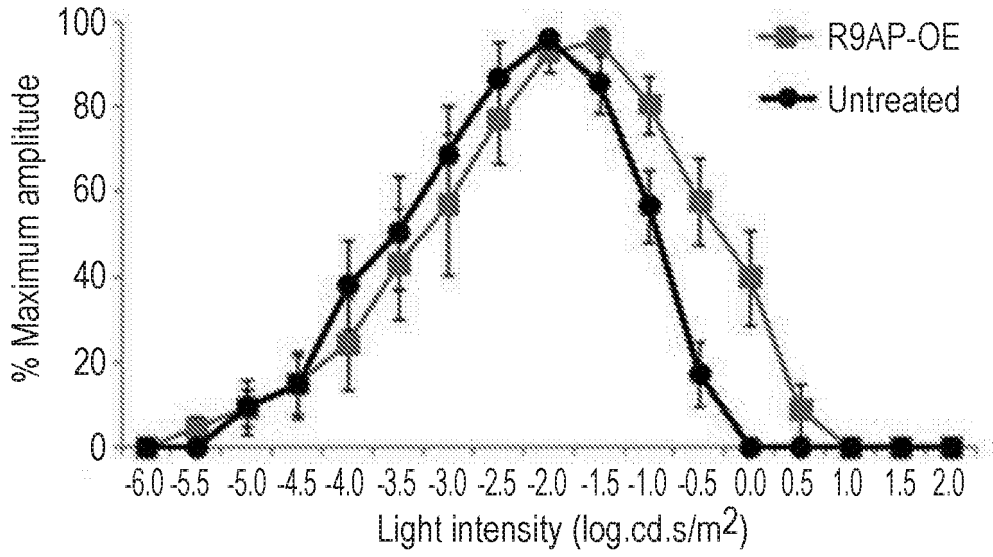
R9AP-OE
Untreated
% Maximum amplitude
100
80
60
40
20
0
-6.0 -5.5 -5.0 -4.5 -4.0 -3.5 -3.0 -2.5 -2.0 -1.5 -1.0 -0.5 0.0 0.5 1.0 1.5 2.0
Light intensity (log.cd.s/m2)

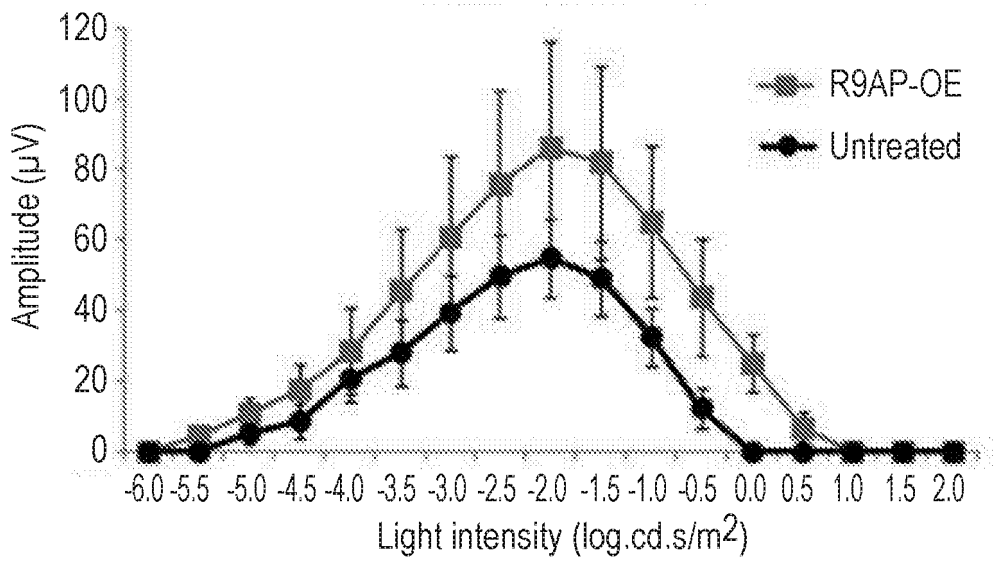
R9AP-OE
Untreated
Amplitude (µV)
120
100
80
60
40
20
0
-6.0 -5.5 -5.0 -4.5 -4.0 -3.5 -3.0 -2.5 -2.0 -1.5 -1.0 -0.5 0.0 0.5 1.0 1.5 2.0
Light intensity (log.cd.s/m2)

Fig. 11

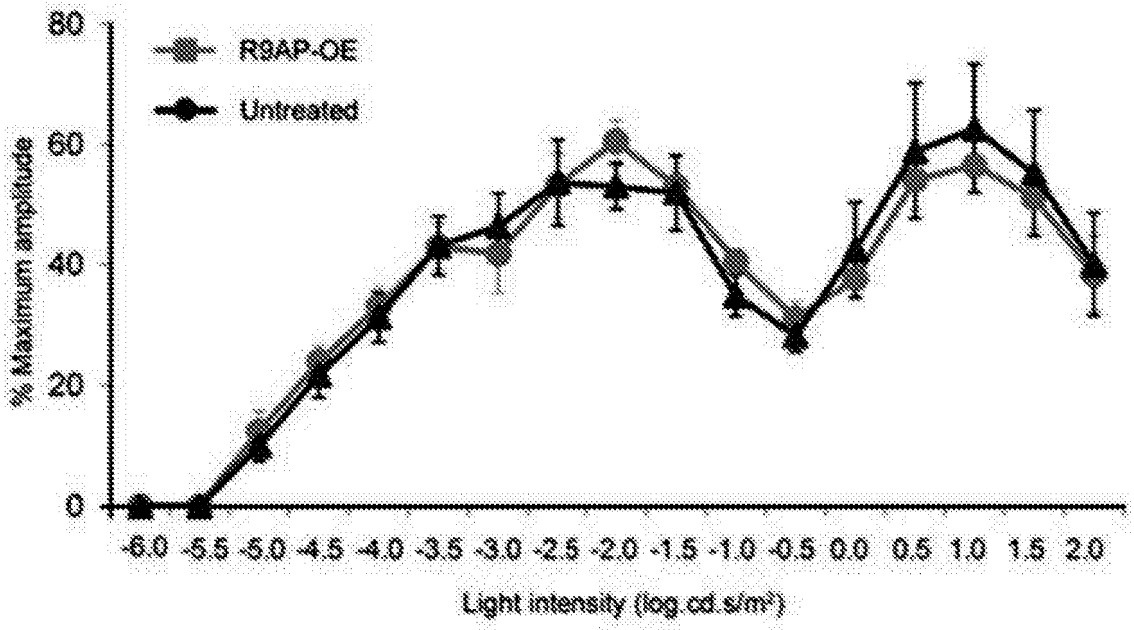
80
60
40
20
0
% Maximum amplitude
R9AP-OE
Untreated
-6.0 -5.5 -5.0 -4.5 -4.0 -3.5 -3.0 -2.5 -2.0 -1.5 -1.0 -0.5 0.0 0.5 1.0 1.5 2.0
Light intensity (log cd.s/m²)

Fig. 12

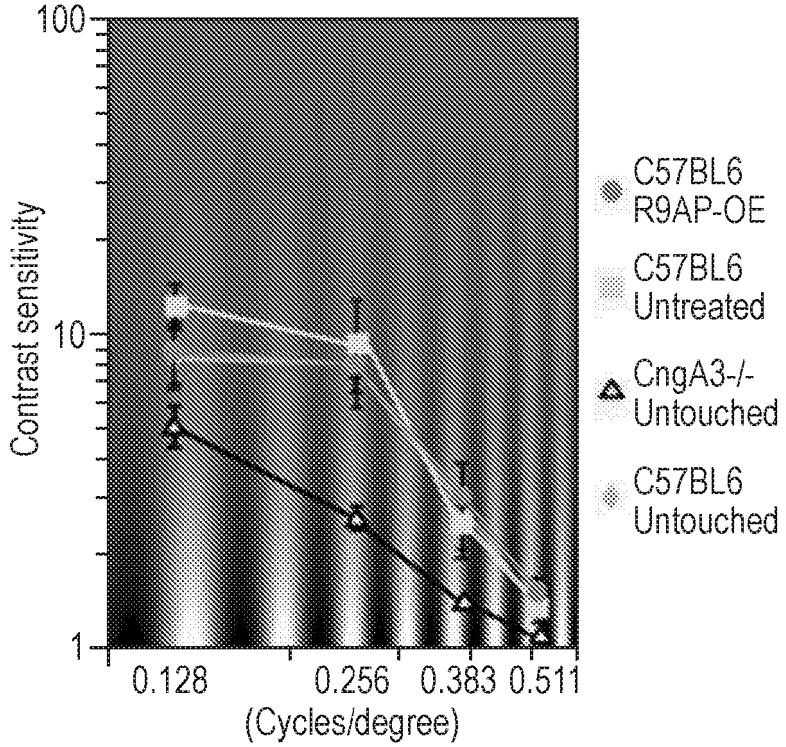
100
10
1
Contrast sensitivity
0.128
0.256
0.383
0.511
(Cycles/degree)
C57BL6 R9AP-OE
C57BL6 Untreated
CngA3-/- Untouched
C57BL6 Untouched

INTERNATIONAL SEARCH REPORT

International application No
PCT/GB2016/050419

A. CLASSIFICATION OF SUBJECT MATTER
INV. A61K48/00
ADD.

According to International Patent Classification (IPC) or to both national classification and IPC

B. FIELDS SEARCHED

Minimum documentation searched (classification system followed by classification symbols)
A61K C12N

Documentation searched other than minimum documentation to the extent that such documents are included in the fields searched

Electronic data base consulted during the international search (name of data base and, where practicable, search terms used)
EPO-Internal, WPI Data, BIOSIS, CHEM ABS Data, EMBASE

C. DOCUMENTS CONSIDERED TO BE RELEVANT

Category*	Citation of document, with indication, where appropriate, of the relevant passages	Relevant to claim No.
X	WO 2009/127705 A1 (NOVARTIS FORSCHUNGSSTIFTUNG [CH]; BALYA DAVID [CH]; BUSSKAMP VOLKER [C) 22 October 2009 (2009-10-22) claims 1-15; figure 1	19-22
X	WO 2013/124477 A1 (INST NAT SANTE RECH MED) 29 August 2013 (2013-08-29) page 3, line 31 - page 4, line 8 page 7, line 9 - line 17 page 9, line 12 - line 14	19-21
X	WO 2012/167109 A2 (MASSACHUSETTS EYE & EAR INFIRM) 6 December 2012 (2012-12-06) examples 1-4	19-21

-/--

[X] Further documents are listed in the continuation of Box C.

[X] See patent family annex.

* Special categories of cited documents :

"A" document defining the general state of the art which is not considered to be of particular relevance

"E" earlier application or patent but published on or after the international filing date

"L" document which may throw doubts on priority claim(s) or which is cited to establish the publication date of another citation or other special reason (as specified)

"O" document referring to an oral disclosure, use, exhibition or other means

"P" document published prior to the international filing date but later than the priority date claimed

"T" later document published after the international filing date or priority date and not in conflict with the application but cited to understand the principle or theory underlying the invention

"X" document of particular relevance; the claimed invention cannot be considered novel or cannot be considered to involve an inventive step when the document is taken alone

"Y" document of particular relevance; the claimed invention cannot be considered to involve an inventive step when the document is combined with one or more other such documents, such combination being obvious to a person skilled in the art

"&" document member of the same patent family

Date of the actual completion of the international search	Date of mailing of the international search report
19 April 2016	29/04/2016

Name and mailing address of the ISA/	Authorized officer
European Patent Office, P.B. 5818 Patentlaan 2 NL - 2280 HV Rijswijk Tel. (+31-70) 340-2040, Fax: (+31-70) 340-3016	Lewis, Birgit

2

Form PCT/ISA/210 (second sheet) (April 2005)

C(Continuation). DOCUMENTS CONSIDERED TO BE RELEVANT

Category*	Citation of document, with indication, where appropriate, of the relevant passages	Relevant to claim No.
X	ELSA LHÉRITEAU ET AL: "Successful Gene Therapy in the RPGRIP1-deficient Dog: a Large Model of Cone-Rod Dystrophy", MOLECULAR THERAPY, vol. 22, no. 2, 4 October 2013 (2013-10-04), pages 265-277, XP055266023, GB ISSN: 1525-0016, DOI: 10.1038/mt.2013.232 abstract figure 2	19-21
X	KOJI M. NISHIGUCHI ET AL: "Gene therapy restores vision in rd1 mice after removal of a confounding mutation in Gpr179", NATURE COMMUNICATIONS, vol. 6, 23 January 2015 (2015-01-23), page 6006, XP055266591, DOI: 10.1038/ncomms7006 page 3, left-hand column, paragraph 2 - right-hand column, line 2	19-21
A	XUE HAN ET AL: "A High-Light Sensitivity Optical Neural Silencer: Development and Application to Optogenetic Control of Non-Human Primate Cortex", FRONTIERS IN SYSTEMS NEUROSCIENCE, vol. 5, 13 April 2011 (2011-04-13), XP055265835, DOI: 10.3389/fnsys.2011.00018 the whole document	1-26
A	M. E. BURNS ET AL: "Lessons from Photoreceptors: Turning Off G-Protein Signaling in Living Cells", PHYSIOLOGY, vol. 25, no. 2, 1 April 2010 (2010-04-01), pages 72-84, XP055266715, US ISSN: 1548-9213, DOI: 10.1152/physiol.00001.2010 cited in the application figure 1 page 76, right-hand column, paragraph 2 page 81, right-hand column, paragraph 2	1-26

2

INTERNATIONAL SEARCH REPORT

Information on patent family members

International application No
PCT/GB2016/050419

Patent document cited in search report	Publication date	Patent family member(s)	Publication date
WO 2009127705 A1	22-10-2009	AU 2009237585 A1	22-10-2009
		BR PI0911426 A2	29-09-2015
		CA 2721635 A1	22-10-2009
		CN 101970013 A	09-02-2011
		EA 201001621 A1	30-06-2011
		EP 2271369 A1	12-01-2011
		EP 2679246 A2	01-01-2014
		ES 2474721 T3	09-07-2014
		JP 2011516091 A	26-05-2011
		JP 2015128440 A	16-07-2015
		KR 20100136550 A	28-12-2010
		PT 2271369 E	10-07-2014
		WO 2009127705 A1	22-10-2009
WO 2013124477 A1	29-08-2013	US 2015038557 A1	05-02-2015
		WO 2013124477 A1	29-08-2013
WO 2012167109 A2	06-12-2012	US 2014364488 A1	11-12-2014
		WO 2012167109 A2	06-12-2012

(19)中华人民共和国国家知识产权局

(12)发明专利申请

(10)申请公布号 CN 107530449 A
(43)申请公布日 2018.01.02

(21)申请号 201680023264.6

(22)申请日 2016.02.19

(30)优先权数据
1503008.3 2015.02.23 GB

(85)PCT国际申请进入国家阶段日
2017.10.20

(86)PCT国际申请的申请数据
PCT/GB2016/050419 2016.02.19

(87)PCT国际申请的公布数据
WO2016/135457 EN 2016.09.01

(71)申请人 UCL商业有限公司
地址 英国伦敦

(72)发明人 M·瑞兹 R·阿里 A·史密斯 K·西口

(74)专利代理机构 北京北翔知识产权代理有限公司 11285
代理人 孙占华 张广育

(51)Int.Cl.
A61K 48/00(2006.01)
A61P 27/02(2006.01)
C12N 15/864(2006.01)

权利要求书2页 说明书21页 附图17页

(54)发明名称

改善视觉的基因疗法

(57)摘要

本发明涉及基因疗法载体改善视觉的用途，所述改善视觉如下进行：通过将编码感光细胞中光敏性基因产物和/或调节内源性光敏性信号传导的基因产物引入到患有视锥细胞功能障碍和/或变性的患者的健康视杆细胞中，从而扩大视杆细胞响应的光强度的范围和/或提高视杆细胞响应光的速度。

CN 107530449 A

1.一种包含编码感光细胞中光敏性基因产物和/或调节内源性光敏性信号传导的基因产物的核酸的载体，其用于在具有视锥细胞功能障碍和/或变性的患者中改善视觉的方法，所述方法通过将所述核酸引入到所述患者的视网膜中的健康视杆细胞中并在其中表达所述基因产物，从而扩大视杆细胞响应的光强度的范围和/或提高视杆细胞响应光的速度。

2.根据权利要求1使用的载体，其中所述核酸编码以光刺激之后导致视杆超极化(外向电流)的方式改变膜电导的蛋白。

3.根据权利要求2使用的载体，其中所述核酸编码(a)光敏性或光门控G偶联膜蛋白、离子通道、离子泵或离子转运蛋白；(b)RGS9复合物成员；或(c)另一种增加内源性视杆信号传导机制的速度的蛋白。

4.根据权利要求3使用的载体，其中所述光门控分子是ArchT、Jaws(cruxhalorhodopsin)、iC1C2，或所述RGS9复合物成员是R9AP。

5.根据前述权利要求中任一项使用的载体，所述载体为病毒载体。

6.根据权利要求5使用的载体，所述载体为腺相关病毒(AAV)载体。

7.根据权利要求6使用的载体，所述载体的衣壳源自AAV8。

8.根据权利要求6或7使用的AAV载体，所述载体的基因组源自AAV2。

9.根据前述权利要求中任一项使用的载体，其中所述患者患有黄斑变性、全色盲或利伯先天性黑矇。

10.根据权利要求9使用的载体，其中所述黄斑变性为年龄相关性黄斑变性(AMD)、遗传性黄斑变性病症或遗传性视锥营养不良。

11.根据权利要求10使用的载体，其中所述AMD是湿性AMD或新生血管性AMD或地图状萎缩。

12.根据前述权利要求中任一项使用的载体，其中视杆细胞信号传导被扩大到中间视觉或明视觉照明范围。

13.根据前述权利要求中任一项使用的载体，其中所述视杆表现出改善的调节强度和/或更快的激活/失活动力学。

14.根据前述权利要求中任一项使用的载体，其中在体外将所述载体引入到视杆细胞，然后移植到视网膜中。

15.根据前述权利要求中任一项使用的载体，其中所述患者的中间视觉和/或明视觉得到改善。

16.根据前述权利要求中任一项使用的载体，其中所述核酸在光感受器特异性启动子或光感受器优选的启动子的控制下表达。

17.根据权利要求16使用的载体，其中所述光感受器特异性启动子或光感受器优选的启动子是视杆特异性启动子或视杆优选的启动子。

18.根据权利要求17使用的载体，其中所述核酸在视紫红质(Rho)、神经视网膜特异性的亮氨酸拉链蛋白(NRL)或磷酸二酯酶6B(PDE6B)启动子的控制下表达。

19.包含权利要求1至4中任一项中所定义的核酸的表达盒，所述核酸与权利要求17或18中所定义的视杆特异性启动子或视杆优选的启动子可操作地连接。

20.包含权利要求19的表达盒的载体。

21.权利要求20的载体，其为权利要求5至8中任一项所定义的病毒载体。

22.包含权利要求20或21的载体的宿主细胞。

23.权利要求1至8、16、17、19或20中任一项所定义的载体用于制备用于如权利要求1或9至15中任一项中所定义的改善视觉的药物的用途。

24.一种在具有视锥细胞功能障碍的患者中改善视觉的方法，所述方法通过将编码光敏性基因产物的核酸引入到所述患者的视网膜中的健康视杆细胞中并在其中表达所述基因产物，从而扩大视杆细胞响应的光强度的范围和/或提高视杆细胞响应光的速度。

25.权利要求24的方法，其中所述载体如权利要求1至8、16、17、19或20中任一项所定义。

26.权利要求23或24的方法，其中如权利要求1或9至15中任一项所定义来改善视觉。

改善视觉的基因疗法

技术领域

[0001] 本发明涉及基因治疗载体用于改善患者的视觉的用途。

背景技术

[0002] 在许多哺乳动物物种(包括小鼠和人)中,在暗光下调节视觉的视杆细胞(rod photoreceptor)的数目远超过视锥细胞(cone photoreceptor)的数目(Curcio et al,2000)。然而,在照明使视锥整日运作的工业化世界中,视杆介导的视觉的重要性降低。许多从出生起缺少视杆功能的患者只是偶然被发现,实际上无法识别出他们异常的视觉(Dryja,2000)。相反,当存在视锥功能障碍时,患者总是具有症状,并且通常患有视觉障碍(取决于他们的视锥功能障碍的程度)。然而在一些情况下,仅(或主要是)视锥损失或功能障碍,视杆相对被保留。例如,全色盲是严重的遗传性视网膜营养不良,患者从出生时视锥功能完全丧失,但是可能具有正常的视杆功能(Hess et al,1986;Nishiguchi et al,2005)。多种基因(包括CNGA3(Kohl et al 1998)和PDE6C(Chang et al,2009;Thiadens et al,2009))中的突变与该疾病相关。每一种致病基因编码视锥光转导级联的必需组分,所述视锥光转导级联通过引起感光细胞的超极化而将光转化为电信号。在年龄相关性黄斑变性(AMD)中,视觉损伤主要是由富含视锥的黄斑中央凹的变性引起的。因此,患者丧失中心视觉和敏锐度,但是通常具有相对保存良好的外周斑,因此具有一些有用的受限于缺乏中央凹外部视锥的残余视觉。

[0003] 视杆对光高度灵敏,这使视杆在昏暗条件下感知少量的光。相反,视锥的灵敏度较低,但是能够在日光中处理大量光并连续传导视觉信号。这种功能差异部分是由于光信号传导的失活机制——由RGS9、R9AP(也称为RGS9BP)和Gβ5组成的GTPase复合物——的效率导致的。RGS9是水解与G蛋白偶联的GTP的催化组分,而R9AP和Gβ5是必需组成型亚基(Burns et al,2009;Burns et al,2010)。重要的是,R9AP将所述复合物连接到光感受器外段(在那里还发生光转导信号传导)处的圆盘膜(Baseler et al,2002)。R9AP的表达决定了GTPase复合物的水平,以使超出R9AP而产生的任何RGS9可能快速被降解(Martyemyanov et al,2009)。鼠视杆中R9AP的过表达足以增加GTPase活性,并且足以大幅加快它们的失活动力学,如单细胞记录所证明的(Krispel et al,2006)。据估计,视锥中RGS9表达比视杆中的RGS9表达高约10倍(Cowan et al,1998;Zhang et al,2003)。这为视锥从曝光中快速恢复并因此保持对连续光刺激的功能性的能力提供了基础。这还使视锥响应于更快速的刺激。实际上,在临床上,具有由RGS9或R9AP中的遗传缺陷引起的光转导级联的延迟失活或具有缓慢的视觉(bradyopsia)的患者具有严重的视锥介导的视觉损伤,包括昼盲症和看见移动物体的能力下降(Nishiguchi et al,2004;Michaelides et al,2010)。同时,视杆介导的视觉受到相同突变的影响较小。

[0004] 一些黄斑变性病症,例如年龄相关性黄斑变性(AMD)和遗传性黄斑变性病症也表现出视锥功能障碍,但是正常或损伤更少的视杆功能。在发达国家,黄斑变性是失明最主要的原因,并且因为AMD的发病率在生命中每10年就会变为原来的4倍,预期未来AMD病例将随

着寿命的增加而增多。用于治疗AMD的药物已经占英国国家卫生服务部的全部药物预算的1％以上。尽管晚期AMD患者可接受训练以将视线移向中央凹外，然而视杆细胞的低更新率和低漂白阈值限制了所产生的视觉质量。

发明内容

[0005] 使用缺少视锥功能的小鼠，我们证明了AAV介导的Rgs9锚定蛋白(R9AP)——介导光转导级联失活的GTPase复合物的关键组分——的过表达导致视杆驱动的视网膜电图的脱敏和“明视偏移(photopic shift)”。治疗在损失暗视(更低的光水平)功能的情况下使视杆比未经治疗的细胞响应于更亮的光(最高达约2.0log)。使用经治疗的视网膜的多电极阵列测量表明，视网膜神经节细胞通过表现出明视光水平的分级响应，也反映出视杆的“明视偏移”。通过对响应于旋转正旋光栅的头部追踪移动进行定量来测量的对比敏感度函数表明，在室内光条件下敏感度提高最多达25倍，并且更快响应于反复的刺激。此外，在这些小鼠中可漂白的视紫红质水平的生化测量表明，视循环没有限制视杆功能。

[0006] 本发明人还在视杆细胞中表达了快速光驱动质子泵ArchT(Han et al,2011)。将携带视紫红质启动子(Rho)控制下的ArchT-EGFP的AAV8粒子经视网膜下注射到成年小鼠中。Rho-ArchT-EGFP的表达局限于视杆细胞膜。ArchT的表达允许非常快的光响应，而固有的视杆响应被保留并且与在非转导的视杆细胞中观察到的响应相当。总的来说，ArchT表达并未改变视杆细胞对暗视刺激的响应能力，但是它确实赋予了额外的以对更高水平的照明的快速非漂白响应作出响应的能力。本发明人还发现，经转导的视杆能够可靠地保持这种快速“类似于视锥的”传输，因为表达ArchT的视锥使维持的视网膜神经节细胞(RGC)在高光强度下和与视锥细胞的频率接近的频率下产生脉冲(spike)。在缺少视锥介导的视觉的CNGA3$^{-/-}$和PDE6C$^{-/-}$小鼠中Rho-ArchT-EGFP的表达还扩大了这些小鼠对亮光刺激的敏感度，并且赋予这些小鼠敏捷的视觉。表达ArchT的小鼠能够跟随的刺激的最大频率类似于视锥细胞的频率。

[0007] 这些结果共同表明，在用编码视锥所特有的光敏蛋白的基因或编码提高内源性视杆信号传导机制速度的分子的基因转导健康视杆细胞之后，视杆表现得更像视锥，并因此能够补偿视锥的功能障碍。这可用于治疗许多视觉疾病，在这些疾病中，视锥功能降低，但是至少保留一些健康的视杆。这与之前的目的在于恢复视锥丧失的功能的方法不同(Busskamp et al,2010;美国专利申请No.2012258530)。以本发明的方法改变视杆功能的优势在于，视锥具有功能障碍但是能够被修复的病症(例如在视网膜变性的早期，当感光细胞功能丧失但是感光细胞至双极突触完整时)是罕见的，而视锥功能障碍更严重或进入晚期并且无法被修复，或视锥完全丧失，但是至少保留一些健康的视杆细胞的病症是常见的(参见上文)。此外，本发明使得能够产生“假中央凹”——在中央凹视锥丧失或功能障碍的病症中改善视觉的一小片类似视锥的视杆。

[0008] 因此，本发明提供了包含编码感光细胞中光敏性基因产物和/或调节内源性光敏性信号传导的基因产物的核酸的载体，其用于在具有视锥细胞功能障碍和/或变性的患者中改善视觉的方法，所述方法通过将所述核酸引入到所述患者的视网膜中的健康视杆细胞中并在其中表达所述基因产物，从而扩大视杆细胞响应的光强度的范围和/或提高视杆细胞响应光的速度。

[0009] 本发明还提供了如上文定义的载体，包含所述载体的宿主细胞，以及使用所述载体进行治疗的方法。

附图说明

[0010] 图1：视杆细胞中ArchT的表达产生快速光驱动的电流。

[0011] (a)上方的图：在视紫红质启动子控制下的ArchT-EGFP的AAV8介导的转导(绿色，参见左图)。未观察到视锥的重叠(紫色：视锥抑制蛋白，参见中图；白色：DAPI，参见右图)。下方的图：还可在突触水平上观察到表达特异性。(b)ArchT-EGFP定位于视杆细胞膜，包括内段和外段。(c)在表达ArchT-EGFP的视杆末端(绿色，左峰)和视锥抑制蛋白阳性的视锥末端(紫色，右峰)中的荧光定量显示出两个独特的带，其分别对应于视杆和视锥突触定位的亚层(n＝22)。(d)来自表达ArchT的视杆细胞的细胞体的单细胞记录。保存了响应于10ms 530nm光脉冲(绿色，参见垂直条)的固有的视杆光转导介导的电流(上方的迹线)。ArchT产生的电流更快(下方的迹线)。比例尺：(a)上方的图：50μm；(a)下方的图和(b)：10μm。

[0012] 图2：ArchT表达驱动视杆中的高频率响应并快速传输到视网膜神经节细胞。

[0013] (a)未经注射的C57BL6视网膜中固有的视杆光引起的电流。(b)ArchT介导的电流能够跟随高得多的刺激频率。(c)响应对刺激呈现(presentation)是时间锁定的(绿色垂直条)。(d)表达ArchT的视杆稳定地响应最高达80Hz的频率刺激，而固有的视杆响应在约20Hz下降低。(e)显示出ArchT表达的总结数据并未改变视杆细胞的固有响应，而ArchT响应在更亮的光水平下开始。(f)来自$PDE6C^{-/-}$表达ArchT的视网膜的多电极阵列记录。固有的视杆响应无法引发20Hz以上的可靠视网膜神经节细胞脉冲。相反，ArchT介导的视杆激活促使视网膜神经节细胞的快速脉冲至与视锥细胞相当的水平。

[0014] 图3：ArchT介导的视杆激活促使对快速高光强度刺激的行为响应

[0015] (a)上方的图：恐惧条件反射行为的示意图。简言之，视觉刺激与点击成对出现。24小时后，在新环境中检验冻结行为。下方的图：未经注射的$CNGA3^{-/-}$和$PDE6C^{-/-}$小鼠无法学会任务(各图中左侧柱组)。然而，ArchT表达成功促使小鼠中的冻结行为(各图中右侧柱组)。(b)视动测试。表达ArchT的小鼠能够在与视锥可靠地跟随的频率相当的频率下跟随刺激。

[0016] 图4：Cnga3-/-小鼠中视杆中AAV介导的R9AP过表达和加速的a波失活。

[0017] A.用rRAAV2/8.Rho.mR9ap处理的Cnga3-/-眼中RGS9表达增加。与未经处理的眼(右)相比，在经处理的眼(左)中，R9AP过表达导致整个光感受器层中针对RGS9的免疫反应性增加(红)。蛋白质印迹表明，在过表达R9AP的眼中，视网膜和视网膜色素上皮(RPE)中RGS9表达均增加(下图)。在经处理的眼的RPE中还检测到少量RGS9蛋白。这可能反映了吞噬细胞圆盘膜内包含的过量蛋白的“溢出”。比例尺表示25μm。

[0018] B.用rAAV2/8.Rho.mR9ap和rAAV2/8.CMV.mR9ap处理的Cnga3-/-眼中a波振幅恢复的速度增加。来自相同动物的经处理(上)和未经处理的(下)眼的探测闪光的代表性ERG迹线(黑色迹线，参见在时程中间具有峰的迹线)和第二闪光的代表性ERG迹线(红色迹线)以2秒的刺激间时距(ISI)展示。注意到，在经处理的眼中，第二闪光产生的小a波(箭头)是清晰可见的，而在未经处理的另一只眼中a波是不可见的(箭头)。在经处理和未经处理的眼中，不同ISI下a波恢复的图。用rAAV2/8.CMV.mR9ap(n＝5)或rAAV2/8.Rho.mR9ap(n＝7)注射的眼比未经处理的眼(n＝5)具有更快的恢复动力学，所述未经处理的眼在更短的ISI下是最

可见的。数据表示为平均值±平均值的标准误差。OE:过表达。

[0019] 图5:在Cnga3-/-小鼠中通过R9AP的过表达从视杆获得明视功能

[0020] A.在Cnga3-/-小鼠的视杆中,通过R9AP的过表达而导致的响应阈值的升高和6Hz ERG的明视偏移。来自Cnga3-/-小鼠的代表性6Hz ERG迹线,所述小鼠的一只眼用rAAV2/8.CMV.mR9ap处理,另一只眼未处理(上图)。ERG迹线以0.5log.cd.s/m^2梯度从上至下从针对最暗闪光(-6.0log cd.s/m^2)的响应到针对最亮闪光(2.0log cd.s/m^2;底部)的响应而进行比对。注意到,响应出现的低阈值闪光强度增大,与之相联系的是对更亮闪光的响应阈值升高。这导致在用rAAV2/8.CMV.mR9ap处理的眼中视网膜功能的"明视偏移"。总结6Hz ERG结果,其证明了在用rAAV2/8.CMV.mR9ap或rAAV2/8.Rho.mR9ap(下图)处理之后视网膜功能的明视偏移。来自视杆功能缺陷的Gnat1-/-小鼠的ERG响应代表视锥介导的功能。同时,来自C57BL6小鼠的响应源自视杆细胞和视锥细胞。数据表示为相对于最大响应的%振幅,并且表示为平均值±平均值的标准误差。从用rAAV2/8.CMV.mR9ap处理的Cnga3-/-小鼠(Cnga3-/-CMV.R9ap;N=8)、用rAAV2/8.Rho.mR9ap处理的Cnga3-/-小鼠(Cnga3-/-Rho.R9ap;N=6)、未处理的Cnga3-/-小鼠(Cnga3-/-未处理的;N=8)、未处理的Gnat1-/-小鼠(Gnat1-/-未处理的;N=6)和未处理的C57BL6小鼠(C57BL6未处理的;N=6)记录ERG。

[0021] B.在用rAAV2/8.CMV.mR9ap处理的Cnga3-/-眼中,对长闪光的视网膜响应增加。空心矩形表示闪光的持续时间。注意到在用rAAV2/8.CMV.mR9ap处理的眼中,光刺激的持续时间增加时,响应是可检测的。相反,当在相同条件下同时记录时,未经处理的对侧眼显示出很少的响应或没有响应。

[0022] C.在用rAAV2/8.CMV.mR9ap处理的Cnga3-/-眼中,在明视条件下视网膜功能的增强。注意到经处理的眼在明视记录条件(20cd/m^2的白色背景光)下表现出响应,而同时记录的未经处理的对侧眼保持未响应。

[0023] 图6:在过表达R9AP的眼中,改变的光感受器信号向双极细胞的有效传输。

[0024] A.代表性的ERG迹线。使用饱和闪光(1.9log cd.s/m^2),在Cnga3-/-小鼠中注射rAAV2/8.CMV.mR9ap之后,记录ERG(红色迹线,下方的迹线)。将对侧眼用作未经处理的对照(黑色迹线,上方的迹线)。

[0025] B.闪光对双极细胞的延迟激活。在经处理的和未经处理的眼中,测量从ERG响应到饱和闪光(1.9log cd.s/m^2)的a波和b波隐含期。

[0026] C.从一只眼用rAAV2/8.CMV.mR9ap处理(红色曲线),另一只眼未处理(黑色曲线)的Cnga3-/-小鼠记录的a波和b波振幅的强度响应曲线。所有数据表示为平均值±平均值的标准误差。OE:过表达。

[0027] 图7:在Cnga3-/-小鼠中R9AP过表达之后,可持续的视觉感知的增加。

[0028] A.通过光动力学响应测量的改善的对比敏感度函数。在用rAAV2/8.Rho.mR9ap处理的Cnga3-/-小鼠的左眼中,差异化地测量针对正弦光栅的顺时针(代表经处理的左眼)和逆时针(代表未经处理的右眼)头部追踪移动的对比敏感度函数(CSF)。经处理的眼(红色曲线)的CSF比未经处理的眼(蓝色曲线)的CSF更好,所述未经处理的眼的CSF类似于未受影响的Cnga3-/-小鼠的CSF(黑色曲线;两只眼的平均值)。注意到经处理的眼的CSF等于(如果不是稍微好于)未受影响的野生型对照的CSF(绿色;两只眼的平均值)。对于全部组,N=5。所有数据表示为平均值±平均值的标准误差。OE:过表达。

[0029] B.在延长暴露于验光学测试之后，持续的视紫红质水平。使用扫描式分光光度计(绿色虚线框中的左图)的眼样品光吸收的代表性记录。从完全光漂白之前测量的眼样品的吸收(红色迹线)减去之后测量的眼样品的吸收(蓝色迹线，300和400nm之间的上方迹线)表示约380nm处的λmin峰值(对应于释放的光产物)，以及约500nm处的λmax峰值(代表样品中可漂白的视紫红质的量)(绿色虚线框中的右图)。暴露于7.0mW白光5分钟之后，通过测量Cnga3-/-小鼠中用rAAV2/8.Rho.mR9ap处理或未处理的瞳孔完全放大的眼中的差异光谱(λmax)来评估视紫红质漂白速度(左下图；平均值±平均值的标准误差)。还在rAAV2/8.Rho.mR9ap的单侧注射之后Cnga3-/-小鼠暴露于验光学测试最多达120分钟之后，测量视紫红质水平(右下图；各时间点N＝3)。灰色面积表示过夜暗适应之后从未受影响的Cnga3-/-小鼠(N＝8)记录的视紫红质水平(平均值±标准差)。点状线表示平均值。注意到在Cnga3-/-小鼠的用rAAV2/8.Rho.mR9ap处理的眼和未经处理的眼中，视紫红质水平保持稳定持续至少2小时。具有误差棒的数据表示为平均值±平均值的标准误差。

[0030] 图8：在Pde6c-/-小鼠中，R9AP的过表达增大了视杆光响应的恢复速率。

[0031] 与未经处理的对侧眼(σ＝约 11.46秒)相比，用rAAV2/8.CMV.mR9ap注射的Pde6c-/-眼(σ＝约5.75秒)中a波振幅50％恢复的时间常数(σ)降低约50％，这与治疗后光转导的加速失活一致。N＝6。具有误差棒的数据表示为平均值±平均值的标准误差。

[0032] 图9：在Pde6c-/-小鼠中，R9AP过表达导致强度响应曲线的“明视偏移”。

[0033] 在Pde6c-/-小鼠(N＝6)中，与未经处理的对侧眼相比，用rAAV2/8.CMV.mR9ap注射的眼表现出对增加的闪光强度的6HzERG响应的明视偏移。数据表示为相对于最大响应的％振幅，并且表示为平均值±平均值的标准误差。

[0034] 图10：在Cnga3-/-小鼠中，rAAV2/8.CMV.mR9ap注射后5个月时R9AP过表达的持续影响，没有清楚的视网膜变性的证据。

[0035] 针对最大振幅归一化的响应特征证明了对6Hz闪光的强度响应曲线的“明视偏移”(上图)。没有归一化的相同数据未示出在经处理的眼中振幅减小的证据(下图)。N＝5。数据表示为平均值±平均值的标准误差。

[0036] 图11：用rAAV2/8.Rho.mR9ap处理野生小鼠未显示出对6HzERG强度响应曲线的明显影响。

[0037] 在C57BL6小鼠(N＝5)中，与未经处理的对侧眼相比，用rAAV2/8.Rho.mR9ap处理的眼在6Hz ERG强度响应曲线中显示出没有偏移。数据表示为平均值±平均值的标准误差。

[0038] 图12：在C57BL6小鼠中，R9AP过表达之后视觉感知未增强。

[0039] 在仅用rAAV2/8.Rho.mR9ap处理左眼的C57BL6小鼠中，差异化地测量针对旋转正弦光栅的顺时针(代表经处理的左眼)和逆时针(代表未经处理的右眼)头部追踪移动的对比敏感度函数(CSF)。经处理的眼的CSF(粉色曲线)和未经处理的眼的CSF(浅蓝色曲线)显示出类似的结果，类似于未受影响的C57BL6小鼠的结果(绿色曲线；两只眼的平均值)。对于全部组，N＝5。数据表示为平均值±平均值的标准误差。OE：过表达。

具体实施方式

[0040] 本发明的载体包含这样的核酸，其表达产生基因产物(通常是蛋白质)，该基因产物将影响本文所述的眼病症的治疗，所述核酸与启动子可操作地连接以形成表达盒。

[0041] 核酸和基因产物

[0042] 本发明的载体包含编码基因产物的核酸，所述基因产物是光敏性的和/或在感光细胞中调节内源性光敏性信号传导，并且通过扩大视杆细胞响应的光强度范围和/或提高视杆细胞响应光的速度，使用本发明的核酸转导的视杆的性能更像视锥。因此，蛋白质本身可以是直接光敏性的，例如，它可以以导致光刺激后的超极化(外向电流)的方式改变视杆中的膜电导。这样的蛋白质例如为光敏性或光门控G偶联膜蛋白、离子通道、离子泵或离子转运蛋白。优选的光敏性蛋白包括ArchT、Jaws(cruxhalorhodopsin)(Chuong et al,2014)和iC1C2。或者，蛋白可自身不是直接光敏性的，但是可间接调节视杆感光细胞中的光敏性信号传导。这样的蛋白的实例为RGS9复合物成员，特别是R9AP(还称为RGS9BP)和Gβ5。或者，核酸可编码提高内源性视杆信号传导机制速度的任何其他基因产物。在所有这些情况下，序列可编码野生型蛋白或保留野生型蛋白活性的突变体或变体或截短形式。核酸也可以是为在靶细胞型中表达而经密码子优化的。

[0043] 在基因产物表达之后，视杆将以比普通强度更高的强度，表现出比未转导的视杆更强和/或更快的对光刺激的调节。实例包括提高的调节强度和/或更快的激活/失活动力学。因此，相对于未转导的视杆，根据本发明转导的视杆对中间视觉和/或明视觉范围中的照明反应更强和/或更快。优选地，视杆对暗视照明条件的响应未受影响或未受到实质影响，即视杆获得对更亮的光的强烈和/或快速响应的能力而不丧失对暗光响应的能力。

[0044] 启动子和其他调控元件

[0045] 在表达构建体中，编码基因产物的核酸通常可操作地连接至启动子。启动子可以是组成型的，但是优选为感光细胞特异性的或感光细胞优选的启动子，更优选为视杆特异性启动子或视杆优选的启动子，例如视紫红质(Rho)、神经视网膜特异性的亮氨酸拉链蛋白(NRL)或磷酸二酯酶6B(PDE6B)启动子。纳入于表达盒中的启动子区可以为任何长度，只要它有效驱动基因产物的表达，优选感光细胞特异性的表达或感光细胞优选的表达，或视杆特异性的表达或视杆优选的表达。

[0046] 感光细胞特异性启动子意指驱动仅在或基本上仅在感光细胞中表达的启动子，例如驱动在感光细胞中比在任何其他细胞型中强至少100倍的表达的启动子。视杆特异性启动子意指驱动仅在或基本上仅在视杆中表达的启动子，例如驱动在视杆中比在任何其他细胞型(包括视锥)中强至少100倍的表达的启动子。感光细胞优选的启动子意指优选在感光细胞中表达，但是也可在其他组织中驱动一定程度的表达的启动子，例如驱动在感光细胞中比在任何其他细胞类型中强至少2倍、至少5倍、至少10倍、至少20倍或至少50倍的表达的启动子。视杆优选的启动子意指优选在视杆中表达，但是也可在其他组织中驱动一定程度的表达的启动子，例如驱动在视杆中比在任何其他细胞类型(包括视锥)中强至少2倍、至少5倍、至少10倍、至少20倍或至少50倍的表达的启动子。

[0047] 除启动子之外，还可存在一种或多种其他调控元件，例如增强子。

[0048] 载体

[0049] 本发明的载体可以为任何类型，例如可以为质粒载体或微环DNA。

[0050] 然而，本发明的载体通常是病毒载体。病毒载体可例如基于单纯疱疹病毒、腺病毒或慢病毒。病毒载体可以是腺相关病毒(AAV)载体或其衍生物。病毒载体衍生物可以是嵌合、改组或衣壳修饰的衍生物。

[0051] 病毒载体可包含来自AAV天然来源的血清型、分离株或进化枝的AAV基因组。血清型可例如为AAV2、AAV5或AAV8。

[0052] 基因疗法的功效通常取决于供体DNA的充分而有效的递送。该过程通常由病毒载体介导。腺相关病毒(AAV)——细小病毒家族成员——通常用于基因疗法。包含病毒基因的野生型AAV将它们的基因组物质插入到宿主细胞的19号染色体中。AAV单链DNA基因组包含两个反向末端重复(ITR)和两个开放阅读框,包含结构(cap)和包装(rep)基因。

[0053] 对于治疗目的,除治疗性基因之外仅需要的顺式序列为ITR。因此,AAV病毒是被修饰的:从基因组除去病毒基因,产生重组AAV(rAAV)。这仅包含治疗性基因,两个ITR。病毒基因的去除使rAAV不能主动地将其基因组插入到宿主细胞DNA中。相反,rAAV基因组经由ITR融合,形成环状、游离的结构,或插入到预先存在的染色体断裂中。对于病毒产生,以辅助质粒的形式,反式提供已从rAAV去除的结构基因和包装基因。AAV是特别引人注意的载体,因为它通常是非致病性的;大多数人在他们生命过程中被这种病毒感染而未受到有害影响。

[0054] 眼组织的免疫赦免——解剖学屏障和免疫调控因子的结果——使眼在很大程度上免于AAV可在其他组织中引发的有害免疫应答(Taylor 2009)。

[0055] AAV载体受限于相对小的包装能力(约4.8kb)和转导后缓慢开始的表达。尽管存在这些小缺陷,AAV已成为视网膜基因疗法中最常使用的病毒载体。

[0056] 大多数病毒构建体基于AAV血清型2(AAV2)。AAV2通过硫酸肝素蛋白聚糖受体结合于靶细胞。类似于全部AAV血清型的基因组,AAV2基因组能够被包封于多种不同的衣壳蛋白中。AAV2可被包装在它的天然AAV2衣壳(AAV2/2)中或可与其他衣壳进行假型化(例如,AAV2基因组于AAV1衣壳中;AAV2/1、AAV2基因组于AAV5衣壳中;AAV2/5和AAV2基因组于AAV8衣壳中;AAV2/8)。

[0057] rAAV通过血清型特异性的受体介导的内吞作用而转导细胞。影响rAAV转基因表达动力学的主要因素是病毒粒子在内体内部脱壳的速率。这进一步取决于包封遗传物质的衣壳的类型(Ibid.)。脱壳之后,经由互补链的从头合成,通过形成双链分子而稳定线性单链rAAV基因组。使用自身互补的DNA可通过产生双链转基因DNA而绕过这一阶段。Natkunarajah et al(2008)发现,与单链AAV2/8相比,自身互补的AAV2/8基因表达起始更快并且表达量更高。因此,当与标准单链构建体的转基因表达相比时,通过避开与第二链合成相关的时间延迟,提高了基因表达水平。随后的调查其他AAV假型(例如AAV2/5)中自身互补的DNA的作用的研究产生了类似的结果。该技术的一个限制是,由于AAV具有约4.8kb的包装能力,自身互补的重组基因组必须是适当大小的(即约2.3kb或更小)。

[0058] 除了修饰包装能力,AAV2基因组与其他AAV衣壳的假型化能够改变细胞特异性和转基因表达的动力学。据报道,AAV2/8比AAV2/2或AAV2/5更有效地转导感光细胞(Natkunarajah et al.2008)。

[0059] 因此,本发明的载体可包含腺相关病毒(AAV)基因组或其衍生物。

[0060] AAV基因组是编码产生AAV病毒粒子所需的功能的多聚核苷酸序列。这些功能包括AAV在宿主细胞中复制和包装周期中运行的那些,包括将AAV基因组包入AAV病毒粒子的衣壳内。天然存在的AAV病毒是复制缺陷的并且依赖于提供的反式辅助功能以完成复制和包装周期。因此,在另外除去AAV rep和cap基因的情况下,本发明的载体的AAV基因组是复制缺陷型的。

[0061] AAV基因组可以是正义或反义单链形式，或者是双链形式。双链形式的使用使得避开靶细胞中的DNA复制步骤，因此能够加速转基因表达。AAV基因组可以来自任何天然来源的AAV血清型或分离株或进化枝。如本领域技术人员已知的，可根据各种生物系统对天然存在的AAV病毒进行分类。

[0062] 通常，按照AAV病毒的血清型来提及它们。血清型对应于AAV的变异亚种，其由于衣壳表面抗原的表达特征而具有独特的反应性，这可用于将其与其他变异亚种区分开。通常，具有特定AAV血清型的病毒无法有效地与特异性针对任何其他AAV亚型的中和抗体进行交叉反应。AAV亚型包括AAV1、AAV2、AAV3、AAV4、AAV5、AAV6、AAV7、AAV8、AAV9、AAV10和AAV11，以及重组血清型，例如最近从灵长类动物脑鉴定的Rec2和Rec3。在本发明的载体中，基因组可源自任何AAV血清型。衣壳也可源自任何AAV血清型。基因组和衣壳可源自相同血清型或不同血清型。

[0063] 在本发明的载体中，优选基因组源自AAV血清型2(AAV2)、AAV血清型4(AAV4)、AAV血清型5(AAV5)或AAV血清型8(AAV8)。最优选基因组源自AAV2，但是其他特别适用于本发明的血清型包括AAV4、AAV5和AAV8，其有效转导眼中的组织，例如视网膜色素上皮。优选衣壳源自AAV5或AAV8，特别是AAV8。

[0064] 对AAV血清型的综述可参见Choi et al(Curr Gene Ther.2005;5(3);299-310)和Wu et al(Molecular Therapy.2006;14(3),316-327)。用于本发明的AAV基因组序列或AAV基因组元件的序列(包括ITR序列、rep或cap基因)可源自以下AAV全基因组序列的登录号：腺相关病毒1 NC_002077、AF063497；腺相关病毒2 NC_001401；腺相关病毒3 NC_001729；腺相关病毒3B NC_001863；腺相关病毒4 NC_001829；腺相关病毒5 Y18065、AF085716；腺相关病毒6 NC_001862；鸟类AAV ATCC VR-865AY186198、AY629583、NC_004828；鸟类AAV毒株DA-1 NC_006263、AY629583；牛AAV NC_005889、AY388617。

[0065] AAV病毒也可按照进化枝或克隆来提及它们。这是指天然来源的AAV病毒的系统发生关系，通常是指可追溯到共同祖先的AAV病毒的系统发生群，并且包括其所有后代。另外，AAV病毒可按照具体的分离株(即在自然界发现的具体AAV病毒的遗传分离株)来提及。术语遗传分离株描述了这样的AAV病毒群体，其与其他天然存在的AAV病毒进行了有限的遗传混合，从而在遗传水平上定义了可识别的独特的群体。

[0066] 可用于本发明的AAV的进化枝和分离株的实例包括：

[0067] 进化枝A：AAV1 NC_002077、AF063497、AAV6 NC_001862、Hu.48 AY530611、Hu 43AY530606、Hu 44AY530607、Hu 46AY530609；

[0068] 进化枝B：Hu.19 AY530584、Hu.20 AY530586、Hu 23AY530589、Hu22 AY530588、Hu24 AY530590、Hu21 AY530587、Hu27AY530592、Hu28 AY530593、Hu 29AY530594、Hu63AY530624、Hu64 AY530625、Hu13 AY530578、Hu56 AY530618、Hu57AY530619、Hu49 AY530612、Hu58 AY530620、Hu34 AY530598、Hu35AY530599、AAV2 NC_001401、Hu45 AY530608、Hu47 AY530610、Hu51 AY530613、Hu52 AY530614、Hu T41 AY695378、Hu S17 AY695376、Hu T88 AY695375、Hu T71 AY695374、Hu T70 AY695373、Hu T40AY695372、Hu T32AY695371、Hu T17 AY695370、Hu LG15 AY695377；

[0069] 进化枝C：Hu9 AY530629、Hu10 AY530576、Hu11 AY530577、Hu53 AY530615、Hu55 AY530617、Hu54 AY530616、Hu7 AY530628、Hu18 AY530583、Hu15 AY530580、Hu16

AY530581、Hu25 AY530591、Hu60 AY530622、Ch5 AY243021、Hu3 AY530595、Hu1 AY530575、Hu4 AY530602 Hu2、AY530585、Hu61 AY530623；

[0070] 进化枝D：Rh62 AY530573、Rh48 AY530561、Rh54 AY530567、Rh55 AY530568、Cy2 AY243020、AAV7 AF513851、Rh35 AY243000、Rh37 AY242998、Rh36 AY242999、Cy6 AY243016、Cy4 AY243018、Cy3 AY243019、Cy5 AY243017、Rh13 AY243013；

[0071] 进化枝E：Rh38 AY530558、Hu66 AY530626、Hu42 AY530605、Hu67 AY530627、Hu40 AY530603、Hu41 AY530604、Hu37 AY530600、Rh40 AY530559、Rh2 AY243007、Bb1 AY243023、Bb2 AY243022、Rh10 AY243015、Hu17 AY530582、Hu6 AY530621、Rh25 AY530557、Pi2 AY530554、Pi1 AY530553、Pi3 AY530555、Rh57 AY530569、Rh50 AY530563、Rh49 AY530562、Hu39 AY530601、Rh58 AY530570、Rh61 AY530572、Rh52 AY530565、Rh53 AY530566、Rh51 AY530564、Rh64 AY530574、Rh43 AY530560、AAV8 AF513852、Rh8 AY242997、Rh1 AY530556；

[0072] 进化枝F：Hu14(AAV9)AY530579、Hu31 AY530596、Hu32 AY530597、克隆分离株AAV5 Y18065、AF085716、AAV 3NC_001729、AAV 3B NC_001863、AAV4 NC_001829、Rh34 AY243001、Rh33 AY243002、Rh32 AY243003。

[0073] 技术人员能够根据他们的公知常识选择用于本发明的适当的AAV血清型、进化枝、克隆或分离株。然而，应理解，本发明还涵盖了可能尚未被鉴定或表征的其他血清型的AAV基因组的用途。AAV血清型决定了AAV病毒感染的组织特异性(或趋向性)。因此，根据本发明用于给予患者的AAV病毒的优选的AAV血清型为对视杆细胞具有天然趋向性或具有视杆细胞高效感染率的那些。

[0074] 通常，天然来源的AAV血清型或分离株或进化枝的AAV基因组包含至少一个反向末端重复序列(ITR)。本发明的载体通常包含两个ITR，优选在基因组的每个末端各一个。ITR序列顺式发挥作用以提供复制的功能起点并且允许载体与细胞基因组的整合和从细胞基因组的切除。优选的ITR序列为AAV2及其变体的那些。AAV基因组通常包含包装基因，例如编码AAV病毒粒子的包装功能的rep和/或cap基因。Rep基因编码蛋白Rep78、Rep68、Rep52和Rep40或其变体中的一种或多种。Cap基因编码一种或多种衣壳蛋白，例如VP1、VP2和VP3或其变体。这些蛋白组成AAV病毒粒子的衣壳。在下文中讨论衣壳变体。

[0075] 优选地，AAV基因组将为给予患者而被衍生化。这样的衍生化是本领域标准的，并且本发明涵盖了任何已知的AAV基因组衍生物和可通过利用本领域已知的技术而产生的衍生物的用途。AAV基因组的衍生化和AAV衣壳的衍生化参见例如上文中引用的Choi et al和Wu et al。

[0076] AAV基因组的衍生物包括允许在体内从本发明的载体表达Rep-1转基因的任何截短或修饰形式的AAV基因组。通常，可显著截短AAV基因组以包含最小病毒序列但仍然保留以上功能。这优选是为了安全性原因以降低载体与野生型病毒重组的风险，同时避免由靶细胞中存在的病毒基因蛋白引起细胞免疫应答。

[0077] 通常，衍生物将包含至少一种反向末端重复序列(ITR)，优选多于一种ITR，例如两种ITR或多种。一种或多种ITR可源自具有不同血清型的AAV基因组，或可以是嵌合或突变ITR。优选的突变ITR具有trs(末端分解位点)缺失。该缺失允许基因组持续复制以产生包含编码序列和互补序列的单链基因组(即自身互补的AAV基因组)。这使得避开靶细胞中的DNA复制，并因此能够加速转基因表达。

[0078] 一种或多种ITR优选在本发明的包含启动子和转基因的表达构建体盒的侧翼。包含的一种或多种ITR优选辅助将本发明的载体包装到病毒粒子中。在优选的实施方案中，ITR元件将是从衍生物的天然AAV基因组中保留的唯一序列。因此，衍生物将优选不包含天然基因组的rep和/或cap基因和天然基因组的任何其他序列。这优选由于上述原因，以及为了降低载体整合到宿主细胞基因组中的可能性。此外，减小AAV基因组的大小使得能够增大将转基因以外的其他序列元件(例如调控元件)纳入到载体中的灵活性。关于AAV2基因组，因此在本发明的衍生物中可除去以下部分：一个反向末端重复(ITR)序列、复制(rep)和衣壳(cap)基因。然而，在一些实施方案中，包括体外实施方案中，衍生物可另外包含一个或多个rep和/或cap基因或AAV基因组的其他病毒序列。

[0079] 衍生物可以是一种或多种天然存在的AAV病毒的嵌合、改组或衣壳修饰的衍生物。本发明涵盖了提供在相同载体内的来自AAV的不同血清型、进化枝或分离株的衣壳蛋白序列。本发明涵盖了将一种血清型的基因组包装到另一种血清型的衣壳中，即假型化。

[0080] 通常选择嵌合、改组或衣壳修饰的衍生物以提供病毒载体的一种或多种所需功能。因此，与包含天然存在的AAV基因组(例如AAV2的基因组)的AAV病毒载体相比，这些衍生物可表现出增加的基因递送效率、降低的免疫原性(体液或细胞)、改变的趋向性范围和/或改善的对特定细胞型的靶向。增加的基因递送效率可受到改善的细胞表面受体或共受体结合、改善的内化作用、改善的细胞内和到细胞核中的运输、改善的病毒离子脱壳和改善的单链基因组向双链形式的转化的影响。增加的效率也可涉及改变的趋向性范围或特定细胞群靶向，以使载体剂量未因给予至不需要载体的组织而被稀释。

[0081] 嵌合的衣壳蛋白包括通过两种或多种天然存在的AAV血清型的衣壳编码序列之间的重组而产生的那些。这可例如通过标记获救法来实施，在标记获救法中，用不同血清型的衣壳序列共转染非传染性的一种血清型的衣壳序列，并且使用定向选择来正选择具有所需特性的衣壳序列。不同血清型的衣壳序列可通过细胞内的同源重组来改变，以产生新型嵌合衣壳蛋白。嵌合的衣壳蛋白也包括通过改造衣壳蛋白序列以将特定的衣壳蛋白结构域、表面环或特定的氨基酸残基转移到两种或多种衣壳蛋白之间(例如两种或多种不同血清型的衣壳蛋白之间)而产生的那些。

[0082] 改组或嵌合的衣壳蛋白也可通过DNA改组或通过易错PCR产生。杂合的AAV衣壳基因可通过以下方法产生：随机使相关AAV基因(例如编码多种不同血清型的衣壳蛋白的那些)的序列片段化，然后在自引发聚合酶反应中重新组装片段，这也可导致序列同源区中的交换。可对以这种方式、通过改组若干血清型的衣壳基因而产生的杂合AAV基因文库进行筛选以鉴定具有所需功能的病毒克隆。类似地，易错PCR可用于使AAV衣壳基因随机突变以产生多种变体文库，然后在文库中正选择所需特性。

[0083] 也可对衣壳基因的序列进行遗传修饰以引入相对于天然野生型序列的特定的缺失、置换或插入。具体地，可通过在衣壳编码序列的开放阅读框内或在衣壳编码序列的N端和/或C端插入非相关蛋白或肽的序列来修饰衣壳基因。

[0084] 非相关蛋白或肽可有利地作为特定细胞型的配体而起作用，从而赋予对靶细胞改善的结合或改善载体靶向至特定细胞群的特异性。

[0085] 非相关蛋白也可以是辅助病毒粒子的纯化(作为产生过程的一部分)的蛋白，即表位或亲和标签。通常将选择插入位点以不影响病毒粒子的其他功能，例如内摄作用、病毒粒

子的运输。技术人员能够根据他们的公知常识鉴定适合的插入位点。特定的位点公开于上文引用的Choi et al中。

[0086] 本发明另外涵盖了以与天然AAV基因组不同的次序和构型提供AAV基因组序列。本发明还涵盖了用来自另一种病毒的序列或用由多于一种病毒的序列组成的嵌合基因置换一种或多种AAV序列或基因。这样的嵌合基因可由来自两种或多种不同病毒物种的相关病毒蛋白的序列组成。

[0087] 本发明的载体为病毒载体形式，其包含本发明的启动子和表达构建体。

[0088] 本发明还提供了包含本发明的载体的AAV病毒粒子。本发明的AAV粒子包括转衣壳形式，其中具有一种血清型的ITR的AAV基因组或衍生物被包装到不同血清型的衣壳中。本发明的AAV粒子还包括嵌合形式，其中来自两种或多种不同血清型的未经修饰的衣壳蛋白混合物组成病毒包膜。AAV粒子还包括经化学修饰的形式，其具有被吸附到衣壳表面的配体。例如，所述配体可包括靶向特定细胞表面受体的抗体。

[0089] 本发明另外提供了包含本发明的载体或AAV病毒粒子的宿主细胞。

[0090] 本发明的载体可通过本领域已知的用于提供基因疗法载体的标准方法来制备。因此，明确确定的公开的结构域转染、包装和纯化方法可用于制备适合的载体制品。

[0091] 如上文所讨论的，本发明的载体除本发明的启动子以外还可包含天然存在的AAV病毒的全基因组或其变体。然而，通常使用衍生基因组，例如具有至少一个反向末端重复序列(ITR)，但是可缺少任何AAV基因(例如rep或cap)的衍生物。

[0092] 在这样的实施方案中，为了将衍生基因组组装到AAV病毒粒子中，在宿主细胞中与衍生基因组组合提供另外的遗传构建体(提供AAV和/或辅助病毒功能)。这些另外的构建体通常包含编码结构AAV衣壳蛋白(即cap、VP1、VP2、VP3)的基因和编码AAV生命周期所需的其他功能的基因(例如rep)。在另外的构建体上提供的结构衣壳蛋白的选择将决定所包装的病毒载体的血清型。

[0093] 用于本发明的特别优选的包装的病毒载体包含与AAV5或AAV8衣壳蛋白组合的衍生的AAV2基因组。

[0094] 如上文提及，AAV病毒无法进行复制，因此通常还在一种或多种另外的构建体上提供辅助病毒功能，优选腺病毒辅助功能以允许AAV复制。

[0095] 在宿主细胞中，全部上述另外的构建体可提供为质粒或其他游离元件，或者可将一种或多种构建体整合到宿主细胞基因组中。

[0096] 药物组合物、剂量和治疗

[0097] 可将本发明的载体配制成药物组合物。这些组合物除载体以外还可包括可药用的赋形剂、载体、缓冲剂、稳定剂或本领域技术人员公知的其他材料。这样的材料应当是无毒的，并且不应当影响活性成分的功效。技术人员根据给药途径(即，本文中的直接视网膜注射、视网膜下注射或玻璃体内注射)可确定载体或其他材料的准确性质。

[0098] 药物组合物通常为液体形式。液体药物组合物通常包括液体载体，例如水、石油、动物油或植物油、矿物油或合成油。可包括生理盐水、氯化镁、右旋糖或其他糖溶液或二醇类，例如乙二醇、丙二醇或聚乙二醇。在一些情况下，可使用表面活性剂，例如普流尼克酸(PF68)0.001％。

[0099] 对于在患处的注射，活性成分为水溶液形式，其无热原并且具有适合的pH、等渗性

和稳定性。本领域相关技术人员能够使用例如等渗载体(例如氯化钠注射剂、林格氏注射剂、乳酸林格氏注射剂、哈特曼注射剂)来制备适合的溶液。根据需要,可包括防腐剂、稳定剂、缓冲剂、抗氧化剂和/或其他添加剂。

[0100] 对于延迟释放,药物组合物中可包括为了缓释而配制的载体,例如根据本领域已知的方法在从生物相容性聚合物形成的微囊中或在脂质体载体系统中。本发明的载体和/或药物组合物可包装成试剂盒。

[0101] 通常,优选本发明的载体的直接视网膜递送、视网膜下递送或玻璃体内递送,通常是通过注射。因此优选递送到视网膜、视网膜下空间或玻璃体内空间。也可在体外将载体引入视杆细胞后将细胞移植到视网膜。

[0102] 本发明的载体和/或药物组合物也可与任何其他用于治疗或预防视觉障碍的疗法结合使用。例如,它们可与已知的使用VEGF拮抗剂(例如抗VEGF抗体如贝伐珠单抗(Bevacizumab)或雷珠单抗(Ranibizumab))或可溶性受体拮抗剂(例如阿柏西普(Aflibercept))的治疗结合使用,用于治疗如本文讨论的AMD或其他眼病。

[0103] 剂量和剂量方案可在负责给予组合物的医学从业者的常规技术范围内确定。本发明的载体的剂量可根据多个参数来确定,特别是根据待被治疗的患者的年龄、体重和病症;给药途径和所需的方案来确定。同样,医生能够确定任何特定患者所需的给药途径和剂量。

[0104] 根据需要转导的视网膜组织的量,典型的单剂量为10^{10}至10^{12}个基因组粒子。基因组粒子在本文中被定义为包含单链DNA分子的AAV衣壳,所述DNA分子可用序列特异性方法(例如实时PCR)来定量。该剂量可被提供为单剂量,但是对于对侧眼或在由于任何原因(例如手术并发症)载体可能未靶向到正确的视网膜区的情况下,可重复该剂量。治疗优选为针对每只眼的单一永久性治疗,但是可以考虑重复注射,例如在未来若干年中和/或使用不同的AAV血清型。

[0105] 治疗

[0106] 本发明的载体可用于治疗任何眼病,其中存在视锥功能障碍、变性或缺失,但是至少保留了一些健康的视杆。视锥功能可全部缺失或部分缺失,例如至少10%、至少25%、至少50%、至少75%、至少80%、至少90%或更多缺失。健康的视杆是在感知暗视水平的光方面能够实现正常或部分视杆功能,例如至少10%、至少25%、至少50%、至少75%或至少90%的正常视杆功能的视杆。

[0107] 可使用本发明的载体来治疗的病症因此包括黄斑变性、全色盲和利伯先天性黑矇。黄斑变性可以是年龄相关性黄斑变性(AMD),例如湿性或新生血管性AMD或地图状萎缩、遗传性黄斑变性病症或遗传性视锥营养不良。在一些实施方案中,本发明将导致产生"假中央凹"——一小片类似于视锥的视杆,其在中央凹视锥丧失或功能障碍的病症中改善视觉。

[0108] 通常,待用本发明的载体治疗的患者为人类患者。他们可以是任何年龄的男性或女性。

[0109] 以下实施例说明本发明。

[0110] 实施例

[0111] 实施例1——ArchT实验方法

[0112] 动物

[0113] 从Harlan实验室(英国Blackthorn)购买野生型小鼠(C57BL/6J)。圈养CNGA3-/-和

PDE6C-/-小鼠。将全部小鼠维持在周期光(12h光照-黑暗)条件下;在光周期中笼照明为7英尺-烛光。所有实验获得当地机构动物护理和使用委员会(英国伦敦,UCL)的批准,并且符合神经科学学会和视觉和眼科学研究协会(Rockville,MD)采用的动物护理和使用准则。

[0114] 质粒构建、病毒产生和注射步骤

[0115] 转基因构建体(ArchT-EGFP)由Prof Ed Boyden(MIT,USA)惠赠,并且包含与荧光蛋白EGFP融合的ArchT基因的cDNA序列。将质粒包装成AAV8以产生重组AAV病毒载体AAV8.hRho.ArchT-EGFP。通过如之前所述的三重瞬时转染法产生重组的AAV8载体。将质粒构建体、AAV血清型特异性包装质粒和辅助质粒与聚乙烯亚胺(Polysciences Inc.)混合以形成转染复合物,然后将该转染复合物添加到293T细胞并放置72h。收集细胞、浓缩并裂解以释放载体。使用AVB Sepharose柱(GE Healthcare)来纯化AAV8。将二者在1X PBS中洗涤并浓缩至体积100-150μL。通过比较从纯化的病毒原种制备的斑点印迹DNA和确定的质粒对照来确定病毒粒子滴度。用于所有实验的纯化的载体浓度为5×10^{12}病毒粒子/mL。如我们组之前所述进行视网膜下注射,其由两次注射组成,每次2μL。

[0116] 免疫组织化学

[0117] 对动物施安乐死术,摘除眼球并取出角膜、晶状体和虹膜。对于视网膜切片,室温下在4%多聚甲醛(PFA)中固定眼杯(eyecup),然后包埋于最适切割温度(OCT)培养基中。径向切出30μm冷冻切片,在PBS中冲洗,并在10%正常山羊血清(NGS)、3%牛血清白蛋白(BSA)和0.1%Triton-X100中封闭。4℃下使用兔抗视锥抑制蛋白(1:500稀释),在封闭液中用一级抗体过夜孵育各样品。PBS洗涤之后,二级抗体(全部1:500稀释,life technologies)(包括山羊抗兔Alexa Fluor 546(#A11035)、山羊抗小鼠Alexa Fluor 633(#A21052)和链霉亲和素、Alexa Fluor 633缀合物(#S21375))的各结合物用于标记样品,然后将这些用DAPI进行反染色,并用DAKO荧光封固剂(DAKO,S3023,Denmark)封固。通过共焦显微镜(Leica DM5500Q)获取图像。

[0118] 单光感受器吸入记录

[0119] 使动物在暗处适应12h,然后开始实验。经由腹膜腔给予小鼠过量的氯胺酮-dormitor麻醉混合物以诱导终端手术级麻醉。然后通过颈椎脱位术处死小鼠并摘除眼球。将眼在弱远红外照明下解剖。将分离的视网膜包埋于1%低熔解琼脂糖溶液中,然后使用vibrotome(leica)切成230μm厚面对面(en face)的切片。将切片封固在记录室中并用包含100μM 9-顺式视黄醛(Sigma)和0.2%BSA(Sigma)的卡波金(95%O_2,5%CO_2)饱和的Ames培养基灌注。在反馈控制(Scientifica)下使用线内加热元件将灌注液的温度保持在37℃。使用Narishige PC-10垂直拉制器从丝状硼硅酸盐玻璃毛细管(Harvard Apparatus Ltd)制造电阻非常低(1-2MΩ)的膜片吸管(patch pipette)。将吸管用外部溶液填充,放置到探头(headstage)上并在尖端施加较小的压力(约30mbar)。使用红外照明,将辅助看见吸管的显微镜放置到视网膜表面,然后降低约50μm到切片中,直到光感受器段显现出完整且整齐的排列。随着吸管尖端缓慢穿过视网膜组织,在吸管尖端施加轻微的负压,使用100ms,10mV测试脉冲以监测经过吸管尖端的阻抗。当阻抗升至约20-30MΩ时,检测光引发的响应。将来自与液芯光导管偶联的LED光源的光刺激(峰波长530nm)传递通过显微镜物镜(Olympus)。使用中性密度滤波器准确控制光刺激的密度。光刺激由方形波脉冲组成,该方形波脉冲用P-Clamp软件(Molecular Devices)编程并经由DAC板(Axon Instruments)(与LED驱动器

(Thorlabs)连接)传递。使用Multiclamp 700B放大器(Molecular Devices)进行电生理记录。在20kHz下将数据数字化。

[0120] MEA记录

[0121] 使动物在暗处适应12h,然后开始实验。经由腹膜腔给予小鼠过量的氯胺酮-dormitor麻醉混合物以诱导终端手术级麻醉。然后通过颈椎脱位术处死小鼠并摘除眼球。在弱红光下,将眼在卡波金(95%O_2,5%CO_2)饱和的Ames培养基(Sigma)中解剖。小心取出角膜和晶状体以从视网膜表面除去尽可能多的玻璃体。从视网膜分离RPE,并且从视网膜"杯"切除横向1-3mm的平瓣(flat petal)。将该视网膜瓣放置在多电极阵列表面上下方的神经节细胞一侧,使用由惰性铂丝(Sigma)和尼龙构成的环形harm以将瓣保持在原位。在记录过程中,将组织用卡波金饱和的Ames培养基(Sigma)灌注,保持在36.5℃的温度下。对于包括暗视或中间视觉条件的记录,制备灌注培养基以包括0.2%BSA(Sigma)中的浓度为100μM的9-顺式视黄醛(Sigma)。使用多孔的60电极记录阵列——由间隔100μm的钨电极(MultiChannel Systems)组成——记录神经节细胞的胞外电势。使用MC Rack软件(MultiChannel Systems),通过MC Card系统将电压改变放大并在50kHz下数字化。

[0122] 电生理数据分析

[0123] 使用IgorPro 6中的定制手写宏指令来分析电生理数据。使用振幅阈值算法来检测突触电流和电势,在该算法中将事件检测的阈值设定为基线噪声(通常约10pA)的标准差的2倍。通过仔细检查所有电生理数据来手动确认检测的电流和电势。

[0124] 恐惧条件反射

[0125] 使用市售的恐惧条件反射系统(Med Associates)训练和测试小鼠。为了确保盲条件,进行训练和测试的实验者始终不知晓小鼠品种和处理条件。简言之,装备由调节箱(20×30cm)组成,所述箱具有被放置在减音隔间内部的不锈钢格栅地板。在训练和测试期间,通过内装的红外数字视频摄像机(采集速率30帧/秒)和红外照明来持续监测小鼠行为。视频冻结软件(Med Associates)用于控制光刺激和电击的传递。光刺激由单次LED(530nm,Thorlabs)5Hz 50ms完全亮度闪光组成,该闪光由放置在调节箱侧板上的Arduino界面(Arduino软件)产生。为了确保训练和测试发生的背景不同,对于测试期,将地板和弧形墙板插入到箱中。将背景用于降低视杆激活的概率,用托吡卡胺(Tropicamide)滴剂使瞳孔放大以增加到达小鼠视网膜的光的量。

[0126] 将小鼠放置到箱内并使其经历一个调节期,该调节期由6对都以2s、0.65mA足部点击结束的5s光刺激组成。试验之间的间隔是假随机的(平均间隔90s)。在训练期之后,使小鼠返回到原来的笼中。训练后24小时,测试小鼠的视觉线索记忆回忆。将小鼠放置在测试箱中并监测共360s。在测试期最后的120s中连续给予调节光刺激。获取所有数据并自动通过VideoFreeze软件(Med Associates)记录。简言之,在将动物放置到箱中之前校准软件。然后软件测量每个视频帧之间发生的像素变化。将移动阈值设定得尽可能低(20个移动指数单位),将连续冻结计数设置为帧率以确保最灵敏的移动读出。为了评估光线索记忆回忆,在光刺激开始之前和开始后的2分钟,求冻结行为的时间百分数的平均值。使用单因素ANOVA来评估统计学显著性。结果表示为平均值±S.E.M。

[0127] 验光学(Optomotry)

[0128] 通过观察小鼠对旋转正旋光栅(OptoMotry,Cerebral Mechanics)的视动反应来

测量视敏度。由于只有颞部到鼻方向上的移动引起追踪反应，根据两只眼对图案旋转的不同敏感度，使用的方案产生右眼和左眼敏感度的独立测量。因此，右眼和左眼分别对逆时针方向(CCW)和顺时针方向(CW)的旋转最敏感。使用不同时间频率的刺激确定反应存在的阈值。使用双盲两次替代性强制选择步骤，其中观察者对图案旋转的方向、对是否是经ArchT处理的或未经处理的CNGA3-/-或PDE6C-/-小鼠或年龄匹配的野生型对照动物(C57BL6)是“不知晓”的。在单独的4天进行4次试验之后，测量测试动物两只眼的视敏度，求平均值或单独分析每只眼的视敏度。在与年龄匹配的等基因对照共同处理之后3-10周，对经注射的小鼠进行测量。

[0129] 实施例2——视杆细胞中的ArchT表达赋予了以快速非漂白响应作出响应的能力

[0130] 优化低光水平的视杆介导的视觉，包括单光子检测。然而，视杆比不上视锥对光反应的快速发生和恢复(Fu et al.,2007,Pugh et al.,1999)。当在病症中(例如在年龄相关性黄斑变性中)视锥介导的视觉丧失时、在中央凹中紧密堆叠的视锥变性时(de Jong 2006)，这种用于确保在不同环境中的可靠视觉的功能差异减弱。研究了视杆是否能够对刺激更快地响应和恢复，这有助于缓解由视锥丧失引起的功能损伤。

[0131] 在视杆细胞中表达快速光驱动的质子泵(Han et al.,2011)。将携带视紫红质启动子(Rho)控制下的ArchT-EGFP的AAV8粒子经视网膜下注射到成年小鼠中。Rho-ArchT-EGFP的表达限于视杆细胞膜(图1a-b)。通过免疫组织化学能够容易地区分表达Rho-ArchT-EGFP的视杆的突触末端和视锥(图1c)。对视锥的分类群进行的定量PCR证实Rho-ArchT-EGFP表达是视杆群特异性的，并且在AAV8注射后最长达6个月未观察到任何明显的毒性征象。ArchT表达允许极其快速的光响应，而固有的视锥响应被保留并且与在非转导的视杆细胞中观察到的响应相当(图1d)。在所有测试小鼠模型中，从表达ArchT的视杆记录的光引发的电流证明了比固有的视杆电流快得多的动力学(图2a-b)。这些动力学使光引发的电流被调整到最高达80Hz，远高于视杆(约为20Hz)(图2a-c)和视锥的极限(Fu et al.,2007)。

[0132] 出乎意料的是，ArchT表达并未改变视杆细胞的特性，然而赋予了以快速非漂白响应作出响应的能力(图2e)。

[0133] 实施例3——表达ArchT的视杆在高光强度下和与视锥细胞的频率接近的频率下驱动持续的RGC脉冲

[0134] 接下来研究了视杆驱动的电路能否跟随比正常更快的视杆驱动的视觉。视杆和视锥途径表现出一些相似性和一些显著差异，因此不清楚视杆电路能否可靠地维持快速的“类似于视锥的”传输(**Wässle** et al.,2004)。视杆已显示出直接接触OFF“视锥”双极细胞(Soucy et al.,1998和Hack et al.,1999)，成对脉冲刺激表明该旁路途径可以与视锥至OFF双极途径一样快(Li et al.,2010)。然而，不清楚该响应如何持续以及视杆(ON)双极细胞能否也保持快速传输。此外，与视锥相比，视杆突触末端具有不同大小和超结构组织，视杆双极细胞不与视网膜神经节细胞(RGC)直接接触，但是仅通过涉及AII无长突细胞的途径接触(**Wässle** et al.,2004)。为了研究视杆途径能够达到的最大速度，进行来自缺少视锥功能的小鼠模型中的RGC的多电极记录，以分离视杆介导的RGC输出。非转导的视网膜中的RGC中的视锥驱动的响应在高光水平下被漂白，并且无法跟随高于约20Hz的刺激频率(图2f)。

[0135] 相反，表达ArchT的视杆在高光强度下和与视锥细胞的频率接近的频率下驱动持

续的RGC脉冲(图2f)。

[0136] 实施例4——Rho-ArchT-EGFP的表达扩大了缺少视锥介导的视觉的小鼠对亮光刺激的灵敏度

[0137] 为了使这种快于正常的视杆视觉有用,推断小鼠应当能够使用ArchT介导的电流以可靠地响应于明亮且快速的刺激。缺少视锥介导的视觉的CNGA3$^{-/-}$和PDE6C$^{-/-}$小鼠(Biel et al.,1999和Change et al.,2009)无法学习恐惧条件反射范式,其中亮光刺激是成对的并且共同以中度足部电击结束(图3a)。然而,Rho-ArchT-EGFP表达扩大了这些小鼠对亮光刺激的敏感度,使小鼠学习视觉刺激和电击之间的关联(图3a)。最终,测试ArchT表达是否赋予CNGA3$^{-/-}$和PDE6C$^{-/-}$小鼠快速视觉。通过视动测试(Umino et al.,2008)对视觉速度的评估表明,表达ArchT的小鼠与没有经历视网膜下病毒注射的小鼠和仅接受GFP载体的小鼠相比,能够更快地追随刺激(图3b)。表达ArchT的小鼠能够追随的刺激的最大频率类似于视锥细胞的频率(图3b)。

[0138] 这些结果共同表明,相对于通过视杆固有的光转导级联,能够更快地驱动视杆,并且视杆驱动的电路能够维持更快的信号传导。重要的是,从视杆的突触释放不需要大电压波动,但是小电流反而能够导致充分的电压变化而显著改变它们的突触传输(Cangiano et al.,2012)。这将本发明的用途扩大到比大多数其他神经元中的活动的光遗传操控所需的平均光水平低若干倍的光水平(Han et al.,2011)。

[0139] 实施例5——RPAP实验方法

[0140] 动物

[0141] 将C57BL6(英国Harlan)、Cnga3-/-(密歇根大学,J.R.Heckenlively)、Pde6c-/-(密歇根州密歇根大学,J.R.Heckenlively)(Chang et al.,2009)和Gnat1-/-(马萨诸塞州,塔夫茨大学医学院,J.Lem)(Calvert et al.,2000)小鼠维持在伦敦大学学院的动物设备中。病毒注射时成年雄性和雌性动物为6-12周龄,并且在注射后至少2周用于实验以使R9AP充分表达。所有使用的小鼠为2至6月龄,并且在给定实验组之间的月龄匹配。全部实验根据神经科学研究中的动物和人类使用政策以及眼和视觉研究中动物使用的ARVO声明进行。将动物维持在标准12/12小时光照-黑暗周期。

[0142] 质粒构建和重组AAV8的产生

[0143] 使用被设计以涵盖全部编码区的引物从鼠视网膜cDNA PCR扩增出鼠R9ap cDNA。在启动子(CMV启动子或牛视紫红质启动子)和SV40多聚腺苷酸化位点之间克隆R9ap cDNA。这些质粒用于产生两种假型化的AAV2/8病毒载体rAAV2/8.CMV.mR9ap和rAAV2/8.Rho.mR9ap,如以下所述。

[0144] 通过之前所述的三次瞬时转染法来产生重组AAV2/8载体(Gao et al.,2002)。将质粒构建体、AAV血清型特异性包装质粒和辅助质粒与聚乙烯亚胺混合以形成转染复合物,然后将该复合物添加到293T细胞并放置72h。收集细胞、浓缩并裂解以释放载体。通过亲和色谱法纯化AAV2/8并使用超滤柱(Sartorius Stedim Biotech,Goettingen,Germany)浓缩,在PBS中洗涤并浓缩至体积100-150μL。通过斑点印迹法或通过实时PCR来确定病毒粒子滴度。使用的纯化的载体浓度为1-2×10^{12}个病毒粒子/mL。

[0145] 视网膜电图(ERG)

[0146] 使用市售的系统(Espion E2,Diagnosys LLC,Lowell,MA),在使小鼠进行过夜黑

暗适应之后从两只眼记录ERG。记录前使用比例为5:3:42的盐酸美托咪啶(1mg/ml)、氯胺酮(100mg/ml)和水的0.007ml/g混合物的腹膜内注射剂来麻醉动物。使用2.5%苯肾上腺素和1.0%托吡卡胺,使瞳孔完全放大。首先放置中线皮下接地(ground)电极和口腔参照电极,然后放置阳性银电极,使其在弱红光照明下轻触角膜中心。将一滴Viscotears 0.2%液体凝胶(Dr.Robert Winzer Pharma/OPD Laboratories,Watford,UK)放置在阳极上方以在记录期间保持角膜润湿,并使小鼠进一步适应黑暗5分钟。带通滤波器截止频率为0.312Hz和1000Hz。使用成对闪光范式来测量光响应的恢复速度,在该范式中呈现了具有相同饱和强度(1.8log.cd.s/m^2)的闪光对,其以不同的刺激间时距(ISI;0.5、1、2、4、8、16、32、64秒)分隔开。在该范式中,第一闪光完全抑制了视杆机制的电响应,这允许通过呈现具有不同ISI的第二闪光来观察视杆功能的功能性恢复的速度。在闪光对之间提供足量的时间(150秒)以允许第一闪光的恢复。然后观察到的a波振幅的恢复应当反映缺乏视锥功能的动物中视杆失活的速度,因为闪光应当仅漂白视紫红质的一部分(0.02%)(Lyubarsky et al.,2004和Weymouth,A.E.&Vingrys 2008)。在之前报道的基础上进行一些修改,来进行暗视6Hz闪光强度系列(Seeliger et al.,2001)。使用17级闪光强度,范围为-6至2log.cd.s/m^2,每级以0.5log单位分隔。对于每一级,适应10秒之后,使用相同的闪光条件,将600毫秒扫射(sweep)平均20次。使用全部为83.3cd/m^2的持续时间为20、100和200毫秒的更长的闪光,也获得了暗适应的响应系列。在以下逐渐增加的光强度下从暗适应的动物获得标准单闪光暗视记录:-6、-5、-4、-3、-2、-1、0、1.0、1.5和1.9log.cd.s/m^2。在20cd/m^2的背景光强度(也用作记录期间的背景光)下,按照5min光适应间隔进行明视闪光记录。使用的明视光强度为-2、-1、0、1、1.5和1.9log.cd.s/m^2。

[0147] 组织学

[0148] rAAV2/8.Rho.mR9ap单侧视网膜下注射后6周,快速摘除Cnga3-/-小鼠的两只眼并快速冷冻于液氮中。将眼冷冻包埋于OCT(RA Lamb,Eastborne,UK)中之后,将眼切成15μm厚的横向切片并在空气中干燥15-30分钟。对于免疫组织化学,将切片预封闭在包含正常驴血清(2%)、牛血清白蛋白(2%)的PBS中1小时,然后在室温下用抗RGS9抗体(1:500;Santa Cruz Biotechnology,SantaCruz,CA)孵育2小时。用PBS冲洗2×15min之后,在室温(RT)下将切片用适合的Alexa 546标记的二级抗体(Invitrogen,Carlsbad,CA)孵育2小时,冲洗并用Hoechst 33342(Sigma-Aldrich,Gillingham,UK)反染色。在共焦显微镜(Leica TCS SP2,Leica Microsystems;Wetzlar,Germany)上观察视网膜切片。

[0149] 蛋白质印迹

[0150] 在rAAV2/8.Rho.mR9ap单侧视网膜下注射后4周,从Cnga3-/-小鼠收集眼。从RPE/脉络膜/巩膜复合物分离神经视网膜之后,使组织在RIPA缓冲液中均质化并在冰上放置20分钟。4℃、16,000g离心样品30分钟并贮存于-20℃直至使用。使用已知方案来进行蛋白质印迹。

[0151] 视动响应和对比敏感度函数

[0152] 通过观察小鼠对旋转正弦光栅(OptoMotry™,Cerebral Mechanics,Lethbridge,AB Canada)的视动响应来测量处理的和未处理的眼的对比敏感度和视敏度。根据两只眼对图案旋转的不同敏感度,使用的方案产生了右眼和左眼敏锐度的独立测量:右眼和左眼分别主要由逆时针和顺时针旋转驱动(Douglas et al.,2005)。将小鼠放置在封闭空间中与

地板隔离的小岛上，所述封闭空间被4个具有平均照明度为62cd/m^2的旋转正弦光栅的监控器围绕。使用双盲两次替代性强制选择步骤，其中观察者对图案旋转的方向、对是否是经处理的或未经处理的Cnga3-/-小鼠或年龄匹配的野生型对照动物(C57BL6)是“不知晓”的。将6Hz下呈现的0.128、0.256、0.383、0.511周/度下测量的对比敏感度定义为100除以产生阈值响应的最低对比百分数。在独立的天中对每只小鼠的两只眼进行4次测试。将数据展示于Campbell-Robson对比敏感度图表上，正弦光栅代表相对空间频率。

[0153] 视紫红质测量

[0154] 在过夜使小鼠完全适应黑暗之后，麻醉小鼠并使瞳孔完全放大以评估视色素漂白的速度。然后将小鼠放置在光盒中，该光盒中的光源(7.0mW)直接照射眼5分钟，然后收集眼。在另一个实验中，将小鼠暴露于与测量各种持续时间(0、30、60、120分钟)的对比敏感度的条件相同的条件。在各时间点摘除小鼠眼并放置于250μL磷酸缓冲盐水中，快速冷冻于不透光管中的液氮中，并保持在-20℃直到使用。在过夜使小鼠适应黑暗之后，在红光照明下于黑暗中收集一些眼。在之前报道(Douglas et al.,1995)的基础上进行一些修改，来进行视紫红质的分光光度法测量。简言之，在室温下融化样品并均质化。此操作和所有随后的操作在使视色素漂白最少的暗红光照明下进行。将50μL正十二烷基β-D-麦芽糖苷(200mM;Sigma-Aldrich,St.Louis,MO)添加到各样品中，并在室温下将所得混合物旋转2h，然后4℃下离心(23,000g)10分钟。除去上清液并放置在Shimadzu UV-2101PC分光光度计(Shimadzu,Kyoto,Japan)中的石英杯中。在对未漂白提取物进行从300nm至700nm的初始扫描之后，将样品暴露于单色光(502nm)3分钟——已表明其足以完全漂白视紫红质(Longbottom et al.,2009)，并进行重新扫描。全部吸收光谱在700nm归零。使用漂白前曲线和漂白后曲线来构建差异光谱，并确定约500nm下的最大光密度，代表所提取的视色素的量。

[0155] 实施例6——视杆中的R9AP过表达盒和增加的光感受器失活速度

[0156] RGS9、Gβ5和R9AP是调控的GTPase复合物的必要成员。为了研究在视杆中AAV介导的R9AP过表达对GTPase复合物的影响，在Cnga3-/-小鼠中检查rAAV2/8.Rho.mR9ap视网膜下注射之后RGS9的水平和分布。这些小鼠具有正常视杆功能，但是缺乏视锥功能，并充当全色盲的模型。4周之后，与未经治疗的视网膜相比，经治疗的视网膜在整个光感受器层中显示出增加的针对RGS9的免疫反应性(图4A)。蛋白质印迹分析进一步确认了在经治疗的视网膜中RGS9蛋白表达增加(图4B)。这些结果表明，使用AAV2/8的R9AP的过表达有效增加了催化组分RGS9和GTPase复合物的水平。

[0157] 接下来通过运用成对闪光ERG(Lyubarsky and Pugh 1996)，研究了AAV2/8介导的R9AP过表达对视杆光转导的功能影响。在该范式中，以可变的刺激间时距传递一对相同的闪光强度，并且测量第二响应相对于第一响应的恢复。在视杆细胞途径中，a波(源自光感受器)恢复的速度取决于失活的速度。发现与未经处理的眼(σ＝约7.38秒)相比，用rAAV2/8.CMV.mR9ap注射的Cnga3-/-眼中a波振幅50％恢复的时间常数(σ)减小约60％(σ＝约2.99秒)(图4C)。类似地，在相同小鼠系(Cnga3-/-)中使用视紫红质启动子(rAAV2/8.Rho.mR9ap;σ＝约2.74秒;图4C)或在另一视锥缺陷的小鼠系(Pde6c-/-;图8)中使用相同病毒(rAAV2/8.CMV.mR9ap)观察到a波恢复的速度增加。这些观察表明，rRAAV2/8.CMV.mR9ap或rAAV2/8.Rho.mR9ap的视网膜下注射通过增加RGS9和GTPase复合物的水平

可显著提高视杆光转导的失活速度。

[0158] 实施例7——通过R9AP过表达的视杆功能的“明视偏移”

[0159] 为了研究在视杆中通过RGS9和GTPase复合物的过表达而实现的失活速度增加是否能够改变光感受器功能的运转范围，使用增加的闪光强度来记录暗适应的6Hz闪光ERG。与未经处理的眼相比，用rAAV2/8.CMV.mR9ap或rAAV2/8.Rho.mR9ap处理的眼显示出增加的对更亮闪光的响应。这导致响应上限的升高最多达约2log单位(图5A)，对最大光响应的影响很小(在经处理的眼中为151±17μV以及在未经处理的眼中为162±29μV；平均值±平均值的标准误差)。如所预期的，这种视杆运转范围的“明视偏移”伴随着响应下限的相互升高最多达约1.5log单位。同时，与未经处理的Cnga3-/-眼相比，均具有功能性视锥的野生型眼和Gnat1-/-眼的ERG响应的上限升高约4.0log单位。将rAAV2/8.Rho.mR9ap注射到Pde6c-/-小鼠中时得到类似的结果(图9)。因此，治疗使视杆响应于更长持续时间的闪光(图5B)，以及响应于视锥分离背景照明下的闪光(图5C)。这些包括未经处理的视杆实际上未显示出响应的情况。

[0160] 总之，这些结果确定，视杆中R9AP过表达导致它们的脱敏，并且使细胞获得明视功能以交换暗视功能。这种对视杆功能的“明视偏移”的治疗性诱导至少持续5个月，而没有明显的视网膜变性证据(图10)。同时，使用相同病毒载体对野生型小鼠的治疗未显示出可测量的视网膜功能变化(图11)。

[0161] 实施例8——视杆双极途径适应改变的视杆功能的传输。

[0162] 本工作确定了视杆中R9AP的过表达导致更快的光感受器失活动力学，并且使神经元响应于更大量的光子。同时，加速失活还应导致光感受器突触末端的神经递质释放的持续时间更短。因此，评估了下游视杆双极信号传导是否受到治疗的影响。首先，通过使用ERG来测量a波(源自光感受器)和b波(源自双极细胞)的隐含期和振幅，研究了对于短的单闪光，信号从光感受器传输到双极细胞的速度和范围(图6a)。总体上，对于a波和b波，观察到经治疗和未经治疗的眼的稍微更小但是几乎相同的强度-响应曲线。观察到的小差异可反映出加速的光感受器失活的真实结果或仅反映出由视网膜下注射诱导的神经损伤。a波隐含期标志着双极细胞驱动的b波不可检测时的时间点。本发明人还观察到a波和b波隐含期的小延迟，表明从光感受器到双极细胞的神经信号传输中存在中等程度的延迟。然而，个体之间ERG响应的相对大的变化表明，视杆响应的小延迟或降低未必转变为视觉功能障碍(Birch and Anderson 1992)。

[0163] 因此，这些结果表明，原则上，双极细胞几乎完全适应光感受器功能的改变，并且重要的是，表现出适当的剂量-响应关系。

[0164] 实施例9——R9ap过表达导致改善的对比敏感度函数

[0165] 接下来，通过使用标准计算机显示器，在可能的最亮记录条件($62cd/m^2$)下测量对旋转正弦光栅的光动力响应，询问通过R9AP过表达的视杆功能的“明视偏移”是否因此转化为光照下改善的视觉表现(Carvalho et al.,2011)。该行为测试的独特优势在于，可单独地研究每只眼的视觉功能；右眼的功能可通过对逆时针(CCW)光栅的响应来检测，左眼的功能通过顺时针(CW)刺激来检测(Douglas et al.,2005)。使用6.0Hz固定时间频率来研究空间对比敏感度函数(CSF)，发现与野生型小鼠相比，Cnga3-/-小鼠具有降低的CSF(图7)。CSF——对比敏感度和视敏度的函数——表现出视觉感知的估计范围(假定动物可在曲线

下而非曲线上感知光栅;图7A)。有趣的是,当比较经处理的和未经处理的眼的对比敏感度时,观察到使用0.128和0.256周/度(c/d)光栅的敏感度分别增加8.0倍(P=0.005)和5.4倍(P=0.011)(图7A,左图)。对于0.383(P=0.056)和0.511(P=0.111)c/d的光栅,未观察到明显的对比敏感度改变。有趣的是,Cnga3-/-小鼠中处理的眼的平均敏感度超过了具有正常视锥功能的野生型对照的平均敏感度。然而,当用相同的病毒构建体处理野生型小鼠时,经处理的眼和未经处理的眼的CSF并无差异(图12)。

[0166] 当查看最大亮度显示器设置时,已确定R9AP过表达导致视觉表现的增加,需要确定这种视觉增加是否是可持续的。这是合理的担忧,因为已知视杆中视色素的再生比视锥中视色素的再生慢得多(Wangand Kefalov 2011)。首先,评估是否治疗导致视色素漂白速度改变。发现经处理的和未经处理的眼暴露于亮光5分钟并未产生残留的可漂白视色素水平的任何差异(图7B,左下图)。其次,在将Cnga3-/-小鼠暴露于进行CSF测量的相同实验条件下不同时间之后,研究眼中可漂白的视紫红质的量。结果表明,对于经处理的和未经处理的眼,在相似地暴露于视觉刺激的2小时中,视色素水平保持稳定而没有减少迹象(图7B,右下图)。这些结果表明,在经处理的Cnga3-/-小鼠中视觉感知的增加由充分供应的视紫红质分子支持,并且是可持续的。

[0167] 参考文献

[0168] Curcio,C.A.,et al.The.Journal of comparative neurology 292,497-523(1990).

[0169] Dryja,T.PAmerican journal of ophthalmology 130,547-563(2000).

[0170] Hess,R.F.&Nordby,K.The.Journal of physiology 371,365-385(1986).

[0171] Nishiguchi,K.M.,et al.Human mutation 25,248-258(2005).

[0172] Kohl,S.,et al.Nature genetics 19,257-259(1998).

[0173] Chang,B.et al.P.N.A.S 106,19581-19586(2009).

[0174] Thiadens,A.A.,et al.American journal of human genetics 85,240-247(2009).

[0175] Burns,M.E.&Pugh,E.N.Biophys J97,1538-1547(2009).

[0176] Burns,M.E.&Pugh,E.N.Physiology 25,72-84(2010).

[0177] Baseler,H.A.,et al.Nature neuroscience 5,364-370(2002).

[0178] Martemyanov,K.A.&Arshavsky,V.Y.Prog Mol Biol Transl 86,205-227(2009).

[0179] Krispel,C.M.,et al.Neuron 51,409-416(2006).

[0180] Cowan,C.W,et al.P.N.A.S.95,5351-5356(1998).

[0181] Zhang,X.,Wensel,T.G.&Kraft,T.W.The Journal of ueuroscience:the official journal of the Society for Neuroscience 23,1287-1297(2003).

[0182] Nishiguchi,K.M.,et al.Nature 427,75-78(2004).

[0183] Michaelides,M.,et al.Ophthalmology 117,120-127e121(2010).

[0184] Han,X.et al.Front Syst Neurosci.5,18(2011).

[0185] Busskamp,V.,et al.Science329,413-417(2010).

[0186] Fu,Y.,Yau,K.W.Pflugets Arch.454,805-819(2007).

[0187] Pugh,E.N.Jr et al.Curr Opin Neurobiol.9,410-418(1999).

[0188] de Jong,P.V.T.M.N Engl JMed 355,1474-1485(2006).

[0189] Wässle,H.Nat Rev Neurosci.5,747-757(2004).

[0190] Soucy,E.et al.Neuron 21,481-493(1998).

[0191] Hack,I.et al.P.N.A.S.96,14130-14135(1999).

[0192] Li,W.et al.Nat Neurosci 13,414-416(2010).

[0193] Biel,M.et al.P.N.A.S.96,7553-7557(1999).

[0194] Umino,Y.et al.J Neurosci 28,189-198(2008).

[0195] Cangiano,L.et al.J Physiol.590,3841-3855(2012).

[0196] Berndt,A.et al.Science 344,420-424(2014).

[0197] Wietek,J.et al.Science 344,409-412(2014).

[0198] Calvert,P.D.et al.P.N.A.S97,13913-13918(2000).

[0199] Gao,G.P.et al.P.N.A.S99,11854-11859(2002).

[0200] Lyubarsky,A.L.,et al.Vision research 44,3235-3251(2004).

[0201] Weymouth,A.E.&Vingrys,A.J.Progress in retinal and eye research 27,1-44(2008).

[0202] Seeliger,M.W.,et al.Nature genetics 29,70-74(2001).

[0203] Douglas,R.M.,et al.Visual neuroscience 22,677-684(2005).

[0204] Douglas,R.H.,et al.Journal of Comparative Physiology a-Sensory Neural and Behavioral Physiology 177,111-122(1995).

[0205] Longbottom,R.,et al.P.N.A.S.106,18728-18733(2009).

[0206] Lyubarsky,A.L.&Pugh,E.N.,Jr.The Journal of neuroscience:the offcial journal of the Society for Neuroscience 16,563-571(1996).

[0207] Birch,D.G.&Anderson,J.L.Archives of ophthalmology 110,1571-1576(1992).

[0208] Carvalho,L.S.,et al.Human molecular genetics 20,3161-3175(2011).

[0209] Wang,J.S.&Kefalov,V.J.Progress in retinal and eye research 30,115-128(2011).

[0210] Taylor,A.W.,Ocular immune privilege,Eye,23,1885-1889(2009).

[0211] Natkunarajah,M.et al.,Assessment of ocular transduction using single-stranded and self-complementary recombinant adeno-associated virus serotype 2/8,Gene Ther.15,463-467(2008).

[0212] Choi,V.W.et al.,AAV hybrid serotypes:improved vectors for gene delivery,Curr.

[0213] Gene Ther.,5,299-310(2005).

[0214] Wu,Z.et al.,Adeno-associated virus serotypes:vector toolkit for human gene therapy,Mol.Ther.,14,316-327(2006).

[0215] Chuong,A.S.et al.,Non-invasive optical inhibition with a red-shifted microbial rhodopsin,Nat Neurosci.,17,1123-1129(2014).

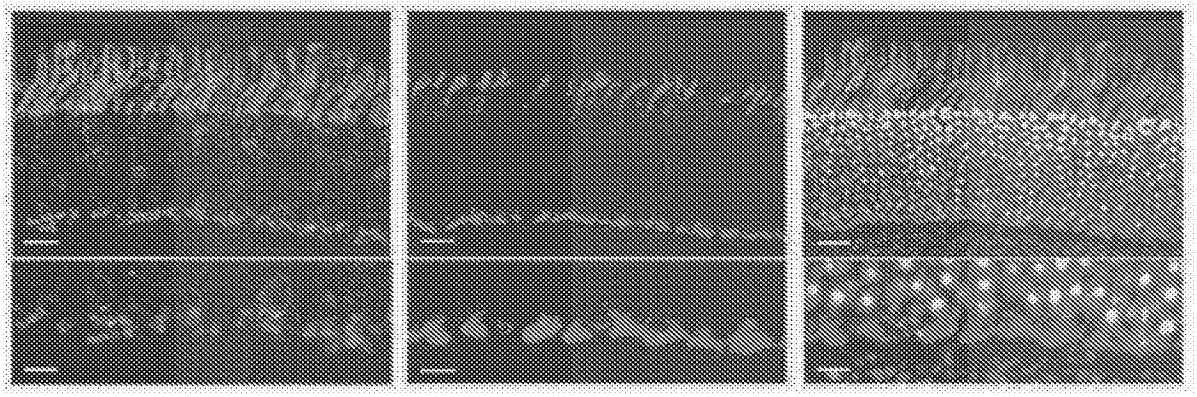

图1a

图1b

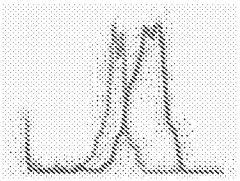

图1c

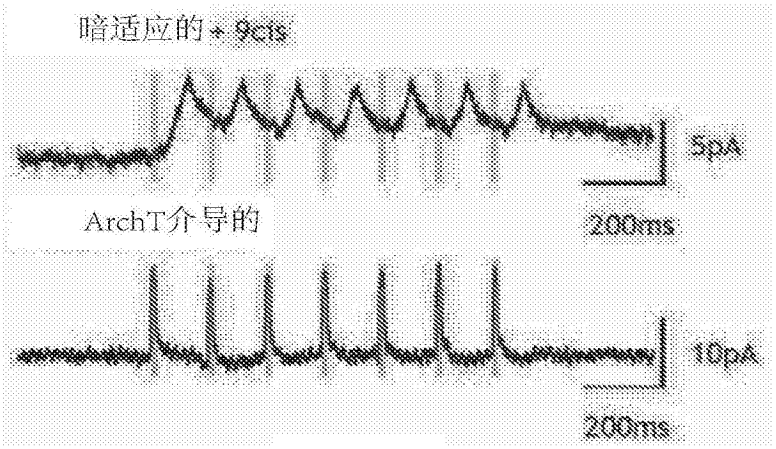
暗适应的+9cis
5pA
200ms
ArchT介导的
10pA
200ms

图1d

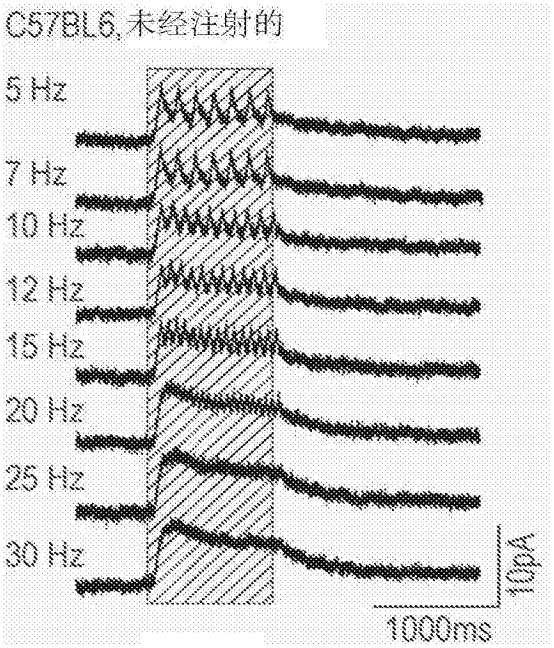
C57BL6,未经注射的
5 Hz
7 Hz
10 Hz
12 Hz
15 Hz
20 Hz
25 Hz
30 Hz
10pA
1000ms

图2a

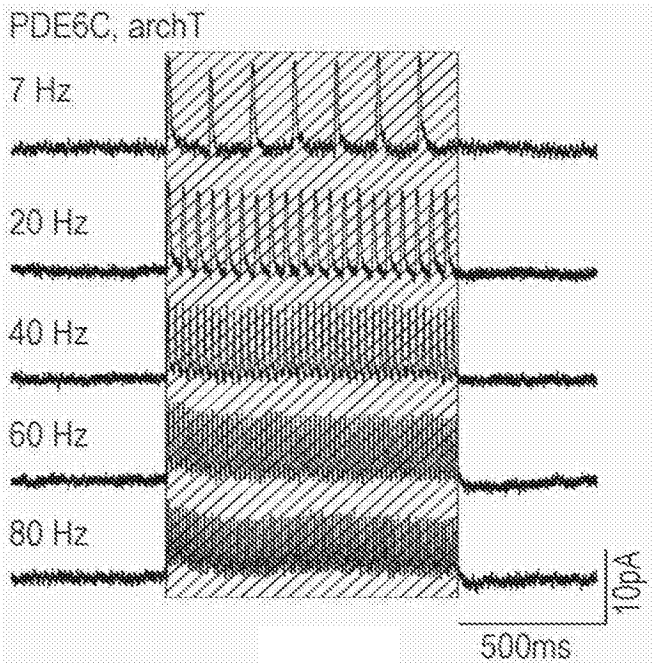
PDE6C, archT
7 Hz
20 Hz
40 Hz
60 Hz
80 Hz
10pA
500ms

图2b

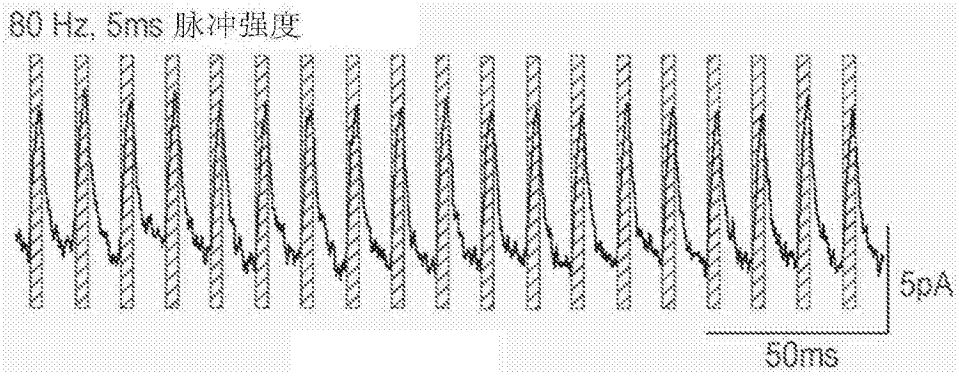
80 Hz, 5ms 脉冲强度
5pA
50ms

图2c

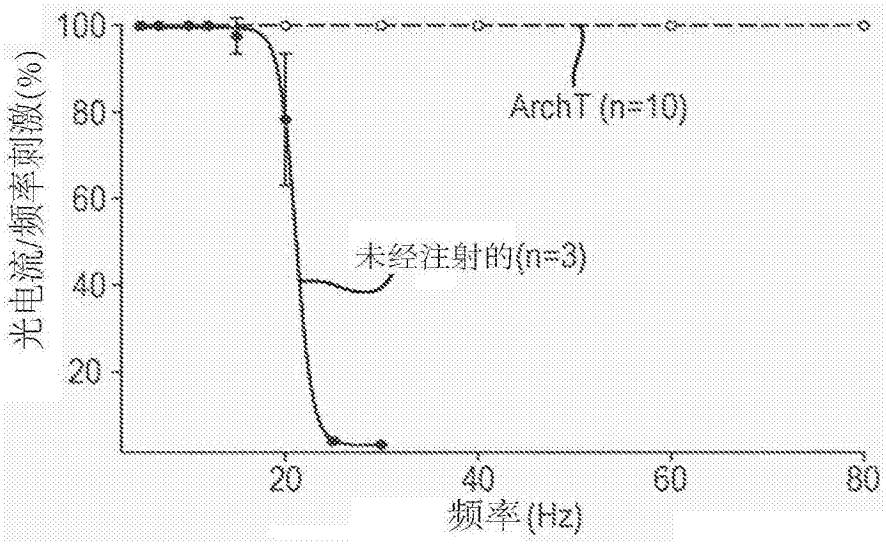
光电流/频率刺激(%)
100
80
60
40
20
ArchT (n=10)
未经注射的(n=3)
20
40
60
80
频率 (Hz)

图2d

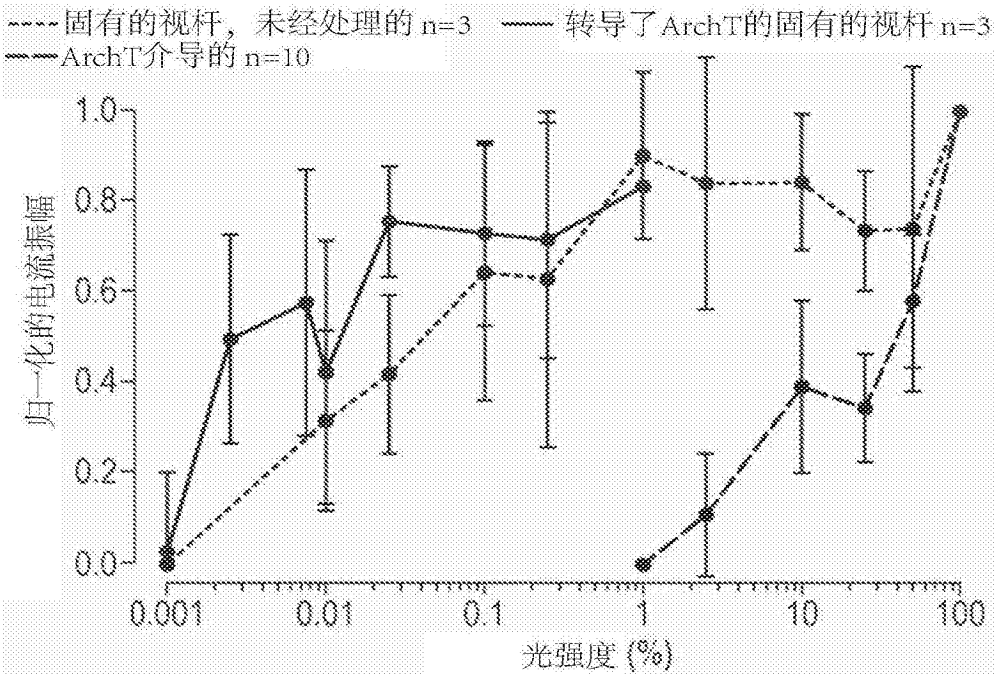
固有的视杆，未经处理的 n=3
转导了ArchT的固有的视杆 n=3
ArchT介导的 n=10
归一化的电流振幅
1.0
0.8
0.6
0.4
0.2
0.0
0.001
0.01
0.1
1
10
100
光强度 (%)

图2e

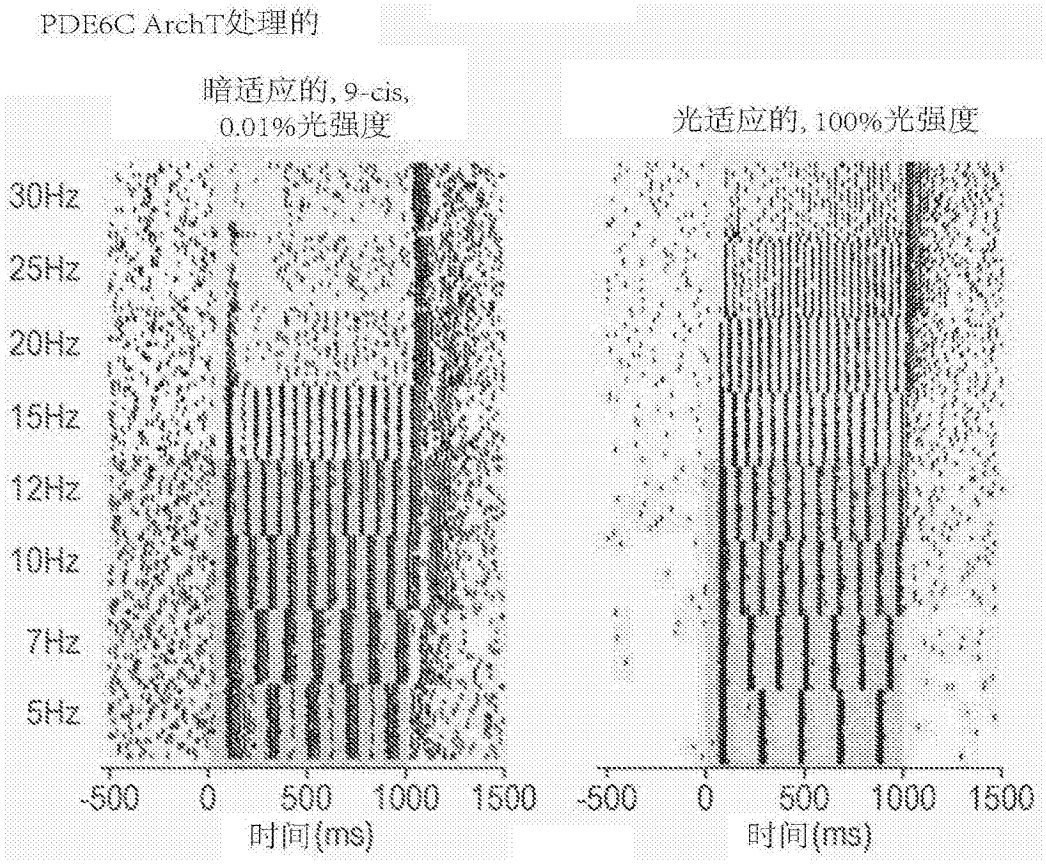
PDE6C ArchT处理的
暗适应的, 9-cis,
0.01%光强度
光适应的, 100%光强度
30Hz
25Hz
20Hz
15Hz
12Hz
10Hz
7Hz
5Hz
-500
0
500
1000
1500
时间(ms)
-500
0
500
1000
1500
时间(ms)

图2f

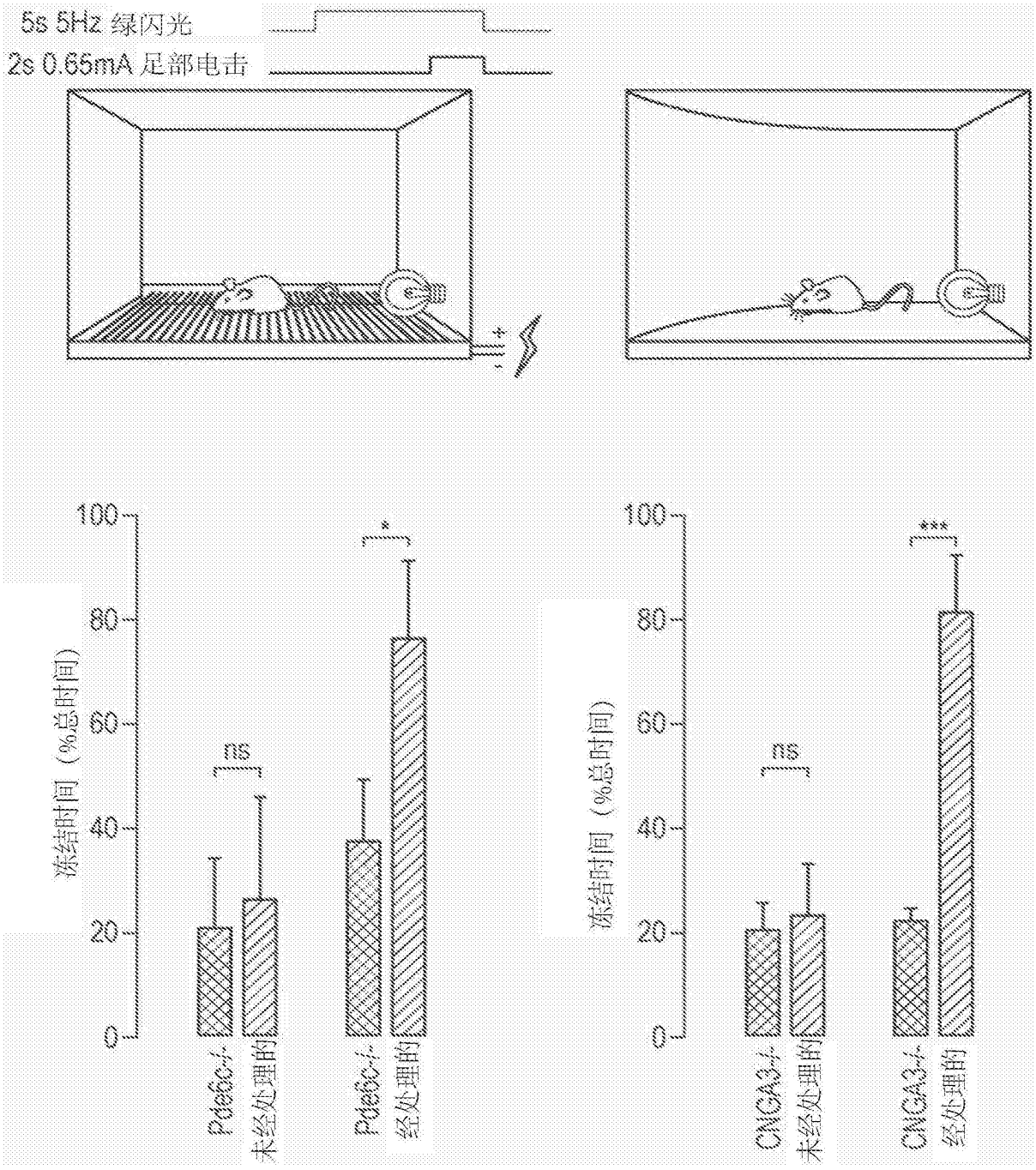
5s 5Hz 绿闪光
2s 0.65mA 足部电击
冻结时间（%总时间）
100
80
60
40
20
0
ns
*
***
P46c-/-
未经处理的
经处理的
CNGA3-/-

图3a

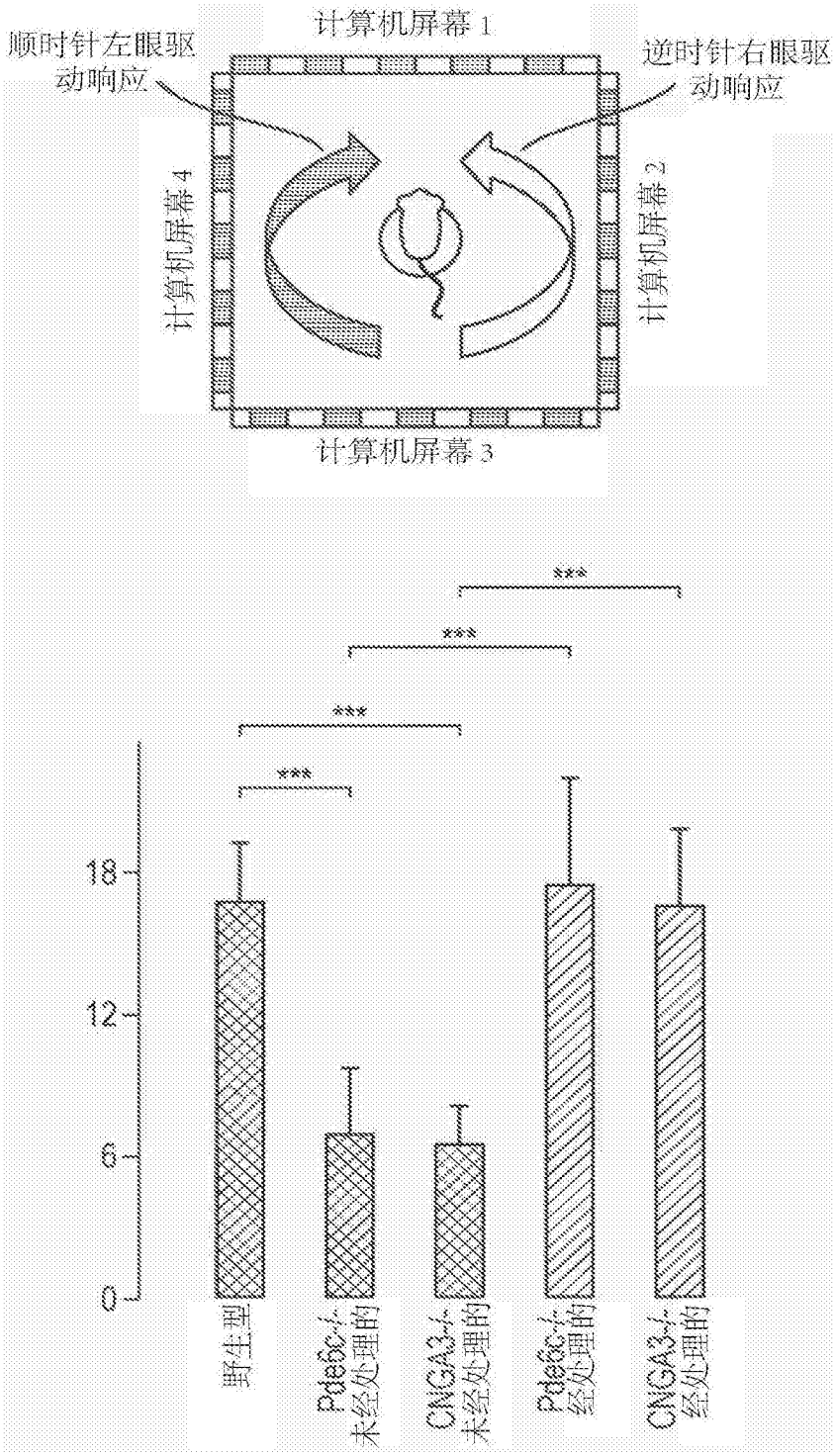
计算机屏幕 1
顺时针左眼驱动响应
逆时针右眼驱动响应
计算机屏幕 4
计算机屏幕 2
计算机屏幕 3
***
***
***
***
18
12
6
0
野生型
Pde6c-/-未经处理的
CNGA3-/-未经处理的
Pde6c-/-经处理的
CNGA3-/-经处理的

图3b

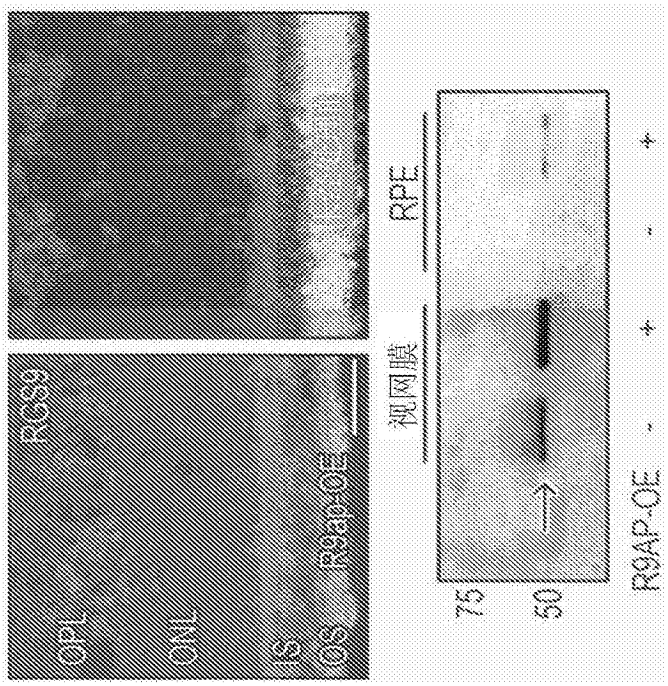

图4a

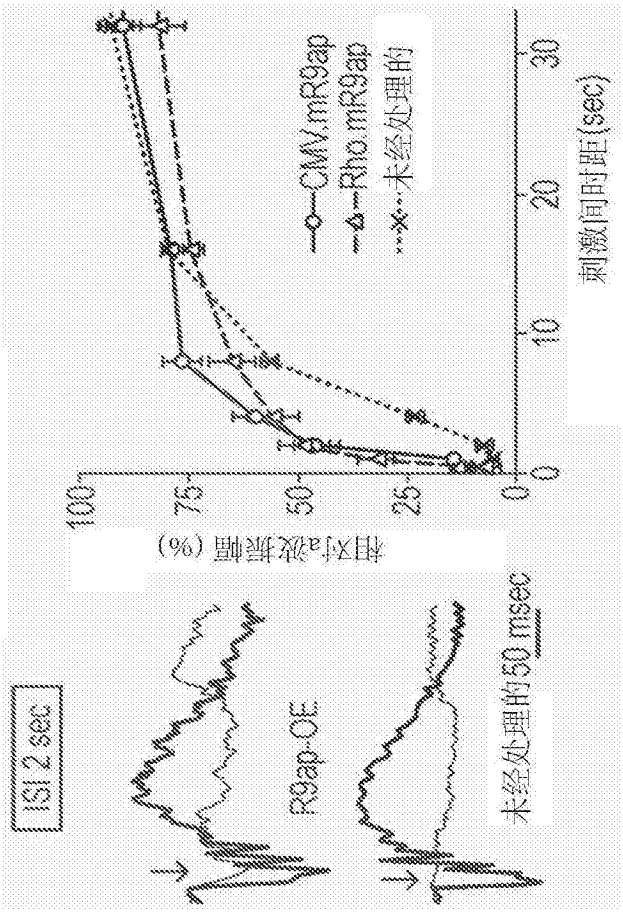
ISI 2 sec
R9ap-OE
未经处理的50 msec
相对a波振幅 (%)
100
75
50
25
0
0
10
20
30
刺激间时距(sec)
CMV.mR9ap
Rho.mR9ap
未经处理的

图4b

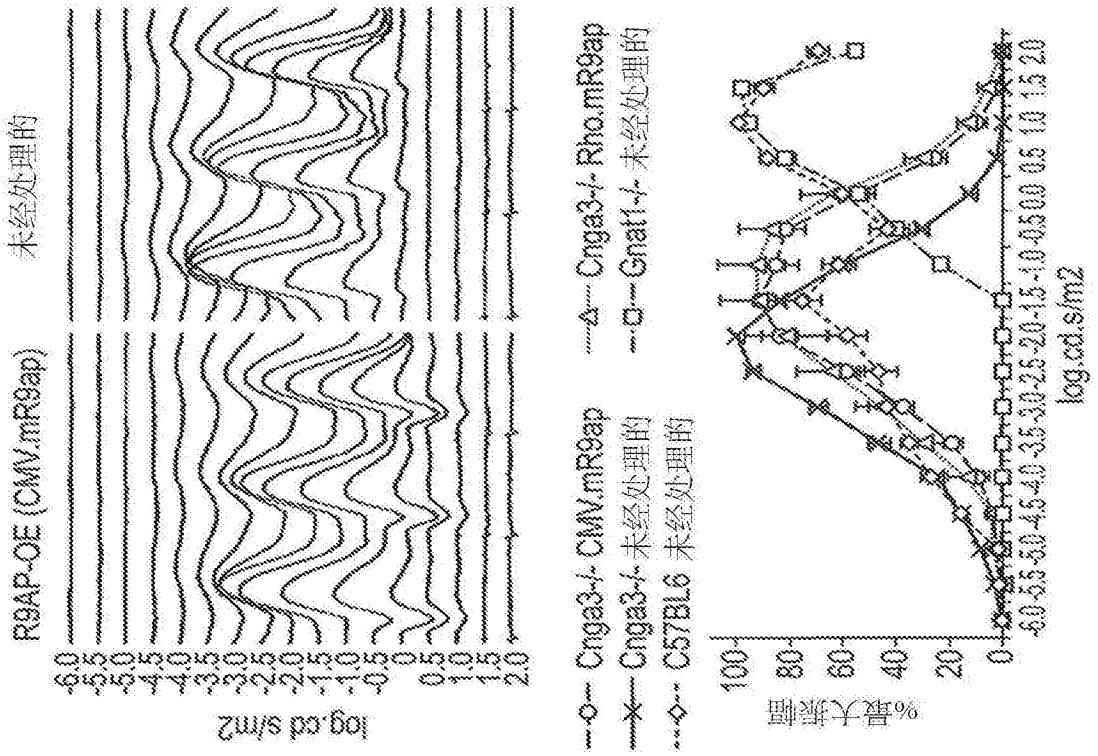
R9AP-OE (CMV.mR9ap)
未经处理的
log.cd s/m2
-6.0
-5.5
-5.0
-4.5
-4.0
-3.5
-3.0
-2.5
-2.0
-1.5
-1.0
-0.5
0
0.5
1.0
1.5
2.0
Cnga3-/- CMV.mR9ap
Cnga3-/- 未经处理的
C57BL6 未经处理的
Cnga3-/- Rho.mR9ap
Gnat1-/- 未经处理的
%最大振幅
100
80
60
40
20
0
-6.0 -5.5 -5.0 -4.5 -4.0 -3.5 -3.0 -2.5 -2.0 -1.5 -1.0 -0.5 0.0 0.5 1.0 1.5 2.0
log.cd.s/m2

图5a

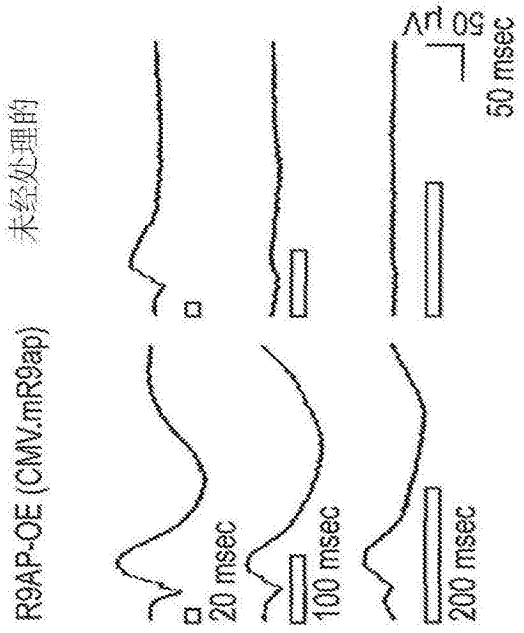
R9AP-OE (CMV.mR9ap)
未经处理的
20 msec
100 msec
200 msec
50 msec
uV

图5b

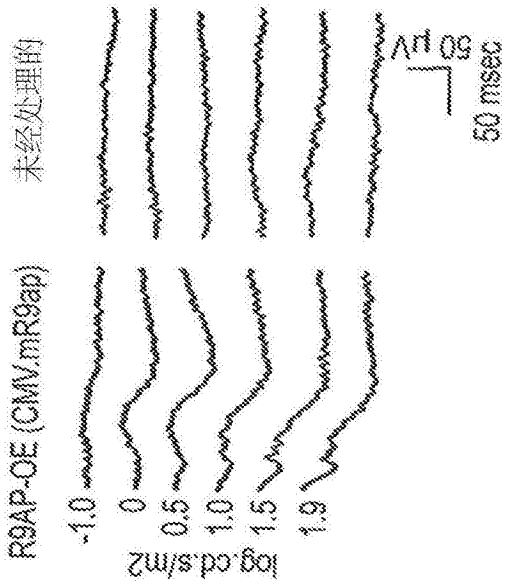
未经处理的
60 μV
50 msec
R9AP-OE (CMV.mR9ap)
-1.0
0
0.5
1.0
1.5
1.9
log cd.s/m2

图5c

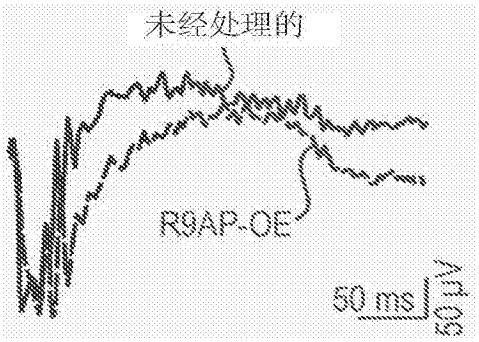
未经处理的
R9AP-OE
50 ms
50 μV

图6a

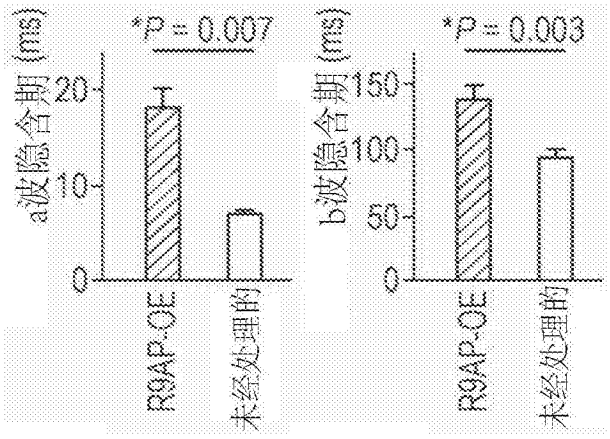
*P = 0.007
a波隐含期 (ms)
20
10
0
R9AP-OE
未经处理的
*P = 0.003
b波隐含期 (ms)
150
100
50
0
R9AP-OE
未经处理的

图6b

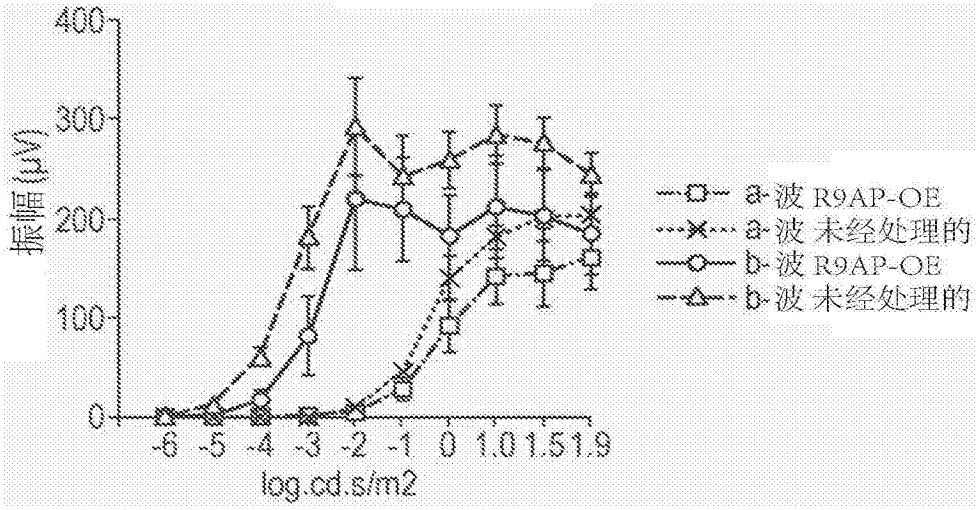
振幅 (μV)
400
300
200
100
0
-6 -5 -4 -3 -2 -1 0 1.0 1.5 1.9
log.cd.s/m2
a-波 R9AP-OE
a-波 未经处理的
b-波 R9AP-OE
b-波 未经处理的

图6c

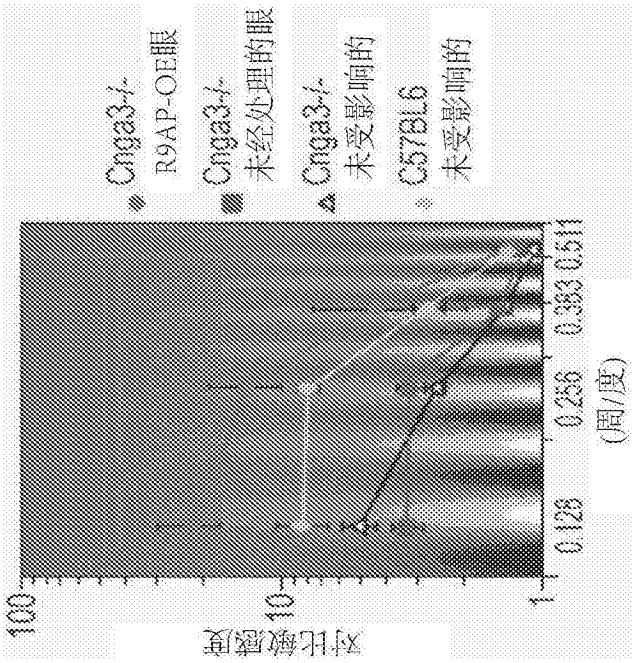
Cnga3-/-
R9AP-OE眼
Cnga3-/-
未经处理的眼
Cnga3-/-
未受影响的
C57BL6
未受影响的
对比敏感度
100
10
1
0.128
0.256
0.383
0.511
(周/度)

图7a

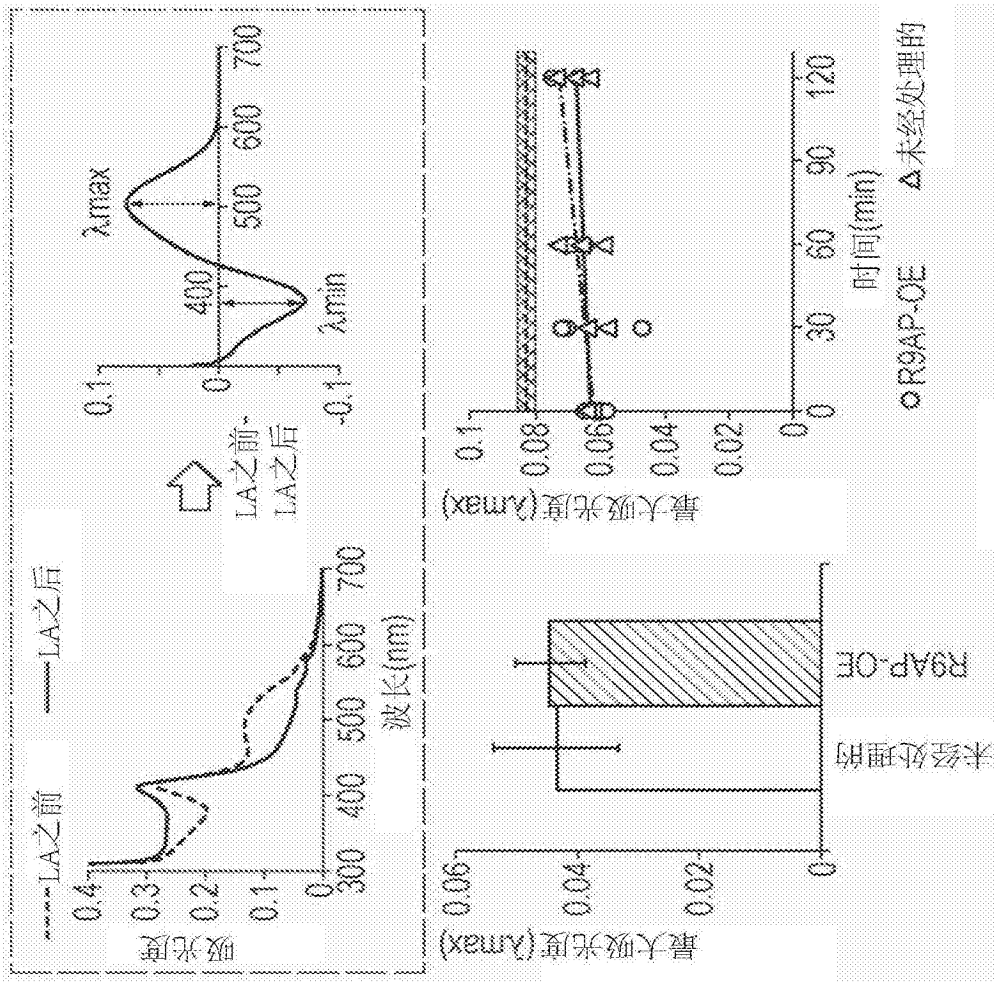
λmax
λmin
400
500
600
700
0.1
0
-0.1
LA之前-
LA之后
LA之前
LA之后
吸光度
波长(nm)
0.4
0.3
0.2
0.1
0
300
400
500
600
700
最大吸光度(λmax)
时间(min)
0
30
60
90
120
0.08
0.06
0.04
0.02
R9AP-OE
△未经处理的
未经处理的
R9AP-OE

图7b

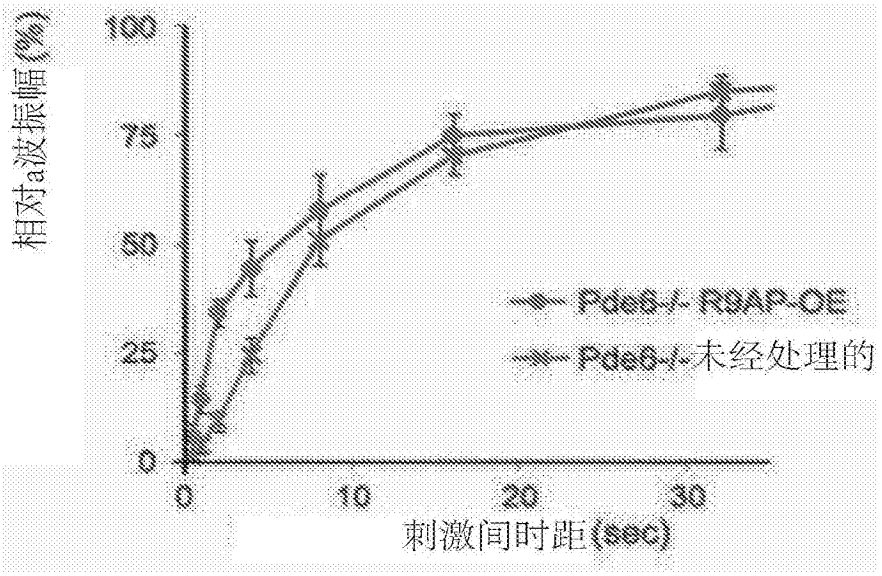
相对a波振幅(%)
100
75
50
25
0
0
10
20
30
刺激间时距(sec)
Pde6-/- R9AP-OE
Pde6-/-未经处理的

图8

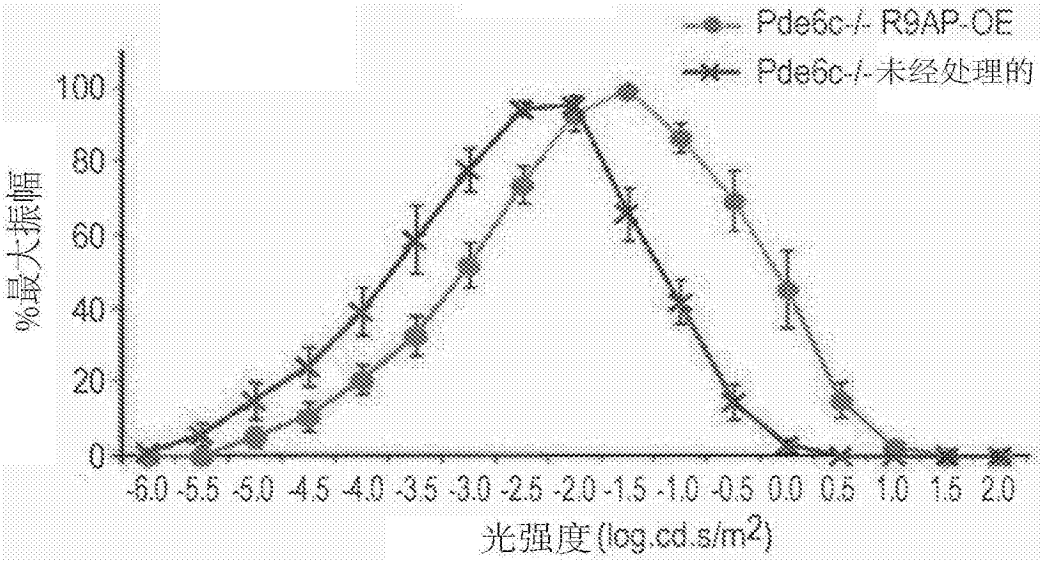
%最大振幅
100
80
60
40
20
0
-6.0 -5.5 -5.0 -4.5 -4.0 -3.5 -3.0 -2.5 -2.0 -1.5 -1.0 -0.5 0.0 0.5 1.0 1.5 2.0
光强度(log cd.s/m2)
Pde6c-/- R9AP-OE
Pde6c-/-未经处理的

图9

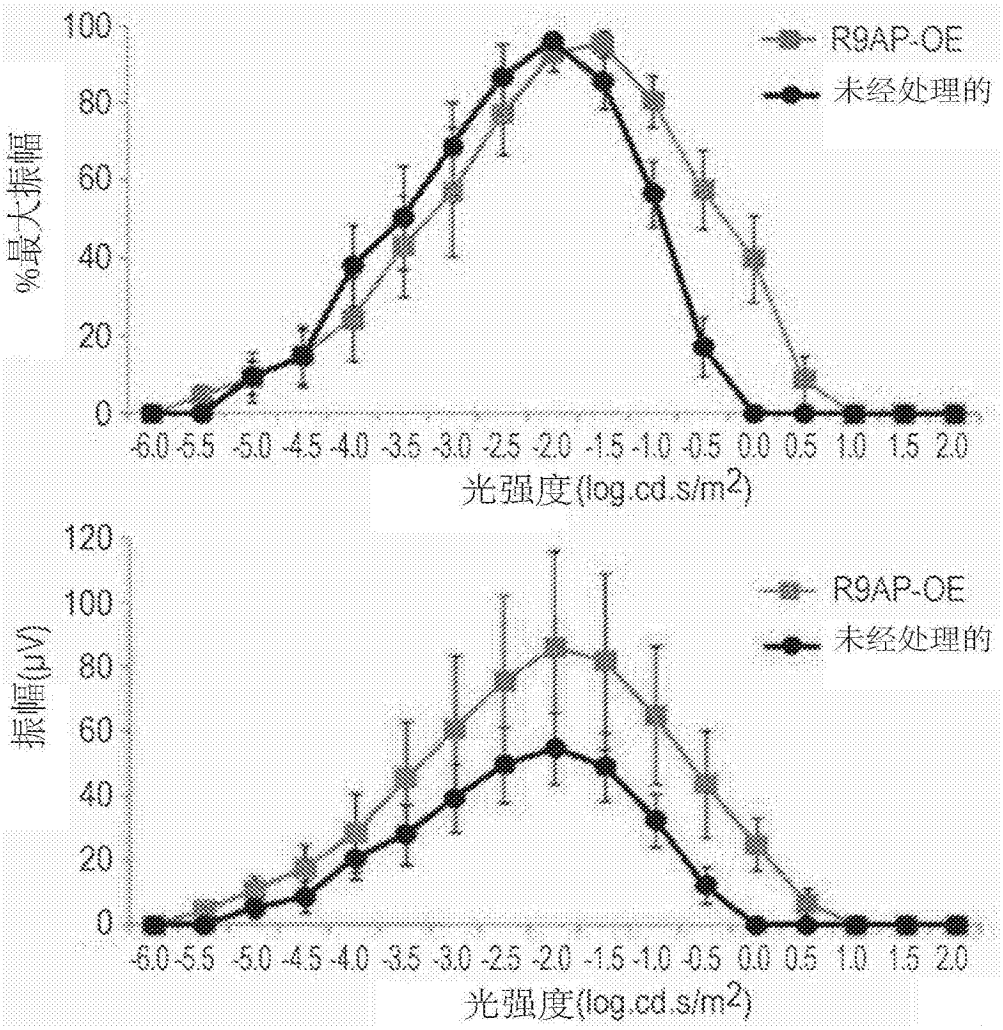
%最大振幅
100
80
60
40
20
0
R9AP-OE
未经处理的
-6.0 -5.5 -5.0 -4.5 -4.0 -3.5 -3.0 -2.5 -2.0 -1.5 -1.0 -0.5 0.0 0.5 1.0 1.5 2.0
光强度(log cd.s/m2)
振幅(μV)
120
100
80
60
40
20
0
R9AP-OE
未经处理的
-6.0 -5.5 -5.0 -4.5 -4.0 -3.5 -3.0 -2.5 -2.0 -1.5 -1.0 -0.5 0.0 0.5 1.0 1.5 2.0
光强度(log cd.s/m2)

图10

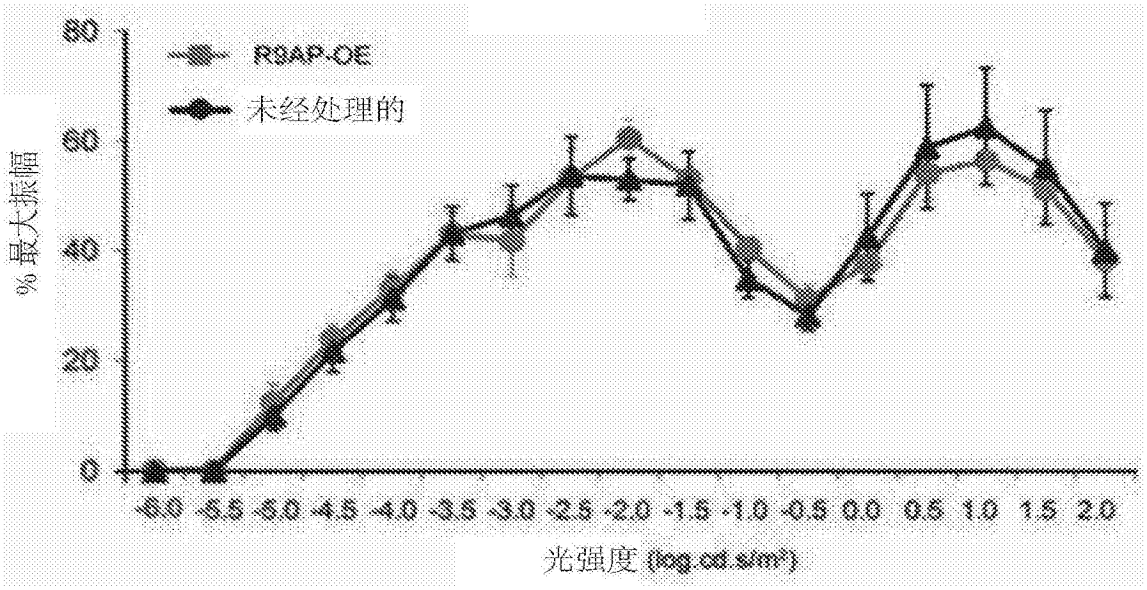
R9AP-OE
未经处理的
% 最大振幅
0
20
40
60
80
-6.0 -5.5 -5.0 -4.5 -4.0 -3.5 -3.0 -2.5 -2.0 -1.5 -1.0 -0.5 0.0 0.5 1.0 1.5 2.0
光强度 (log cd.s/m²)

图11

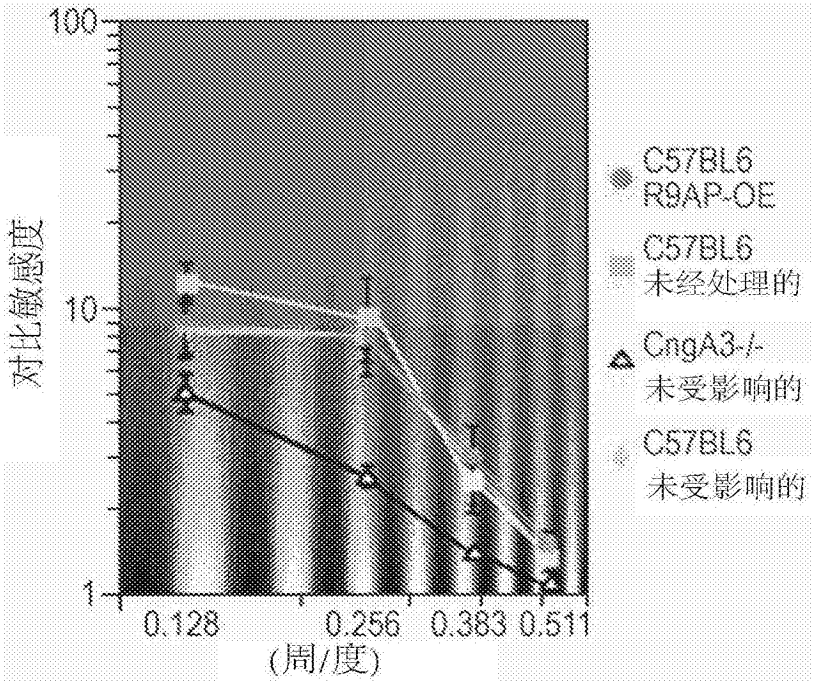
100
10
1
对比敏感度
0.128
0.256
0.383
0.511
(周/度)
C57BL6
R9AP-OE
C57BL6
未经处理的
CngA3-/-
未受影响的
C57BL6
未受影响的

图12